Prolonged T – DC macro-clustering within lymph node microenvironments initiates Th2 differentiation in a site-specific manner

Miranda R. Lyons-Cohen

A dissertation

submitted in partial fulfillment of the

requirements for the degree of

Doctor of Philosophy

University of Washington

2023

Reading Committee:

Michael Y. Gerner, Chair

Elia Tait Wojno

Steven F. Ziegler

Program Authorized to Offer Degree:

Immunology

University of Washington

Abstract

Prolonged T – DC macro-clustering within lymph node microenvironments initiates Th2 differentiation in a site-specific manner

Miranda R. Lyons-Cohen

Chair of the Supervisory Committee:
Michael Y. Gerner
Department of Immunology

T helper 2 (Th2) responses protect against pathogens while also driving allergic inflammation, yet how large-scale Th2 responses are generated in tissue context remains unclear. Here, we used quantitative imaging to investigate early Th2 differentiation within lymph nodes (LNs) following cutaneous allergen administration. Contrary to current models, we observed extensive activation and 'macro-clustering' of early Th2 cells with migratory type-2 dendritic cells (cDC2s) generating specialized Th2-promoting microenvironments. Macro-clustering was integrin mediated and promoted localized cytokine exchange among T cells to reinforce differentiation, which contrasted behavior during Th1 responses. Unexpectedly, formation of Th2 macro-clusters was dependent on the site of skin sensitization. Differences between sites were driven by divergent activation states of migratory cDC2 across dermal tissues, with enhanced costimulatory molecule expression by cDC2 in Th2-generating LNs promoting prolonged T cell activation, macro-clustering, and cytokine sensing. Thus, generation of dedicated Th2 priming micro-environments through enhanced costimulatory molecule signaling initiates Th2 responses *in vivo* and occurs in a skin site-specific manner.

TABLE OF CONTENTS

LIST OF FIGURES

ACKNOWLEDGEMENTS

I am deeply grateful to Michael for letting me explore a new project in the lab and fostering my independence and confidence as a scientist. I wanted to study Th2 cells and you not only supported me but provided the tools, resources, and expertise for me to succeed. We learned a new field together and I feel lucky that I was able to excel due to the support and encouragement I received. Thank you for reading every single training grant, proposal, paper draft, and presentation I ever sent to you. Despite the ups and downs of grad school, I never doubted your commitment to science and to the people in your lab. To all the past and present members of the Gerner Lab: every single one of you taught me something. In your own ways, you all contributed to my successes in grad school whether it was genotyping mice, helping me process tissues, or providing invaluable ideas and feedback during lab meeting. You are all incredible scientists and people, and I can't wait to see the amazing things you all accomplish. Thanks to my brilliant committee members who kept me on track. I always came away from committee meetings feeling more positive and hopeful about myself and my work.

I am forever in debt to my post-bac mentors Don Cook, Jennifer Martinez, and Hideki Nakano at NIEHS who introduced me to the world of Immunology. Don, you took a chance on me when I knew nothing and the skills I learned in your lab were the foundation of my success at UW. Endless thanks to all of you for vouching for me, pushing me when I needed to be pushed, and believing in me.

Thank you to every single person in the department and especially to all the incredible friends I've made along the way. Grad school knocked me down, picked me back up, humbled me in way I couldn't imagine, but ultimately made me a better scientist and person. I attribute this almost

entirely to the kind and brilliant people I was surrounded by. To my classmates: entering class of 2017 truly BEST CLASS. I feel so lucky to be among you and each one of you is a shining star.

To Joey, the most important person, and my former lab mate-turned-fiancé: there are no words to describe how much my life has improved with you in it. Meeting you was the most important thing to happen to me in grad school. Your endless support and optimism has uplifted me and kept me going through grad school. I truly can't explain how incredible it's been to be with someone who knows *exactly* what I'm going through. You believed in me even when I didn't believe in myself. I can't wait to marry you.

To my parents, Amy and Adam: you raised me to value education, and well, here I am after completing 22 years of school! Your pride in me and excitement about my career has keep me motivated. To my sister, Natalie, you are one of the best parts of my life and our bond needs no words (only a knowing blink). Thank you for all your support, love, and baked goods over the years I've been in grad school. I would have had a very different experience without you nearby.

Finally, thank you to Honey: you've always been there with a little lick of encouragement when I most needed it.

DEDICATION

To all the laboratory mice whose lives enabled this work.

Chapter 1. INTRODUCTION TO THE LYMPH NODE

This chapter is adapted from the following publication:

Huang JY*, Lyons-Cohen MR*, Gerner MY. Information flow in the spatiotemporal organization of immune responses. (2022). *Immunol Rev.* Mar;306(1):93-107. doi: 10.1111/imr.13046. Epub 2021 Nov 29. PMID: 34845729; PMCID: PMC8837692.

*contributed equally

Immune responses must be rapid, tightly orchestrated, and tailored to the encountered stimulus. Lymphatic vessels facilitate this process by continuously collecting immunological information (i.e., antigens, immune cells, and soluble mediators) about the current state of peripheral tissues and transporting these via the lymph across the lymphatic system. Lymph nodes (LNs), which are critical meeting points for innate and adaptive immune cells, are strategically located along the lymphatic network to intercept this information. Within LNs, immune cells are spatially organized, allowing them to efficiently respond to information delivered by the lymph, and to either promote immune homeostasis or mount protective immune responses. These responses involve the activation and functional cooperation of multiple distinct cell types and are tailored to the specific inflammatory conditions. The natural patterns of lymph flow can also generate spatial gradients of antigens and agonists within draining LNs, which can in turn further regulate innate cell function and localization, as well as the downstream generation of adaptive immunity. Thus, information transmitted by the lymph shapes the spatiotemporal organization of innate and adaptive immune responses in LNs, in steady state conditions, and during inflammation.

1.1 ROLE OF LYMPH AND LYMPH NODES IN THE IMMUNE RESPONSE

The primary function of the vertebrate cardiovascular system is the regulation of body homeostasis. Blood vasculature supplies oxygen and nutrients to cells and tissues as well as removes waste products for elimination, while the lymphatic system maintains tissue balance by returning interstitial fluids via lymph back into the circulation[1]. In addition to these essential functions, the cardiovascular system is also integrally connected to the organization and function of the immune system[2,3]. Most adaptive lymphocytes and many innate cell types continuously recirculate via the blood, and this promotes rapid trafficking to lymphoid and non-lymphoid organs for surveillance and host defense. The lymphatics, on the other hand, carry information pertaining to the state of peripheral tissues, such as antigens, immune cells, inflammatory mediators, and other soluble molecules[2-7].

Located along the path of lymph return are specialized lymphoid organs, called lymph nodes, which coordinate the information derived from adjacent peripheral tissues via the lymphatics, as well as promote surveillance of this information by the recirculating lymphocytes. Critically, LNs are strategically positioned along the lymphatic network to intercept information transported by the lymph, in order to contain pathogens and limit dissemination, as well as to present this antigenic information to the recirculating T and B cells to initiate adaptive immunity[8]. Antigenic information can be presented by peripheral tissue-derived migratory conventional dendritic cells (cDCs) migrating into the draining lymph node and/or by lymph node resident dendritic cells which capture draining antigens that arrive via lymph flow. These innate cells are localized in a highly organized manner within LNs, and this allows for an extraordinary level of efficiency in sampling of antigens, detection of dangerous insults and pathogens, transmission of signals among

responding innate immune cells and cognate lymphocytes, and the generation of robust antigen-specific adaptive responses specifically tailored to the nature of the stimulus[9-11] (Figure 1.1). Together, this intersection of information gathering via the lymphatic system, adaptive lymphocyte recirculation via blood vessels, and local cellular organization makes LNs ideal hubs for the induction and regulation of immunity, based on the specific organismal needs.

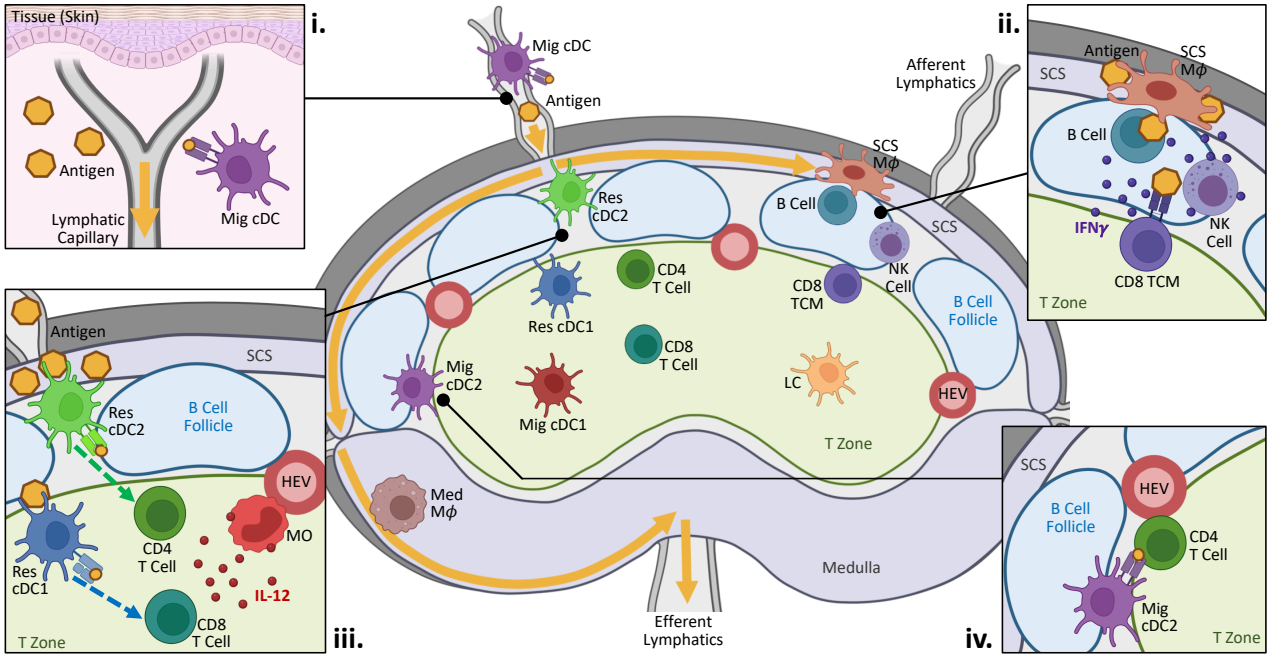

Figure 1.1. Initiation and organization of immune responses within lymph nodes.

Diagram depicts the preferential localization of different immune populations within steady state LNs. Biased spatial positioning is seen for both innate and adaptive cell subsets. (i) At both steady state and during inflammation, information about the state of peripheral tissues is delivered into the nearest LNs via the lymphatics either through direct antigen drainage or active transport by migratory cDCs. (ii & iii) During Type-I inflammation, macrophages and resident cDCs located directly within or proximally to the lymphatic sinuses readily capture antigens and inflammatory agonists. (ii) Innate and adaptive immune cells positioned near the subcapsular sinus initiate early inflammatory responses to promote pathogen containment and clearance. (iii) Resident cDCs also undergo maturation and relocalize into the T cell zone, while inflammatory monocytes infiltrate the LN from the blood. Together, these two cell types functionally cooperate to drive early T cell activation and effector differentiation. Migratory cDC1s can also support Th1 differentiation. (iv) Antigen-bearing migratory cDC2s preferentially position along the T-B border, where they interact with responding CD4 T cells to promote Tfh responses. During Type-II inflammation, these cDCs are also the dominant drivers of Th2 differentiation (also see Figure 1.2). Arrows indicate direction of lymph flow.

Abbreviations: CD8 TCM, central memory CD8 T cell; HEV, high endothelial venule; LC, Langerhans cell; Mϕ, macrophage; Med, medullary; Mig, migratory; MO, monocyte; Res, resident; SCS, subcapsular sinus

1.2 LYMPH NODE ORGANIZATION AND FUNCTION AT STEADY STATE

At both steady state and during inflammation, lymph formed in upstream tissues enters LNs via the afferent lymphatic vessels, passes through the subcapsular and cortical lymphatic sinuses, and then exits via the efferent lymphatic vessels located in the LN medulla to eventually return to the blood circulation. Most LN macrophages, including subcapsular sinus macrophages lining the B cell follicles as well as medullary macrophages, are localized directly within the lymphatic sinuses which enables efficient surveillance of draining lymph and promotes rapid capture of pathogens that arrive via the lymphatics[12,13] (Figure 1.1). LN resident cDCs, and in particular resident cDC2s, also preferentially localize near or directly within the lymphatic sinuses[14,15]. Like macrophages, this enables robust sampling of draining antigens and allows these cells to induce T cell responses during inflammation[15-17]. While some resident cDC1s also reside within these lymphatic sinus regions, most cDC1s are found more evenly distributed throughout the T cell zone and in close association with LN blood vessels[14,18]. Although this reduces their efficiency in sampling of lymph-borne antigens[15,17], more centralized positioning may enhance information exchange with other migratory cDC subsets which localize there, and allow the interception of potentially infected or dying cells during viral infections and cancer[19-21]. These differences in cDC subset positioning have also been recapitulated in human LNs, thus revealing the conservation of cDC subset patterning across species and suggesting likely functional importance for maintenance of homeostasis or host defense[22].

cDCs residing directly within peripheral tissues also constitutively sample local antigens. In the steady state, tonic signaling within tissues induces a fraction of these cells to undergo homeostatic maturation[23-26], and this induces their migration via the lymphatics into the nearest LNs in a CCR7-dependent manner[6,27-29]. Within LNs, different migratory cDC subsets segregate into distinct spatial compartments, and this is observed both at steady state and during inflammation. Specifically for cutaneous LNs, migratory cDC1s and Langerhans cells (ontogenically closely related to macrophages) preferentially migrate into the deep T cell zone, while migratory cDC2s generally localize to the interfollicular regions and outer LN paracortex as discussed above[10,14,18,30,31]. Further segregation of migratory cDC2 subpopulations is seen based on CD301b and SIPRα marker expression. We and other groups have found that $CD301b^{+}$ cDC2s are primarily found at the upper paracortex bordering the B cell follicles, while $SIRP\alpha^{neg}CD301b^{neg}$ migratory cDC2s (also described as "triple negative" cDC2s) predominantly accumulate in the lower cortical ridge bordering the medulla[18,32-34].

At steady state, lymph supplies a large repertoire of tissue-derived self-antigens, including byproducts from apoptotic cells and catabolized extracellular matrix components[4,7]. The dominant role of these steady state cDC populations in LNs is to present captured peripheral self-antigens on MHC molecules to T cells in a non-immunogenic fashion. This is essential for inducing peripheral tolerance to potential self-reactive T cells, which may have escaped central thymic selection and entered the circulation[23,25,26,35]. While cDCs are essential for this process, they can also aberrantly activate self-reactive T cells[36,37]. In these instances, local regulatory T cells help maintain immune quiescence by forming discrete clusters around the autoreactive cells and quickly constraining self-reactive responses[36-40].

1.3 GENERATION OF IMMUNE RESPONSES DURING TYPE-II INFLAMMATION

In contrast to steady state conditions, inflammation of peripheral tissues induces large-scale activation of immune cells both within the affected tissues and the draining LNs to support critical immunological functions. Type-II inflammation is generated in response to exposure to allergens, helminth parasites, venoms, and other irritants which results in innate lymphoid cell type 2 (ILC2) activation and cytokine production, IgE class switching, mucus production, eosinophilia, and smooth muscle contraction. These responses are evolutionarily designed to protect against parasitic helminth infections, but when aberrantly activated, drive allergic disease. Within minutes of exposure to a type-II inducing stimulus, inflammatory mediators and alarmins are released into the tissue parenchyma from barrier surfaces like the skin, lung, and gut to initiate the first line of defense (Figure 1.2). Concurrently, within 24-48 hours of exposure, migratory cDCs residing directly within inflamed tissues also integrate pathogen-derived signals and inflammatory cues, undergo maturation, and traffic to the draining LNs in a CCR7-dependent manner to facilitate the generation of type-II immunity[24,29,41]. The initiation of inflammatory responses at the tissue level and within draining lymph nodes is directed by the release of the canonical type-II cytokines interleukin (IL-)4, IL-5, and IL-13 which are released from activated ILC2s and CD4 T helper 2 (Th2) cells. Th2 cells respond to these environmental cues within tissues and are important drivers of immune responses via the release of cytokines that recruit eosinophils and basophils, drive smooth muscle contraction and mucus production, and induce IgE class switching. Thus, Th2 cells orchestrate many of the downstream effector functions of type-II immune responses, yet how they are generated in lymphoid tissue remains to be fully understood.

We now show the initial generation of Th2 cells requires the promotion of critical innate–adaptive immune cell crosstalk and the formation of specialized microenvironments within LNs to support

Th2 responses. In these settings, peripheral tissue-derived migratory cDC2s, and in particular the IRF4/Klf4-dependent and CD301b$^+$ subsets, appear to play a dominant role in Th2 induction[33,42-47]. Exposure to inflammatory stimuli and alarmins following barrier tissue damage from proteases or helminths leads to a specific program of maturation in local dermal cDC2s, and their migration via the lymphatics to the LN subcapsular sinus[32]. Here, additional CCL8 secretion by activated subcapsular sinus macrophages can synergize with CCR7 chemotactic signaling to promote CD301b$^+$ cDC2 entry into the LN parenchyma[48]. Once in the LN, these CD301b$^+$ cDC2s appear to predominantly localize at the T-B border[33,48]. Given that these spatial patterns are also observed in steady state LNs[18,33], this indicates that such localization is largely intrinsic to the cDC subsets, rather than elicited by the specific inflammatory conditions. In concurrence with migratory cDC2 localization, Th2 cells also appear to accumulate along the T-B border during early differentiation [49-51], suggesting that cellular crosstalk between cDC2s and CD4 T cells within this LN microenvironment may be necessary for optimal Th2 generation. Indeed, in addition to Ebi2, preferential expression of CXCR5 by migratory cDC2s has been in part attributed to their enrichment along the T-B boundary, and this positioning was found critical for induction of Th2 responses during nematode intestinal infection[49,52].

Although migratory cDC2 are required for optimal Th2 differentiation, specific signals provided by these cells to induce Th2 differentiation remain enigmatic[41,47]. Expression of OX40L and Notch ligands on cDCs have been shown important, but whether these molecules selectively promote Th2 responses or more broadly enhance the generation of multiple CD4 T cell helper subsets remains to be demonstrated[53-56]. IL-4 cytokine signaling has been long known to drive expression of the Th2 lineage defining transcription factor, Gata3, and promote differentiation *in vitro*[56].

While the *in vivo* role of IL-4 in Th2 programming and localization has been less clear due to the confounding contributions of IL-4-producing T follicular helper (Tfh) cells[57,58], a more recent study has clarified that IL-4 is indeed critical for generating early Th2 responses *in vivo*[59]. Nevertheless, the very early cellular source of IL-4 to initiate the Th2 differentiation cascade in the LN has not been definitively established, and migratory cDC2s do not appear to express this cytokine. Instead, basophil recruitment to reactive LNs or local NKT cell activation within the interfollicular regions have been proposed as the cellular source/s of IL-4, albeit the precise roles of these innate cells in Th2 differentiation have come under scrutiny[60-64]. cDC-derived IL-10 signals can also elicit Gata3 expression and Th2 responses, indicating that multiple cytokines may mediate this process[65]. Given that several cell types can express IL-10 during inflammation, additional studies to explore the precise role of cDC-derived IL-10 in Th2 priming are necessary. Thus, a combination of multiple stimuli provided by migratory cDC2s, and possibly other cells, as well as the complete absence of Th1 polarizing stimuli, within the peri-follicular microenvironments in LNs mediate the generation of Th2 responses.

It is important to highlight that in addition to Th2 differentiation, migratory cDC2s can also participate in the generation of multiple additional CD4 T helper cell subsets (Th1, Th17 and Tfh), based on the specific nature of encountered agonist[46,66]. This indicates that migratory cDC2s are relatively plastic and can drive divergent T cell helper subtypes though distinct inducible transcriptional programs imparted on them by the signals encountered within the peripheral tissues, rather by their intrinsic propensities to promote one or another form of immunity. In particular, migratory cDC2s have been closely linked with the generation of Tfh responses[47,67-69]. During infection, antigen-bearing migratory cDC2s accumulate at the T-B border[33,49,68], and express the

high affinity IL-2 receptor alpha chain (CD25). This helps augment Tfh differentiation by quenching T cell-derived IL-2 signals, which would otherwise restrict BCL6 expression in responding lymphocytes[67]. Similarly, during intestinal nematode infection, localization of cDC2s near B cell follicles via CXCR5 chemotactic signaling is critical for the induction of both Th2 and Tfh responses[49]. This suggests that the close spatial juxtaposition of migratory cDC2-driven T cell responses with nearby B cell follicles may promote downstream interactions between activated T and cognate B cells and thus elicit Tfh programming[70]. In addition, during certain viral infections, early exposure to IFN-I leads to IL-6 production by migratory cDC2s, and this can help promote Tfh polarization[69]. Surprisingly, while most experimental models have demonstrated the combined loss of Th2 and Tfh responses after broader blockade of cDC2 migration using conditional IRF4 deficiency models[43,68], selective depletion of CD301b$^+$ cDC2s resulted in enhanced generation of Tfh responses[71] suggesting the potential for reciprocal cross-regulation of T cell differentiation by the different migratory cDC2 subsets. Together these data support the model that migratory cDC2s are potent sensors and integrators of information within peripheral tissues and promote the generation of multiple variations of adaptive responses but are critical for the induction of Th2 cells[46].

1.4 THE SIGNAL STRENGTH MODEL: NEW PARADIGMS IN TH2 DIFFERENTIATION

In addition to the signals provided by migratory cDC2s to induce T cell polarization, a new paradigm of Th1 vs Th2 differentiation has recently emerged, collectively resulting in the quantitative and qualitative models which are somewhat divergent from how other T helper cell lineages are thought to be generated[72,73]. The quantitative model posits that the signal strength sensed during initial T cell activation is a major factor regulating T helper cell polarization. Th2

differentiation has been suggested to involve decreased T cell receptor (TCR) signaling, either through reduced TCR affinity, lower levels of peptide MHC (pMHC) complexes presented by antigen-presenting cells (APCs), or through limited sensing of costimulatory molecules[72-74]. Reduced signaling is thought to decrease the longevity of T cell – DC interactions, thus minimizing the ability of T cells to respond to inflammatory cytokines from DCs and ultimately promoting an endogenous program of Th2 polarization[72,75,76]. Confounding this model however is the notion that generally all *in vivo* responses involve polyclonal T cell populations with diverse TCR affinities, yet Th2 cells are not generated in all inflammatory contexts. Additionally, enhanced exposure to costimulatory molecules has been positively and not negatively associated with Th2 differentiation[77-82]. It is also not clear how low-grade stimulation elicits large scale *in vivo* Th2 responses as observed during helminth or allergen exposure, especially given that both result in maturation of cDCs and significant costimulatory molecule expression[53,83-85].

In addition to quantitative signal strength -based factors, qualitative sensing of polarizing cytokines such as IL-4 is important for T cell differentiation *in vivo*, yet APCs do not appear to be the cellular source of this cytokine[86]. Notably, recently activated T cells can produce IL-4 after TCR stimulation independently of the Th2 lineage-defining transcription factor, Gata3, and it has been suggested that paracrine delivery of IL-4 between activated T cells is sufficient for Th2 differentiation[87-90]. Similarly, T cell derived IL-2, also produced downstream of T cell activation and costimulatory signaling, is necessary for Th2 response formation *in vivo*[90,91], and this cytokine is again delivered via paracrine exchange between activated T cells and not provided by APCs[92,93]. In sum, multiple confounding models have been proposed to describe the signals required for Th2 cell differentiation. Migratory cDC2s clearly play a central role in the induction of Th2 cells,

although whether they provide specific inflammatory cues to induce Th2 cell differentiation or more generalizable T cell activation signals is still unknown. The Th2 cytokines IL-4 and IL-2 are required to drive Th2 differentiation, yet the cellular source/s is unclear and does not appear to be APCs. Finally, the signal strength that a T cells receives during the early stages of priming can direct T cell fates yet how this occurs during large scale polyclonal responses is uncertain. Thus, understanding the cellular interactions early signaling events within discrete microenvironments in draining LNs will be critical for understanding Th2 response formation.

1.5 DIFFERENCES BETWEEN THE INITIATION OF TYPE-I AND TYPE-II RESPONSES

It is clear that divergent programs of T cell immunity (e.g., type-I vs. -II) are driven by the distinct participation and activation states of specific innate immune cell subsets in the reactive LNs. It is therefore critical to consider how such innate responses are elicited in the different inflammatory conditions. In this regard, the mechanisms leading to the induction of type-I vs. -II responses are quite distinct (Figure 1.2). Type-I inflammation is initiated by the recognition of microbial and vaccine-derived PAMPs detected by conserved pattern recognition receptors on both innate and stromal populations[24,41,47,94,95]. This elicits a potent multicellular cascade of inflammatory signaling events, including robust resident cDC activation and monocyte influx into dLNs that together drive adaptive immunity. Inflammatory signaling within both barrier sites and LNs likely contribute to functional adaptive responses, and the relative contribution of these is dictated by pathogen tropism, speed of replication, as well as the amount of cellular damage and local inflammation caused by the infection. In the case of vaccination, the formulation of antigen, type/size/charge of adjuvant, as well as the site of immunization will dictate the relative participation of tissue vs. LN -derived innate responses in driving T cell immunity[96,97].

In contrast to type-I responses, type-II inflammation of cutaneous tissues does not appear to elicit strong LN resident innate responses, as characterized by the absence of resident cDC activation, lack of IFNγ production by innate cells, and minimal monocyte influx and IL-12 expression[16,46,98]. In fact, absence of such stimuli (i.e., IFNγ and IL-12) may be essential for promoting Th2 immunity, as these signals can readily override the program of Th2 differentiation[76,99]. Consistent with this, migratory cDC1s, which constitutively secrete IL-12 within LNs, can inhibit Th2 responses, while genetic ablation of cDC1s can enhance Th2 immunity and promote control of nematode infection of the intestine[100], or increase house dust mite induced airway inflammation[101].

Instead, type-II responses are thought to be initiated by the recognition of "patterns of pathogenesis" in the form of allergens, venoms, adjuvants, cell death, tissue stress and destruction, and the release of non-specific alarm signals from barrier tissues, that together act on several tissue-localized immune cell types[102]. Protease activity is likely one major upstream trigger of type-II immunity, and most clinically relevant allergens have protease activity which can cause local activation and release of alarmins from the epithelial cells, as well as cleave epithelial tight junctions in affected barrier surfaces[103-106]. Helminth parasites, which drive potent type-II responses, also employ proteases for migration through host tissues[107,108], thereby causing widespread tissue damage. Other forms of cell death, such as migration-induced cell shattering of mononuclear phagocytes, have also been recently associated with Th2 differentiation[109]. Thus, the initiation of adaptive immunity during type-II settings is likely to be critically dependent on innate cell sensing of local signals induced by tissue damage directly within the inflamed site as opposed to TLR-mediated sensing by cells within draining LNs.

Several immune cell populations reside in the skin, which together form complex cellular networks that function to maintain barrier integrity as well as promote immune responses. cDCs within these networks physically interact with and integrate signals from multiple distinct cell types before migrating into the nearest LN to instruct T cell responses[41,110,111] (Figure 1.2). With regards to Th2 generation, barrier tissue damage elicits the release of specific inflammatory mediators (i.e., IL-33, IL-18, IL-25, and TSLP), and these signals can act directly or indirectly on locally pre-positioned cDC2s, as well as several other nearby cell types, to induce their activation[56,103,112]. In particular, TSLP released by damaged epithelial cells activates cDCs within the skin, and this can drive the upregulation of OX40L and other costimulatory molecules on cDCs, as well as promote their accumulation within draining LNs for induction of certain Th2 responses[34,54,113,114]. Similarly, IL-33 can also lead to the maturation and upregulation of co-stimulatory molecules in cDCs, suppress IL-12 expression, as well as mediate their migration to LNs[83,115-117].

In addition, other responding immune cell types also potentiate indirect cDC2 activation in the skin. Mast cells have been shown to directly interact with cDCs within the dermis[118], and can release inflammatory mediators to induce the maturation and migration of neighboring cDCs to the skin-draining LNs[111,118-120]. Activated ILC2s can further amplify cDC responses through the production of the type-II cytokine, IL-13[121,122]. In many tissues, including the skin, ILC2s predominantly reside within the adventitial cuffs, sites highly enriched with small blood vessels, lymphatics, peripheral nerves, as well as other key components of immunity[123,124]. Notably, $CD301b^{+}$ cDC2s can colocalize with ILC2s within these niches[123], suggesting that crosstalk between these two cell types may preferentially take place within this unique tissue

microenvironment. More recently, a role for neuronal signaling has also been demonstrated in type-II responses. Within the dermis, CD301b$^+$ cDC2s can be found closely associated with the sensory neurons. TRPV1$^+$ sensory neurons in particular can respond to allergens, and upon activation, locally release the neuropeptide Substance P to promote CD301b$^+$ cDC2 migration into draining LNs and subsequent generation of Th2 responses[125]. Finally, an additional role for IFN-I signaling in cDC2-mediated type-II immunity has also been noted[32,126].

Thus, in contrast to anti-microbial type-I responses which are characterized by broad-scale induction of innate cell activation through conserved microbial pattern recognition receptors and cytokine signaling in both peripheral tissues and draining LNs, type-II responses appear highly dependent on the activation of multiple cell lineages within peripheral tissues in response to local tissue damage. Combined action of these cells appears to impart a unique differentiation trajectory for the locally distributed dermal cDC2 cells, which in turn migrate to draining LNs to elicit the corresponding Th2 responses. Together, this indicates that the induction of type-I vs. -II signatures of adaptive immunity are initiated as evolutionarily conserved mechanisms allowing either protection against microbial pathogenesis vs. wound repair and healing of tissue damage, respectively[104].

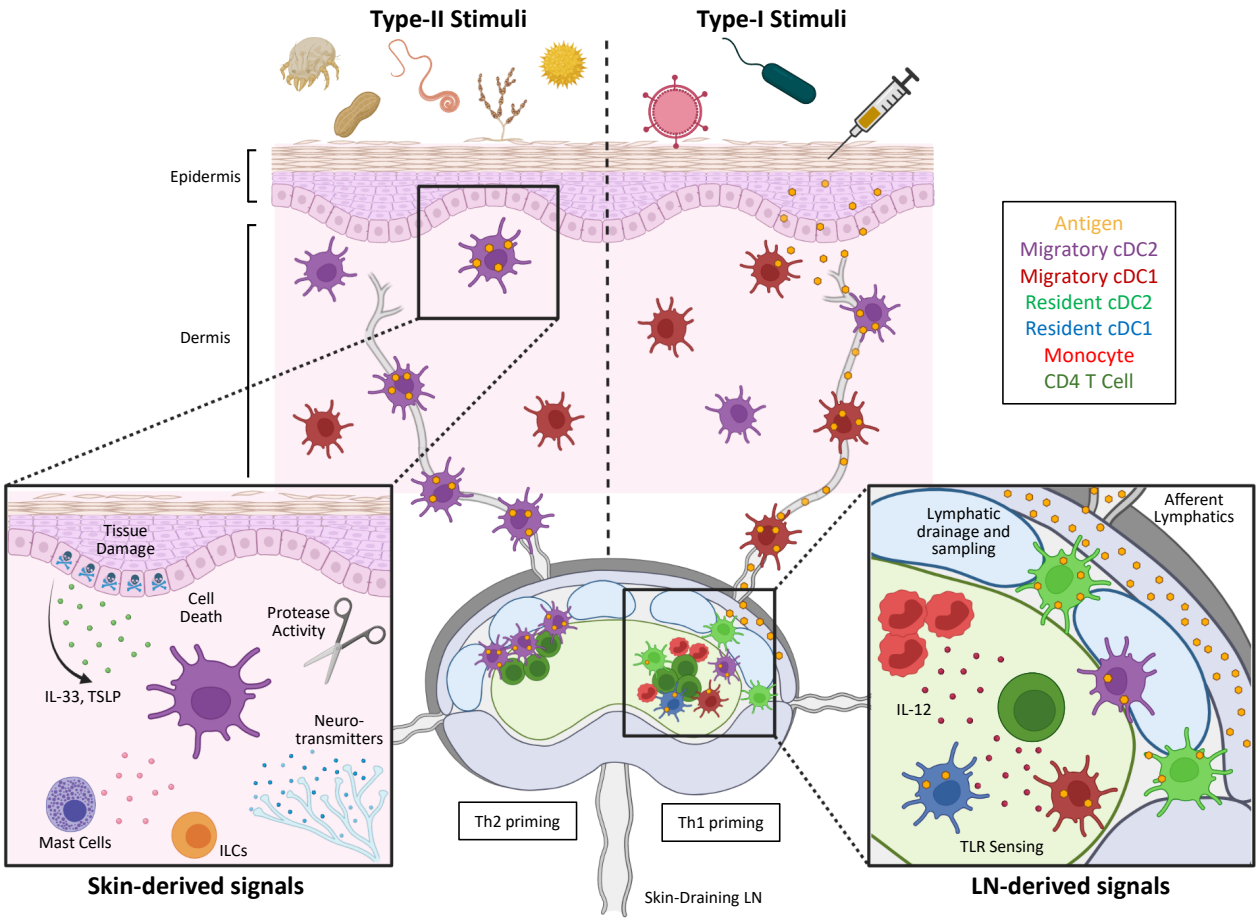

Figure 1.2. Distinct immunological programs involved in the initiation of type-I vs type-II immunity.

Type-II responses (left) are elicited in response to multiple skin-derived stimuli generated due to tissue damage and cell death. Various epithelial-derived alarmins, as well as mast cell-, neuronal-, and ILC-derived signals are integrated by the local dermal cDC2s, which next migrate into LNs to induce Th2 cell differentiation at the T-B border. In contrast, Type-I inflammatory settings (right) are elicited in response to innate sensing of microbe-associated molecular patterns and downstream inflammatory cytokines. In settings of ample antigen and agonist drainage to LNs, T cell responses are primarily induced through cooperation between LN-resident cDCs and blood-derived monocytes, as well as through participation of additional innate cell types (also see Figure 1.1). During highly tropic infections, peripheral tissue-derived dermal cDC1 and cDC2s more dominantly promote the generation of responses. Location of early activated Th1 and Th2 T cells depends on the positioning of specific antigen-presenting cDC subsets, as well as the chemokine receptors expressed on the responding cells.

1.6 THE TH2 PARADOX

Although much work has gone into understanding the specific signals and cell types that initiate type-II immunity, Th2 cell differentiation presents an immunological paradox due to the vast array of upstream triggers that appear to have very few shared biological or chemical properties. In contrast to type-I responses discussed above which are initiated by highly conserved microbial features that are detected by equally conserved pattern recognition receptors on DCs and innate cells, Th2 responses can be induced by parasites, allergens, enzymes, heavy metals, antibiotics, chemicals, irritants and a variety of other compounds[86]. One emerging notion discussed above is that the commonality in these disparate upstream triggers is the overall damage and pattern of pathogenesis they can impart on the host organism. That is, most type-II inducing compounds have noxious activity and trigger tissue perturbations and damage typically caused by protease activity[86,102,104]. Therefore, the modes of initiation of type-II responses could differ based on the tissue or stimulus experienced but converges on the local instruction of DCs within tissues based on the release of known inflammatory alarmins such as IL-33 and TSLP. Unlike type-I responses, direct sensing of immunogenic activity by DCs is not required to initiate type-II responses and only occurs in some models[86]. Thus, although the subset/s of DC and the cytokines involved in driving type-II immune responses are known, the modalities of type-II initiation remain enigmatic. In sum, it is clear that the paradigms developed to study Th1 cell differentiation are not widely applicable to all T helper cell subsets and the exact mechanisms initiating Th2 cell differentiation remain unknown.

Chapter 2. GENERATION OF TH2 MICROENVIRONMENTS IN SKIN DRAINING LYMPH NODES

2.1 INTRODUCTION

This and all following chapters are adapted from the following publication:

Lyons-Cohen M.R., Shamskhou E.A., Gerner M.Y. (2023). Prolonged T cell – DC macro-clustering within lymph node microenvironments initiates Th2 cell differentiation in a site-specific manner. bioRxiv 2023.07.07.547554; doi: https://doi.org/10.1101/2023.07.07.547554

Within draining LNs, multiple innate and adaptive subsets must meet to generate protective immune responses. As APCs mature they increase surface expression of MHC and costimulatory molecules, thus facilitating enhanced antigen presentation and subsequent scanning by and activation of cognate T cells[16]. Optimal Th2 differentiation involves both selective engagement with appropriately activated cDC2 at the T-B border and avoidance of cDC1 populations within the deeper T cell zone[76,100,101]. How such selectivity is achieved *in vivo* is unknown, although recent quantitative imaging studies demonstrated that different cDC subsets are non-equivalently spatially distributed within LNs, which could allow for preferential engagement vs. avoidance of specific DC subsets by responding T cells in distinct tissue compartments[15]. Indeed, during type-I inflammation, the spatial positioning of specific innate subsets, including monocytes and activated cDCs, establishes the formation of dedicated microenvironments in the deep T cell zone to generate effector Th1 and CD8 T cell responses[16,127]. In contrast, CD301b$^+$ and Sirpα-expressing cDC2s localize at the T-B border where early Th2 cells are also found[18,33,49,51]. This suggests an underexplored spatial component of Th2 differentiation in which LN microenvironments populated by appropriately instructed myeloid subsets drive T cell differentiation towards distinct

helper lineages. We investigated the early localization of Th2 cells and identified the formation of dedicated Th2 microenvironments within skin draining LNs after exposure to the allergen papain, a cysteine protease and a clinically relevant allergen that drives robust induction of type-II immunity after cutaneous administration, as well as other Th2 inducing stimuli[33]. We identified the populations of migratory dermal DCs most closely associated with Th2 microenvironments and contrasted these findings with early T cell localization after exposure to the Th1 promoting TLR agonist, CpG, finding distinct spatial positioning of different T helper cell subsets and unique associations with myeloid cells. Furthermore, we surprisingly observed major differences in Th2 response formation within distinct skin draining LNs after exposure to the same stimulus, which was not recapitulated in Th1 settings. Within the skin itself we observed differences in CD301b$^+$ DC maturation and rounding as well as dendritic epidermal T cell (DETC) coverage suggesting potential differences in immune cell composition within distinct skin regions. Thus, we identified unique Th2 promoting microenvironments within some skin-draining LNs composed of highly activated Th2 cells surrounded by CD301b$^+$ dermal DCs which were not present in Th1 conditions. In addition, we established that cutaneous skin sites have differential abilities to drive Th2 responses.

2.2 RESULTS

To examine the early processes governing *in situ* Th2 differentiation, we crossed Ovalbumin (OVA)-specific TCR-transgenic OT-II mice to IL-4 mRNA reporters[128] to generate 4get-GFP OT-II mice (4get-GFP.OT-II) on a CD45.2 congenic background. We then adoptively transferred naïve 4get-GFP.OT-II CD4 T cells into CD45.1$^+$ recipient B6 mice, administered papain plus OVA intradermally in the ear pinnae one day later, and examined the localization and phenotype of

activated OT-II cells in auricular (Au) draining LNs 2-3 days after immunization using quantitative multiparameter microscopy. CD62L blocking antibody was also administered 6 hours after immunization to minimize the impact of asynchronous activation of naïve T cells recruited into LNs late into the response[129]. We observed formation of extensive macro-clusters of OT-II cells located primarily at the T-B border of draining LNs (Figure 2.1A), and the clustered cells expressed high levels of IRF4 and Ki67, indicative of T cell activation and proliferation (Figure 2.1A, 2.1B region 1 inset). Cells within the clusters also expressed high quantities of the Th2 lineage-defining transcription factor, Gata3, and were positive for the 4get-GFP reporter signal, indicating IL-4 mRNA transcription. In contrast, fewer activated OT-II cells outside the macro-clusters expressed Gata3 and 4get-GFP (Figure 2.1A, 2.1B region 2 inset), suggesting that the macro-clusters represented regions where T cells underwent their earliest stages of Th2 lineage commitment detectable with this approach. Large Th2 macro-clusters at the T-B border were also observed when examining endogenous CD4 T cell responses after papain inoculation of 4get-GFP mice, indicating that this macro-clustering phenomenon was occurring during polyclonal endogenous T cell activation, and was not an artifact of high precursor frequency after adoptive transfer (Figure 2.2A, B). We also investigated whether macro-clusters were observed after infection with the parasitic helminth, *Nippostrongylus brasiliensis* (*N.b.*) which drives potent Th2 responses. *N.b.* first transits through the skin to reach the vasculature before establishing an infection in the intestines. Therefore, we investigated the Th2 response in LNs draining different organs which matched the progression of infection through the host. Macro-clusters of IRF4, Gata3 and 4get-GFP-expressing polyclonal Th2 cells were detected in Inguinal (Ing) skin draining LNs 3 days post inoculation and in mesenteric LNs 6 days post infection with *N.b.*, a timepoint when

the parasite establishes robust infection in the intestine and induces Th2 priming[130] (Figure 2.2B, C).

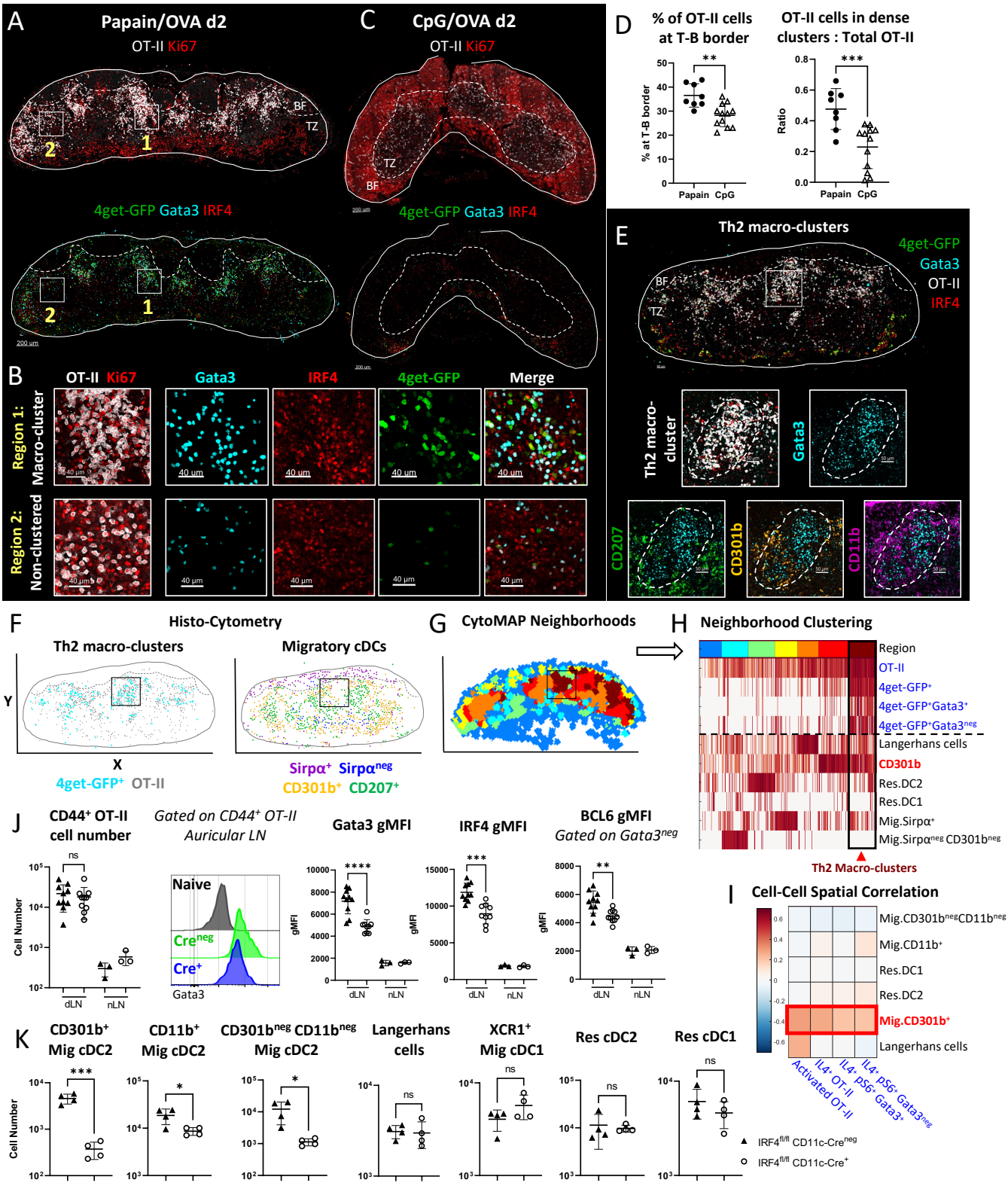

Figure 2.1. Generation of Th2 microenvironments in draining LNs.

A-I) Naïve Ly5.2 4get.OT-II T cells were transferred to Ly5.1 mice and injected with the indicated adjuvants plus OVA in the ear pinnae. Mice were treated intraperitoneally with α-CD62L blocking antibody 6 hours post immunization and dLNs were harvested and assessed by histo-cytometry at 48 hours. A-B) Representative images depicting OT-II macro-clustering at the T-B border in Papain OVA immunized dLNs with B) macro-clustered and non-clustered regions highlighted in insets with the indicated markers shown. C) Representative images depicting OT-II responses in dLNs after CpG OVA immunization. D) Histo-cytometry analyses of OT-II localization with respect to the T-B border and the ratio of macro-clustered vs. total OT-II are shown. E-I) dLN tissue sections were analyzed for association of Th2 cells with myeloid cells. E) Representative image demonstrating Th2 macro-clusters and different myeloid cell markers. F-I) Spatial distribution analysis of myeloid cells and activated ($IRF4^{+}Ki67^{+}$) T cell subsets was performed using CytoMAP. F) Histo-cytometric analysis of the localization of 4get-GFP^{+} OT-II cells and the indicated migratory cDC subsets. G) 50μm raster scan neighborhoods of a representative dLN were plotted on a X,Y positional plot and color-coded using neighborhood clustering. H) Heatmap demonstrating the cellular composition for the different neighborhood clusters (color code depicted at the top as in G). Th2 regions (dark red) enriched with $CD301b^{+}$ DCs are highlighted (arrowhead). I) Cell-cell spatial correlation of the indicated T cell subsets and myeloid cell populations. J-K) Naïve Ly5.1 OT-II T cells were transferred into CD11c-Cre^{+} $IRF4^{fl/fl}$ or CD11c-Cre^{neg} $IRF4^{fl/fl}$ Ly5.2 mice and immunized with papain OVA in the ear pinnae, treated with α-CD62L blocking antibody at 6 hours, and dLNs were harvested and assessed by flow cytometry at 48 hours. J) $CD44^{+}$ OT-II cell number is shown with representative histograms of Gata3 gMFI of $CD44^{+}$ OT-II cells, IRF4 gMFI, and BCL6 gMFI on $Gata3^{neg}$ $CD44^{+}$ OT-II cells. K) Quantification of the indicated myeloid cells subsets in CD11c-Cre^{+} $IRF4^{fl/fl}$ or CD11c-Cre^{neg} $IRF4^{fl/fl}$ mice.

BF = B cell follicles; TZ = T cell zone. Dashed lines represent T-B border. Figures A-I are representative of 5 independent experiments. Figures J-K are representative of 3 independent experiments.

As a comparison, we examined responses after OVA plus CpG immunization, which promotes Th1 differentiation via TLR9 signaling[16]. CpG OVA immunization elicited robust OT-II activation and proliferation indicated by Ki67 expression, but these T cells had undetectable Gata3 and 4get-GFP expression, corresponding to a lack of Th2 differentiation in these settings (Figure 2.1C). Of note, as previously described, CpG also induced large-scale B cell activation and Ki67 expression within the B cell follicles (Figure 2.1C)[131]**.** In contrast to papain induced responses, CpG immunization did not elicit the formation of dense T cell macro-clusters and instead generated much smaller cell clusters that were more diffusely distributed throughout the T cell zone and the

outer LN paracortex, consistent with past findings on behavior of CD4 T cells during Th1 differentiation[16,127] (Figure 2.1C-D).

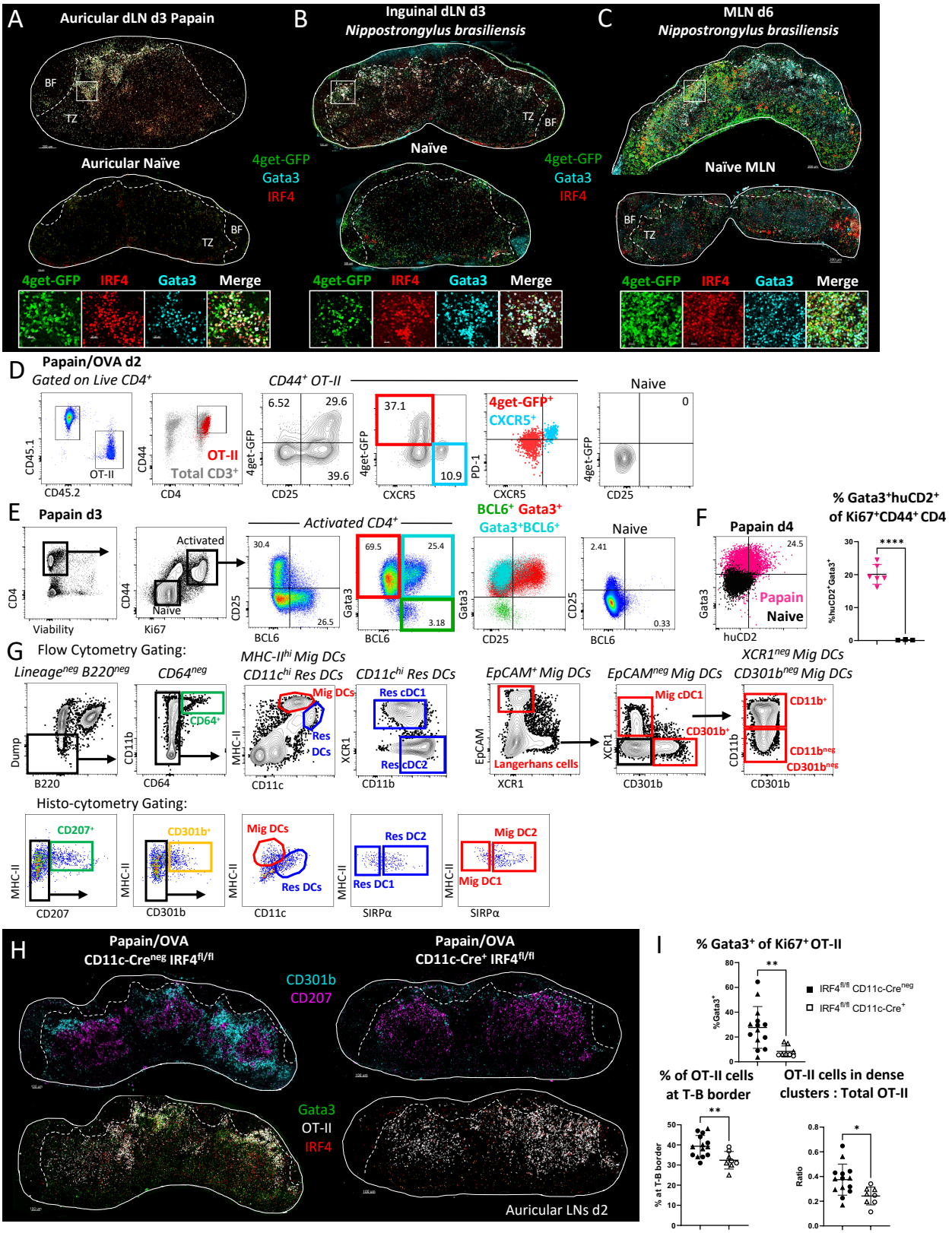

Figure 2.2. Cellular composition of Th2 microenvironments after papain immunization or *N.b.* infection.

A) 4get-GFP mice were immunized in the ear pinnae with papain and auricular dLNs or non-draining naïve LNs were harvested for confocal microscopy 3 days later. Representative images and zoom ins are shown with the indicated markers. B-C) 4get-GFP mice were inoculated subcutaneously at the tail base with 500 *N.b.* L3 larvae and the draining inguinal LNs or mesenteric LN (MLN) or LNs from naïve mice were harvested 3 or 6 days later for confocal microscopy. Representative image and zoom in depicting Th2 macro-clustering in the MLN with the indicated markers is shown. D) Naïve Ly5.2 4get.OT-II T cells were transferred to Ly5.1 mice and injected with papain OVA in the ear pinnae, treated with α-CD62L blocking antibody at 6 hours, and harvested for flow cytometry 48 hours later. Representative gating for T follicular helper (Tfh) and T effector (Teff) OT-II cells is shown with the indicated markers. E) B6 mice were immunized with papain in the ear pinnae and auricular dLNs were harvested 3 days later for flow cytometry. Representative gating for endogenous T cell activation is shown with Gata3, BCL6, and CD25 identifying Tfh and Teff T cells. F) $KN2^{+/-}$ mice were immunized with papain in the ear pinnae and auricular dLNs or naïve lymph nodes (nLN) were harvested 4 days later for flow cytometry. Representative plot and quantification of huCD2 and Gata3 expression is shown. G) Representative myeloid gating schemes for flow cytometry (top) and histo-cytometry (bottom). H-I) Naïve Ly5.1 OT-II T cells were transferred into CD11c-Cre^{+} $IRF4^{fl/fl}$ or CD11c-Cre^{neg} $IRF4^{fl/fl}$ Ly5.2 mice and immunized with papain OVA in the ear pinnae, treated with α-CD62L blocking antibody at 6 hours, and dLNs were harvested and assessed by confocal microscopy at 48 hours. Representative imaging depicting myeloid cell localization and OT-II cell differentiation with the indicated markers are shown. I) Histo-cytometry analysis of Gata3 expression in OT-II cells and OT-II localization with respect to the T-B border and the ratio of macro-clustered vs. total OT-II is shown.

BF = B cell follicles; TZ = T cell zone. Dashed lines represent T-B border. A, C-D are representative of 5 independent experiments. B, E-F are representative of 2-3 independent experiments.

Previous studies visualizing IL-4 producing cells in LNs at late time points have been conflated by detection of IL-4 producing Tfh cells within B cell follicles[57,59], so we examined Tfh markers on the responding 4get-GFP^{+} T cells 2-3 days after papain OVA treatment. We found that most of the 4get-GFP^{+} cells displayed high levels of the high affinity IL-2 receptor, CD25, and low levels of CXCR5 and PD-1 staining (Figure 2.2C), indicating early effector T cell and not Tfh differentiation[132-134]. Similarly, endogenous activated ($CD44^{+}Ki67^{+}$) $Gata3^{+}$ CD4 T cells expressed CD25 and lacked BCL6 expression, while a separate population of $CD25^{neg}$ cells co-expressed Gata3 and BCL6, indicating bifurcation of effector lineages (Figure 2.2D)[135-138]. To

verify that IL-4 mRNA competent 4get-GFP^{+} T cells also produced IL-4 protein, we examined responses in KN2$^{+/-}$ reporter mice which express human CD2 (huCD2) on the surface of T cells actively producing IL-4 protein[139]. We found abundant huCD2 expression on endogenous responding Gata3^{+} CD44^{+}Ki67^{+} CD4 T cells suggesting active IL-4 protein production (Figure 2.2E).

To investigate which specific myeloid cell population/s were associated with the Th2 macro-clusters, we next co-stained sections of papain-immunized auricular draining LNs with various innate cell markers and used histo-cytometry and CytoMAP to analyze myeloid cell composition and distribution[14,18]. Neighborhood clustering analysis identified distinct LN regions populated by different myeloid cell subsets (Figure 2.1E-G; 2.2F). As previously reported, migratory cDC2s, including Sirpα^{+}CD301b^{+} and Sirpα^{+}CD301b^{neg} subsets were predominantly localized in the outer T zone regions, with CD301b^{+} cDC2s localized at the T-B border and in close proximity to the Th2 macro-clusters[33,49,140](Figure 2.1E-F). Of note, we observed relatively limited direct interdigitation of CD301b^{+} cDC2s within the inner regions of the macro-clusters, and they instead appeared to physically surround the border of proliferating Th2 cells. In contrast to CD301b^{+} cells, Sirpα^{+}CD207^{+} Langerhans cells and cDC1s were predominantly distributed within the deeper T cell zone and appeared spatially segregated from the Th2-dense regions (Figure 2.1E-G). Quantitative spatial distribution analysis across multiple LNs using CytoMAP confirmed these observations, demonstrating that CD301b^{+} cDC2s were the dominant myeloid cell subset enriched in Th2 macro-cluster containing tissue neighborhoods, and that CD301b^{+} cDC2s and Th2 cells had a strong positive spatial correlation with one another (Figure 2.1G-I). Together these data

demonstrate the formation of Th2 microenvironments in draining LNs can be defined by macro-clustering of early differentiating Th2 cells and surrounded by CD301b^{+} migratory cDC2s.

cDC2s have been previously demonstrated to drive Th2 polarization, but not T cell proliferation, after papain immunization[33,141,142]. To examine the requirement of migratory cDC2s for Th2 responses in our model, we examined OT-II cell responses in IRF4$^{fl/fl}$ CD11c-Cre^{+} mice which exhibit impaired cDC2 migration from peripheral tissues into LNs, while keeping other cDC populations intact[42,43] (Figure 2.1K). Indeed, as compared to Cre^{neg} littermate controls, loss of migratory cDC2 in IRF4$^{fl/fl}$ CD11c-Cre^{+} animals significantly reduced Gata3 and IRF4 expression in the responding OT-II cells without altering their clonal expansion, suggesting abrogated Th2 differentiation but not priming[142] (Figure 2.1J). Moreover, T cell macro-clustering at the T-B border was also significantly disrupted in Cre^{+} mice as compared to Cre^{neg} littermate controls, and the OT-II cells displayed reduced Gata3 and pS6 expression, reduced cluster density, and limited localization at the T-B border (Figure 2.2G-H). In addition to Th2 responses, cDC2s have also been reported to promote Tfh differentiation[47,67,68], and we indeed noted reduced BCL6 expression in responding CD44^{+} Gata3^{neg} OT-II cells in IRF4$^{fl/fl}$ CD11c-Cre^{+} mice (Figure 2.1J), suggesting that migratory cDC2s mediate the initiation of both Th2 and Tfh immunity. Altogether, these data indicate that cutaneous papain administration into the ear pinnae induces the formation of Th2-promoting microenvironments at the T-B border composed of macro-clusters of highly activated, early differentiating Th2 cells and migratory cDC2s, and that this clustering behavior is also distinct from that observed during Th1 differentiation after TLR agonist immunization.

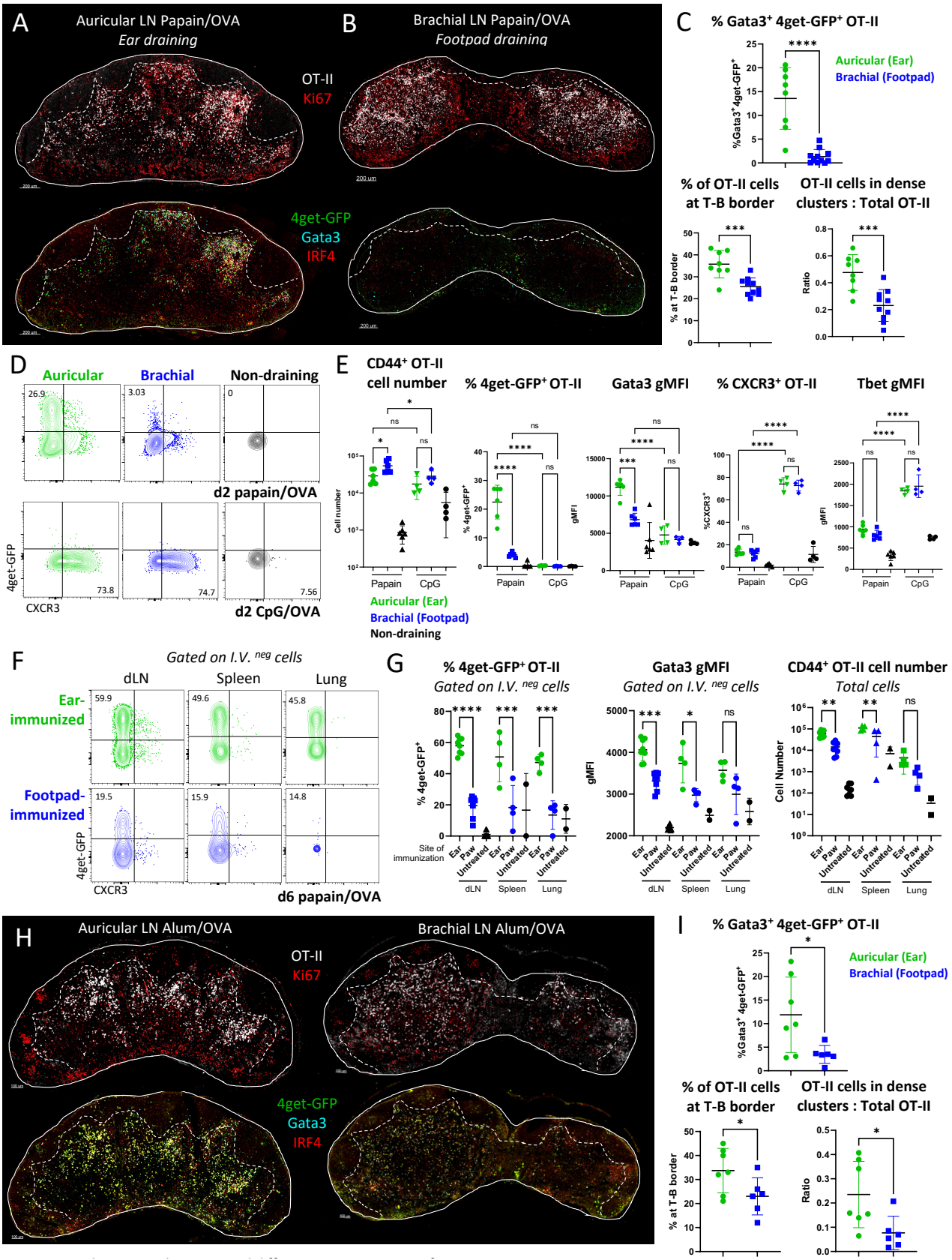

Figure 2.3. Th2 macro-clustering and differentiation is site-specific.

A-E) Naïve Ly5.2 4get.OT-II cells were transferred to Ly5.1 mice and injected with the indicated adjuvant plus OVA in the ear pinnae or front footpad, treated intraperitoneally with α-CD62L 6 hours post immunization, and dLNs were harvested and assessed by histo-cytometry and flow cytometry at 48 hours. Representative images depicting OT-II macro-clustering and expression of the indicated markers in A) auricular vs B) brachial dLNs. C) Histo-cytometry analysis of the percent activated OT-II co-expressing 4get-GFP and Gata3, OT-II localization, and the ratio of macro-clustered vs. total OT-II in the indicated LNs. D-E) Representative plots and quantification of $CD44^+$ OT-II cell number, frequency of 4get-GFP^+ and $CXCR3^+$ cells, and Gata3 and Tbet gMFI of $CD44^+$ OT-II cells. F-G) $0.5x10^6$ naïve Ly5.2 4get.OT-II cells were transferred to Ly5.1 mice then injected with papain OVA in the ear pinnae or front footpad. 6 days later, cells were labeled intravenously, and dLNs, spleen, and lung were harvested and assessed by flow cytometry. Representative plots and quantification of frequency of 4get-GFP^+ and Gata3 gMFI of $I.V.^{neg}$ $CD44^+$ OT-II cells and total $CD44^+$ OT-II cell number are shown. H-I) Naïve Ly5.2 4get.OT-II cells were transferred to Ly5.1 mice and injected with the Alum plus OVA in the ear pinnae or front footpad, treated intraperitoneally with α-CD62L 6 hours post immunization, and dLNs were harvested and assessed by histo-cytometry at 48 hours. H) Representative images depicting OT-II macro-clustering and expression of the indicated markers and I) histo-cytometry analysis of the percent activated OT-II co-expressing 4get-GFP and Gata3, OT-II localization, and the ratio of macro-clustered vs. total OT-II in the indicated LNs.

Au = auricular; Br = brachial; IV = intravenous. Dashed lines represent T-B border. A-E are representative of 5 independent experiments. F-G are representative of 2 independent experiments.

Cutaneous exposure to allergens and associated antigens can occur in distinct anatomical locations. Surprisingly, when administering papain OVA into distinct skin sites, we observed major differences in Th2 response induction within the corresponding skin draining LNs. As above, auricular LNs draining ear pinnae generated extensive early Th2 macro-clustering at the T-B border (Figure 2.3A). In contrast, the equivalent dose of papain and antigen administered in the footpad led to minimal Th2 differentiation in the draining brachial (Br) LNs (Figure 2.3B-C). Instead of macro-clustering at the T-B border, most OT-II T cells in brachial LNs were more homogenously distributed and localized in smaller clusters throughout the T cell zone and expressed significantly less Gata3 and 4get-GFP as detected by histo- and flow cytometry (Figure 2.3A-E). Decreased Th2 response formation was not due to general lack of T cell activation, as

following footpad immunization brachial LN OT-II T cells expressed abundant Ki67 and underwent equivalent or even greater levels of early proliferation as compared to those in auricular draining LNs (Figure 2.3B, E).

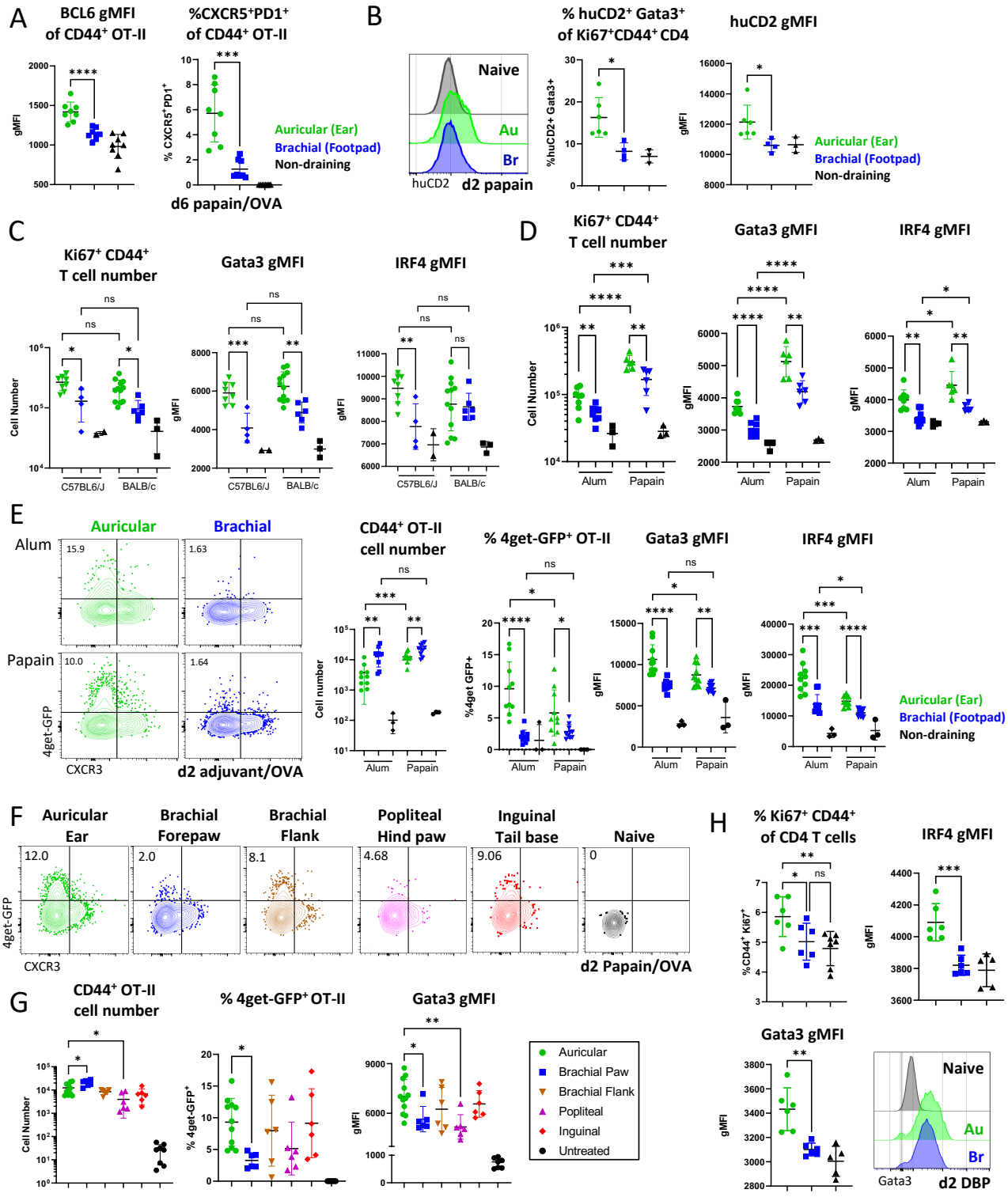

Figure 2.4. Site-specific Th2 responses are maintained across mouse strains and adjuvants.

A) 0.5x10^6 naïve Ly5.2 4get.OT-II cells were transferred to Ly5.1 mice and injected with papain OVA in the ear pinnae or front footpad and dLNs, were harvested and assessed by flow cytometry

6 days later. BCL6 gMFI of $CD44^+$ OT-II cells and frequency of $CXCR5^+PD\text{-}1^+$ $CD44^+$ OT-II cells are shown. B) $KN2^{+/-}$ mice were immunized with papain in the ear pinnae or front footpad and dLNs were assessed by flow cytometry 2 days later. Representative plot and frequency of $KN2^+Gata3^+$ and KN2 gMFI of $CD44^+Ki67^+$ CD4 cells are shown. C) B6 or Balb/c mice were immunized in the ear pinnae and front footpad with papain and dLNs were harvested at day 3 for flow cytometry. Activated $CD44^+Ki67^+$ T cell number, and Gata3 and IRF4 gMFI of $CD44^+Ki67^+$ T cells are shown. D) B6 mice were immunized in the ear pinnae and front footpad with papain or Alum OVA and dLNs were harvested at day 3 for flow cytometry. Activated $CD44^+Ki67^+$ T cell number, and Gata3 and IRF4 gMFI of $CD44^+Ki67^+$ T cells are shown. E) Naïve Ly5.2 4get.OT-II cells were transferred to Ly5.1 mice, injected with papain OVA or Alum OVA in the ear pinnae or front footpad, treated intraperitoneally with α-CD62L 6 hours post immunization and dLNs were harvested and assessed by flow cytometry at 48 hours. Representative plots, $CD44^+$ OT-II cell number, expression of 4get-GFP of $CD44^+$ OT-II cells, and Gata3 and IRF4 gMFI of $CD44^+$ OT-II cells are shown. F-G) Naïve Ly5.2 4get.OT-II cells were transferred to Ly5.1 mice, and injected with papain OVA in the ear pinnae, front footpad, hind footpad, dorsal flank skin, or tail base. Mice were treated intraperitoneally with α-CD62L 6 hours post immunization and dLNs were harvested and assessed by flow cytometry at 48 hours. Representative plots, $CD44^+$ OT-II cell number, frequency of 4get-GFP^+ cells and Gata3 gMFI of $CD44^+$ OT-II cells are shown. H) DBP was topically applied (painted) onto the ear or front footpad skin of mice. dLNs were harvested for flow cytometry 48 hours later. Activated $CD44^+Ki67^+$ T cell number, and Gata3 and IRF4 gMFI of $CD44^+Ki67^+$ T cells are shown. A-G are representative of 2-3 independent experiments. H is representative of 4 independent experiments.

Site-specific differences between the ear and footpad were maintained for at least 6 days and across peripheral organs, with significantly reduced frequencies of effector Th2 OT-II cells also found in the parenchyma of the lung and spleen, suggesting that divergent T cell responses were maintained even after OT-II cells migrated out of the original site of priming (Figure 2.3F-G). Despite the similar initial clonal bursts, by day 6, OT-II cells primed in auricular draining LNs exhibited increased expansion as compared to those primed in brachial draining LNs and greater numbers of OT-II cells disseminated to the spleen and lungs (Figure 2.3G). At these later time points, the auricular draining LNs also exhibited increased frequency of $CXCR5^+PD\text{-}1^+$ Tfh OT-II cells, and the cells also expressed a greater amount BCL6, suggesting that both Th2 and Tfh responses were linked to the specific skin site of immunization (Figure 2.4A). Site-specific Th2 differences were also observed for endogenous CD4 T cells in $KN2^{+/-}$ reporter mice, with a significant reduction of

IL-4 protein producing Gata3^{+} CD4 T cells in footpad draining brachial LNs (Figure 2.4B). Th2 response differences across immunization sites were also observed in Balb/c mice, indicating that this phenomenon was conserved across mouse strains with differential abilities to drive type-II immunity[143] (Figure 2.4C). We further examined site-specific Th2 response formation after immunization with the non-protease adjuvant, Alum, injected with OVA in endogenous T cell and OT-II settings. We found Alum OVA immunization also elicited robust OT-II macro-clustering at the T-B border in auricular draining LNs, and these responses were reduced as compared to Alum OVA immunization in the brachials as seen by expression of Gata3, 4get-GFP, and IRF4 (Figure 2.3H-I). We also examined Th2 responses after Alum OVA immunization by flow cytometry in polyclonal and OT-II settings and observed similar site-specific Th2 responses, although the overall magnitude of response was dictated by the adjuvant (Figure 2.4D-E). These data suggest that immunization with Alum OVA was able to elicit similar site-specific responses as Papain OVA indicating that Th2 macro-cluster formation can be recapitulated in non-protease mediated immunization settings. Finally, we examined Th1 differentiation settings after CpG OVA immunization in distinct cutaneous tissues. In stark contrast to type-II inflammation settings, CpG OVA resulted in equivalent expansion, Tbet expression, and CXCR3 expression in responding OT-II cells in both auricular and brachial LNs, indicating comparable Th1 response formation between the different sites (Figure 2.3E). Comparable Th1 responses across these distinct LNs were also previously observed with other type-I adjuvants[16].

Non-equivalent Th2 responses in different skin draining LNs may result from intrinsic differences between the LNs, differential lymphatic drainage of antigens and agonists, or fundamental differences in how distinct cutaneous sites program local immune responses. To investigate

whether brachial LNs have an inherent defect in mounting Th2 immunity, we immunized mice with papain OVA in the dorsal skin of the flank, which targets a different skin dermatome but antigen and agonist also drain into brachial LNs. Although generating more heterogeneous responses as compared to footpad inoculation, likely due to more diffuse agonist dispersal across the subcutaneous tissue compartment, flank injection resulted in Th2 induction in brachial LNs, which was more analogous to that found in auricular LNs with ear immunization (Figure 2.4F-G). We also tested other cutaneous sites, including the hind paw and the tail base which drain the popliteal and inguinal LNs, respectively. Similar to brachial LN responses with forepaw injection, hind paw inoculation also elicited limited Th2 responses in the draining popliteal LNs, with decreased Gata3 expression by activated OT-II cells. In contrast, tail base administration of papain OVA generated heightened Th2 responses within the inguinal draining LNs (Figure 2.4F-G). We next examined whether site-specific Th2 response differences would be maintained in a model which does not involve abundant lymphatic drainage induced by injection. To test this, we painted the ear vs. footpad skin with dibutyl phthalate (DBP) to induce a model of Th2-driven contact hypersensitivity in which antigen and adjuvant are administered epicutaneously and not intradermally[114]. Although DBP painting did not induce as potent of proliferative responses as papain injection, major differences in Th2 differentiation were still observed across the draining LNs, with markedly increased Gata3 and IRF4 expression in responding CD4 T cells within auricular but not brachial draining LNs (Figure 2.4H).

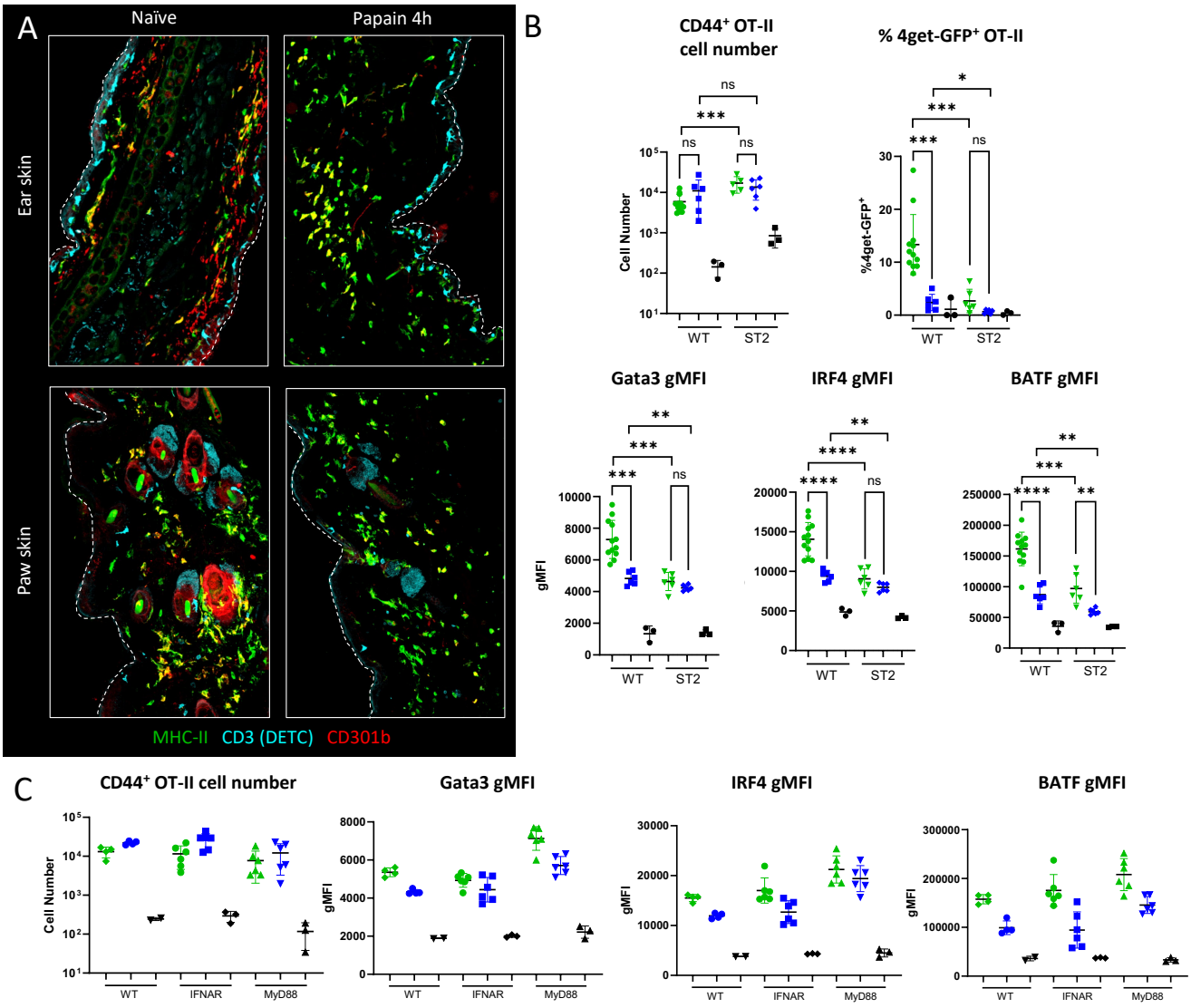

Figure 2.5. Immune cell composition within ear and paw skin.

A) B6 mice were immunized with papain and 4 hours later paw and ear skin or naïve skin was harvested for confocal microscopy. Indicated myeloid cell markers are shown. B) Naïve 4get.OT-II cells were transferred to WT or ST2.KO mice, injected with papain OVA in the ear pinnae or front footpad, treated intraperitoneally with α-CD62L 6 hours post immunization and dLNs were harvested and assessed by flow cytometry at 48 hours. $CD44^+$ OT-II cell number, expression of 4get-GFP of $CD44^+$ OT-II cells, and Gata3, IRF4, and BATF gMFI of $CD44^+$ OT-II cells are shown. C) Naïve Ly5.1 OT-II cells were transferred to WT, IFNAR.KO, or MyD88.KO mice, injected with papain OVA in the ear pinnae or front footpad, treated intraperitoneally with α-CD62L 6 hours post immunization and dLNs were harvested and assessed by flow cytometry at 48 hours. $CD44^+$ OT-II cell number and Gata3, IRF4, and BATF gMFI of $CD44^+$ OT-II cells are shown.

Finally, we tested the hypothesis that these divergent T cell responses were initiated by differences in DC populations within the skin sites themselves. In pilot studies, we imaged naïve ear and paw skin as well as skin 4 hours post papain administration, and found that in both skin types DCs adopted a more rounded phenotype after papain exposure indicative that both sites elicited DC2 activation[144] (Figure 2.5A). However, differences between cutaneous sites were also noted, such as reduced DETC coverage of the outer epidermis in the paw skin in both steady state and after immunization, as well as non-equivalent dispersal of CD301b+ DCs within the dermis prior to papain administration (Figure 2.5A). After immunization, cytokines and alarmins are released from epithelial cells and activate local DCs and other immune populations. To investigate the contribution of various signaling receptors expressed by DCs in the skin that have been implicated in Th2 immunity, we transferred naïve OT-II cells into WT, IFNAR, MyD88, and ST2 KO mice to test the contribution of type-I IFN, TLR4 signaling, and IL-33 respectively[32,61,63,83,85,126]. These data revealed that without affecting OT-II cell expansion, only ST2 mice in which DCs cannot signal through the IL-33 receptor had major defects in Gata3, IRF4, and BATF expression (Figure 2.5B). These data corroborated past findings on the critical role of IL-33 in driving DC activation and Th2 immunity[83,85]. Interestingly and in agreement with previous reports, responding OT-II T cells in MyD88.KO mice displayed increased levels of Gata3, IRF4, and BATF as compared to WT controls, indicating a potential suppressive role of TLR signaling in Th2 differentiation[61] (Figure 2.5C). These data together suggest that while DCs are activated across both skin sites, there are likely fundamental differences in immune cell composition in these tissues, as well as in how dermal DCs are activated by different cytokines after papain administration.

In sum, these findings indicate that distinct cutaneous sites have non-equivalent abilities to drive Th2 macro-clustering and Th2 differentiation, but that these site-specific differences do not necessarily extend to other helper cell lineages, such as Th1 responses. Moreover, non-equivalent responses between sites do not simply result from intrinsic differences between the lymphoid organs or are restricted to injection- or protease-based models, indicating a more generalizable divergence in the ability to drive Th2 responses across distinct skin sites. Differences in immune cell composition or cytokine release within the skin could play a role in site-specific immunity but will require further study.

2.3 DISCUSSION

Here, we used quantitative microscopy to investigate the cellular localization of early differentiating Th2 cells within skin draining LNs. We found that OT-II and endogenous polyclonal T cells were localized within specialized Th2 microenvironments at the T-B border that were surrounded by and closely associated with CD301b$^+$ cDC2s. The formation of these microenvironments, here termed 'macro-clusters,' was found to be a generalizable Th2 phenomenon as we also observed extensive macro-clustering after immunization with Alum OVA and infection with *N.b.* in the skin and gut draining LNs. Wide-spread evidence now exists that migratory cDC2s are required for Th2 differentiation[33,34,42-45]. We similarly find that ablation of cDC2 migration from the skin abrogates Th2, as well as Tfh differentiation in LNs, albeit not necessarily at the cost of reduced early T cell priming[142]. This may be explained by the fact that in settings of ample antigen drainage, lymph node resident cDCs initiate early T cell proliferation, while migratory cDC2s induce downstream Th2 differentiation[15,16,141,142]. Previous studies have noted that neither resident cDCs or migratory cDCs were fully sufficient to induce T cell

proliferation and thus synergy between these populations is likely required to optimize maximal T cell activation and differentiation[142]. A more recent study found a role for LN resident cDCs in inducing Th2 cell development in the lung after exposure to house dust mite[141], but how different DC populations are activated in the lung vs skin remains to be determined. Regardless, we find that mice with impaired migratory cDC2 maturation and migration to the dLN have normal OT-II proliferation, indicating a potential underappreciated role for LN resident cDCs in initiating T cell proliferation in our model.

A key unexpected finding in our work was that not all types of skin generated equivalent Th2 responses in the draining LNs. Our studies primarily focused on the ear vs footpad draining LNs, but additional variation across the skin is likely. A major unanswered question remains as to why different skin sites are non-equivalently activated after exposure to the same agonist and whether this extends to other barrier tissues in mice and humans. Homeostatic tissue signals like IL-13 and IL-18 can impart cDCs and ILC2s with a tissue-specific identity, potentially reflecting intrinsic pre-programming of cDCs and other cells based on skin type residence[121,145,146]. In addition, differences could reflect divergent cDC experiences at the site of immunization with regard to exposure to cytokines or other inflammatory mediators. Many cytokines, including alarmins, are released from epithelial and stromal cells during type-II inflammation and barrier disruption events, and whether these cytokines are equivalently released between skin sites requires further study. We do find a requirement for IL-33 signaling, as OT-II cells transferred into ST2.KO mice displayed reduced Gata3, IRF4, and BATF expression. There could be many additional tissue specific adaptations, such as neuronal composition, mast cell differences, or divergent microbiomes which direct dermal cDC2 maturation and activation[111,118,120,125]. Epidermal barrier thicknesses and other structural differences between skin sites could also contribute[147]. Thus, while

the events that differentially initiate skin-type dependent Th2 response formation are not yet known, we next investigated if differential activation states of migratory cDC2s migrating to draining LNs could account for the observed differences in T cell states between auricular and brachial dLNs.

Chapter 3. COSTIMULATORY MOLECULE EXPRESSION ON MIGRATORY DCS MEDIATES OPTIMAL TH2 DIFFERENTIATION AND SITE-SPECIFIC T CELL RESPONSES

3.1 INTRODUCTION

Not all cDC populations have equivalent capacities to induce Th2 responses. Following barrier tissue damage, locally released alarmins induce the activation of cDC2s, including cells expressing CD301b and variegated levels of Sirpα/CD11b expression[33,53,83]. Activated cDC2s in turn migrate into draining LNs, where they can induce Th2 responses[33,34,42-45,53,83]. cDC2s, however, are also highly plastic and based on the nature of the stimulus can generate diverse helper lineages, including Tfh, Th1, and Th17 cells[32,46,67,68], and the exact molecular mechanisms of how these cells specifically promote Th2 responses during type-II inflammation remain unknown. Given the critical role of cDC2s in driving Th2 differentiation, we next examined the hypothesis that migratory cDC2 responses were non-equivalent for the distinct dermal tissues. RNA sequencing of antigen-bearing migratory cDC2s revealed that differences across the sites were driven by divergent activation states of these cells, with enhanced costimulatory molecule expression by cDC2 in Th2-inducing LNs promoting T cell macro-clustering, cytokine signaling, and Th2 differentiation. We also investigated surface pMHC-II expression, finding that antigen-bearing migratory cDC2s expressed low to undetectable levels, as predicted by the signal strength model. However, this low-grade stimulation was accompanied by high levels of costimulatory molecule expression. Thus, high levels of costimulatory signaling in combination with low TCR signaling appears to promote optimal differentiation of Th2 cells within LN microenvironments.

3.2 RESULTS

We find above that papain OVA immunization across different skin sites leads to non-equivalent generation of Th2 responses. To investigate whether differences across sites were driven by changes in migratory DCs, we immunized mice with papain plus the fluorescent protein EαGFP into the forepaw or ear pinnae[148], and examined the number and phenotype of antigen-bearing migratory DCs in the corresponding draining LNs. Albeit some variation was observed among individual samples, across multiple experiments we found no major differences in the number of total cDC2s, antigen-bearing EαGFP$^+$ cDC2s, or in the amount of EαGFP captured by these cells between the sites (Figure 3.1A-C, 3.2A). The dominant antigen-bearing population in both draining LNs were the CD301b$^+$ cDCs (Figure 3.2B), and their total number did not differ between draining LNs (Figure 3.1C). The overall composition of antigen-bearing cells was also largely similar across the LNs, albeit a modest increase in the frequency of antigen-bearing CD301b$^+$ DCs and CD64$^+$ cells and a corresponding decrease in CD301b^{neg}CD11b^{neg} DCs in brachial LNs was noted (Figure 3.2B).

We also examined the amount of pMHC-II complex presented on the cDC surface using the Y-Ae antibody, which recognizes the Eα peptide presented on I-Ab[148]. Surprisingly, we found that while papain induced robust antigen uptake by migratory cDCs, this was not associated with detectable pMHC-II complex on the cell surface (Figure 3.2C-D). Minor differences in the total number, but not frequency, of EαGFP$^+$ Y-Ae$^+$ migratory DCs were noted between auricular and brachial LNs after papain immunization (Figure 3.2D). In contrast to papain settings, EαGFP plus CpG immunization elicited both antigen uptake and robust surface pMHC-II expression by migratory cDCs (Figure 3.2C-D), demonstrating major differences in how type-I and type-II stimuli impact

MHC-II antigen processing and presentation, and suggesting that during *in vivo* type-II responses to papain, surface pMHC-II expression is relatively limited on migratory DCs. Of note, Eα peptide sequence analysis did not identify papain cleavage sites, indicating that the divergence in pMHC-II complex between papain and CpG conditions was not simply a result of protease mediated degradation of the Eα peptide.

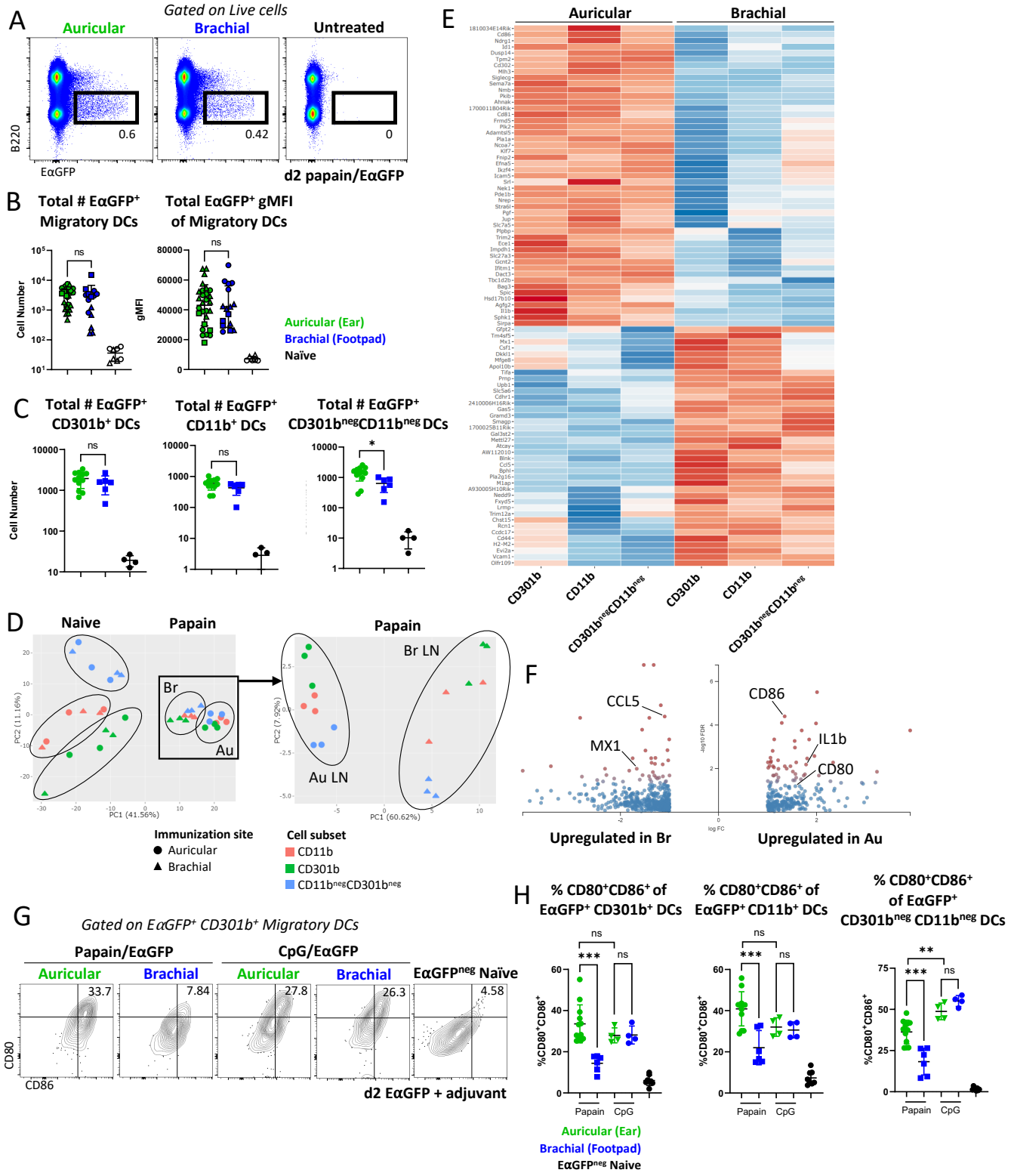

Figure 3.1. Costimulation is enhanced on DCs from auricular LNs.

A-H) B6 mice were immunized in the ear pinnae and front footpad with papain plus EαGFP and the corresponding dLNs were harvested 48 hours later. A) Representative plots showing total EαGFP expression within live cells. B) Quantification of the number of $EαGFP^{+}$ migratory DCs and $EαGFP^{+}$ gMFI of migratory DCs. Symbol shapes represent independent experiments (three total). C) Quantification of total $EαGFP^{+}$ cells for the indicated DC subsets. D-F) $EαGFP^{+}$ DC populations were sorted from dLNs on day 2 for bulk RNA sequencing. DCs were sorted on Live, $CD64^{neg}$, $Lineage^{neg}$ (CD3, CD19, NK1.1), $EαGFP^{+}$, MHC-II^{Hi} $CD11c^{Int}$, $XCR1^{neg}$, $EpCAM^{neg}$, then sorted into $CD11b^{+}$ $CD301b^{+}$, $CD11b^{+}$ $CD301b^{neg}$, and $CD11b^{neg}$ $CD301b^{neg}$ populations. The same gates were used for $EαGFP^{neg}$ DCs in naïve LNs. D) PCA plot of all samples (left) and papain immunized DC populations (right). E) Heatmap of the top 100 DEGs between antigen-bearing migratory DCs from auricular vs. brachial dLNs (FDR<0.05, 2x fold change expression). F) Volcano plot of DEGs between antigen-bearing migratory DCs from auricular and brachial dLNs. Red indicates a FDR<0.05. Genes with a log fold change greater than 2 are shown. G-H) $EαGFP^{+}$ migratory DCs were assessed for surface CD80 and CD86 expression by flow cytometry. G) Representative flow plots for $CD301b^{+}$ cDC2s and H) quantification for three indicated DC subsets are shown.

Au = auricular; Br = brachial. A-C, and G-H are representative of 3 independent experiments. D-F are representative of 1 independent RNA sequencing experiment with n=3 per group.

To further interrogate potential differences among migratory cDCs from different cutaneous sources, we next sorted antigen-bearing ($EαGFP^{+}$) migratory cDC2 subsets ($MHC2^{Hi}CD11c^{Int}$ $CD301b^{+/neg}CD11b^{+/neg}$) from auricular and brachial dLNs two days post papain plus EαGFP immunization, or from naïve mice, and performed bulk RNA sequencing. As expected, principal component analysis (PCA) of all samples demonstrated that the primary segregation was driven by the immunization state, with samples clustering based on whether they were obtained from naïve or papain immunized LNs, revealing large-scale transcriptional changes across all cDC populations from both tissues after papain immunization (Figure 3.1D left, 3.2E-F). Of note, IL-12b, which is constitutively expressed by migratory cDCs at steady state[100,101], was downregulated upon papain immunization (Figure 3.2F). When considering only the papain immunized samples, further PCA separation demonstrated that sample divergence on the PCA1 axis was dominantly driven based on the specific LN of origin, indicating major transcriptional differences between the antigen-bearing auricular-derived and brachial-derived cDCs, while also maintaining a secondary

level grouping along the PCA2 axis based on the cell subset (Figure 3.1D right, 3.2E). Of the top 100 differentially expressed genes (DEGs) between sites, DCs from auricular LNs preferentially upregulated genes associated with activation and costimulation including CD80, CD86, PDL1, and PDL2, indicating increased cDC2 maturation (Figure 3.1E-F). Divergent expression of these molecules at the protein level was confirmed by flow cytometry, demonstrating that antigen-bearing migratory cDC2s in auricular LNs following ear pinnae immunization expressed significantly higher levels of CD80 and CD86 costimulatory molecules as compared to their antigen-bearing counterparts from brachial LNs following footpad immunization (Figure 3.1G-H). We further noted increased expression of PD-L1 and PD-L2 on auricular-derived cDC2s at the protein level (Figure 3.2G). Papain-immunized cDC2s also expressed higher levels of CD80 and CD86 as compared to CpG, further demonstrating divergence in how immunization conditions impact migratory cDC activation (Figure 3.1G-H). In several subsets, cDC2 gene signatures in brachial LNs were also enriched in type 1 interferon (IFN) and viral sensing pathways such as expression of the interferon-stimulated gene, MX1, suggesting that additional differences exist between the sites (Figure 3.1F, 3.2H). In contrast, auricular gene signatures were enriched in cytokine-mediated and leukocyte proliferation signaling pathways. Together, these data suggest that while being relatively similar prior to inflammation, cDC2s migrating into LNs from different cutaneous sites exhibit marked differences at the transcriptional and protein levels, and in particular for costimulatory molecule expression.

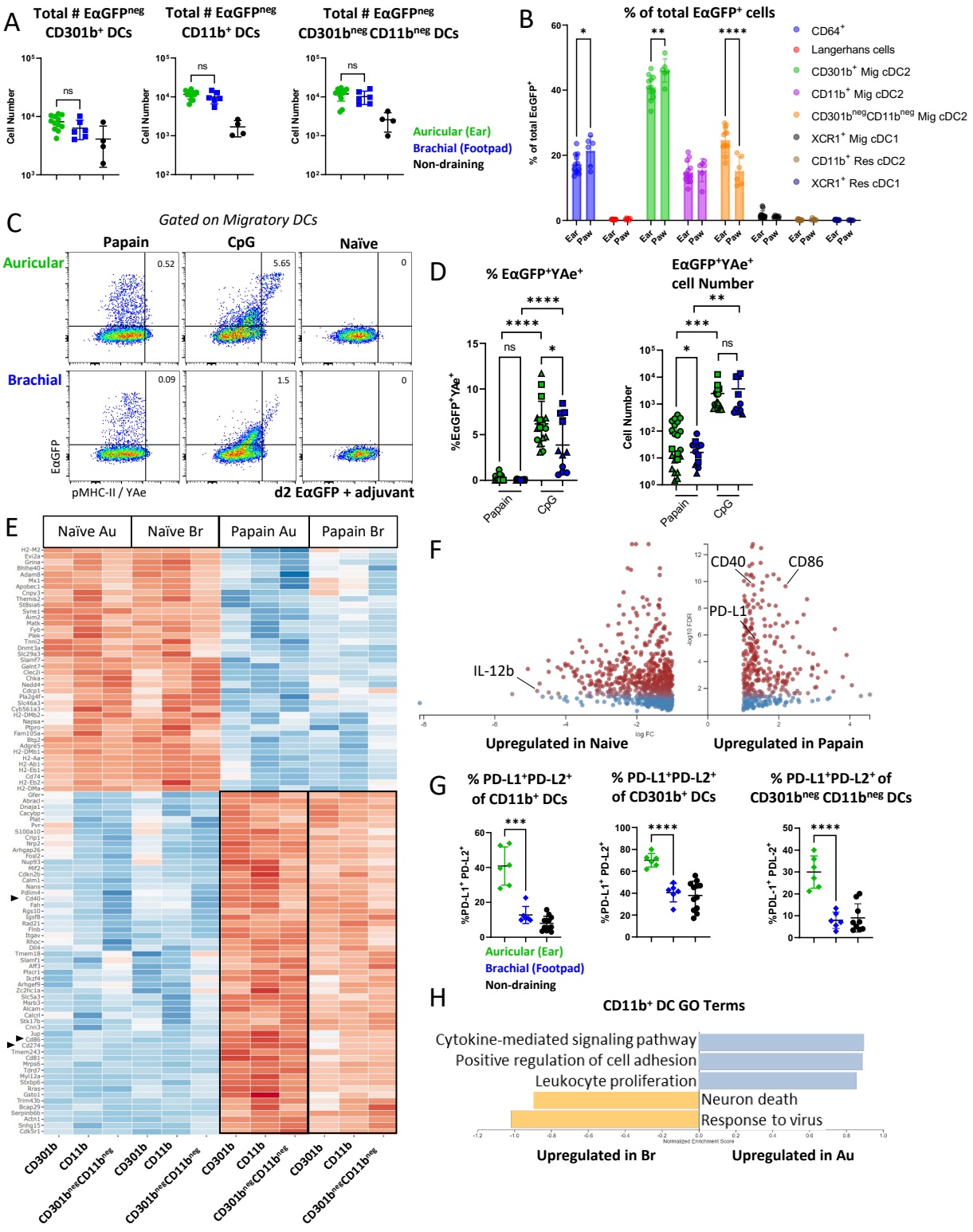

Figure 3.2. Transcriptional signatures of naïve and activated cDC2s.

A-D) B6 mice were immunized in the ear pinnae or front footpad with papain or CpG and EαGFP as indicated and harvested 48 hours later. A) Total number of EαGFP^{neg} cells for the indicated DC subsets. B) Frequency of EαGFP^{+} cells for the indicated cell subsets. C-D) Representative flow plots and quantification showing EαGFP and YAe expression on migratory DCs after immunization with the indicated adjuvant. Symbol shape represents individual experiments (three total). E-F) EαGFP^{+} DC populations were sorted from dLNs on day 2 for bulk RNA sequencing. E) Heatmap of all DEGs with a FDR<0.05 and greater than 2x fold change between naïve and papain immunized DCs from auricular and brachial LNs is shown. F) Volcano plot of DEGs between papain immunized and naïve DCs from auricular and brachial dLNs. Red indicates a FDR<0.05. Genes with a log fold change greater than 2 are shown. G) Migratory DCs were assessed for surface PD-L1 and PD-L2 expression by flow cytometry. Quantification of the frequency of PD-L1 and PD-L2 for the indicated DC subsets is shown. H) GO term enrichment analysis based on all DEGs in EαGFP^{+} CD11b^{+} DC populations between auricular and brachial dLNs. Au = auricular; Br = brachial. A-D, G are representative of 3 independent experiments. E-F and H are representative of 1 independent RNA sequencing experiment with n=3 per group.

Costimulation synergizes with TCR signaling to drive optimized T cell activation and has been implicated in Th2 differentiation[74,77-81,149,150]. Given the costimulatory molecule expression differences on DCs between the sites, we investigated whether activation of signaling pathways downstream of TCR and costimulation were also nonequivalent in activated T cells in different draining LNs. Indeed, we found significantly higher expression of the AP-1 transcription factors, BATF and IRF4, in activated OT-II T cells within the ear draining auricular LNs, indicating non-equivalent engagement of the TCR / costimulatory molecule signaling platform (Figure 3.3A-B, 2.3A-B). Expression of the transcription factors BATF and IRF4 in T cells has been previously associated with Th2 differentiation and IL-4 production[151-159], and we observed a strong positive correlation of these molecules with each other and Gata3 and 4get-GFP expression (Figure 3.3C). Image-based analysis also demonstrated increased phosphorylation of the mTOR signaling protein S6 (pS6), also downstream of TCR / costimulation platform, in T cells within auricular draining LNs (Figure 3.3D). Unexpectedly, in contrast to type-II inflammation, CpG OVA immunization promoted overall reduced levels of pS6 and IRF4 as compared to papain within auricular LNs, and equivalent site-specific expression across both LN sites (Figure 3.3A, D). This indicates that Th2

differentiation is associated with relatively enhanced and not reduced T cell activation, and that site specificity in T cell response induction does not extend to all T helper cell lineages.

To further investigate the role of TCR signaling in Th2 differentiation we transferred naïve 4get.OT-II cells to congenically distinct recipients, immunized with papain OVA, then treated the mice intraperitoneally with anti-PDL1 or anti-PDL2 blocking antibodies to simulate checkpoint blockade mediated enhancement of TCR and costimulatory pathways. Checkpoint blockade (either anti-PD-1, anti-PD-L1, or anti-PD-L2) acts on the TCR and costimulatory pathways to enhance T cell activation[74,160,161]. Indeed, by confocal microscopy we observed sustained macro-clustering at the T-B border after treatment with anti-PD-1 as compared to the isotype control (Figure 3.3E). In addition, OT-II cells expressed increased Gata3 and IRF4 but not 4get-GFP after anti-PD-L1 but not PD-L2 treatment, albeit with decreased T cell expansion possibly due to strong TCR-mediated cell death (Figure 3.3F).

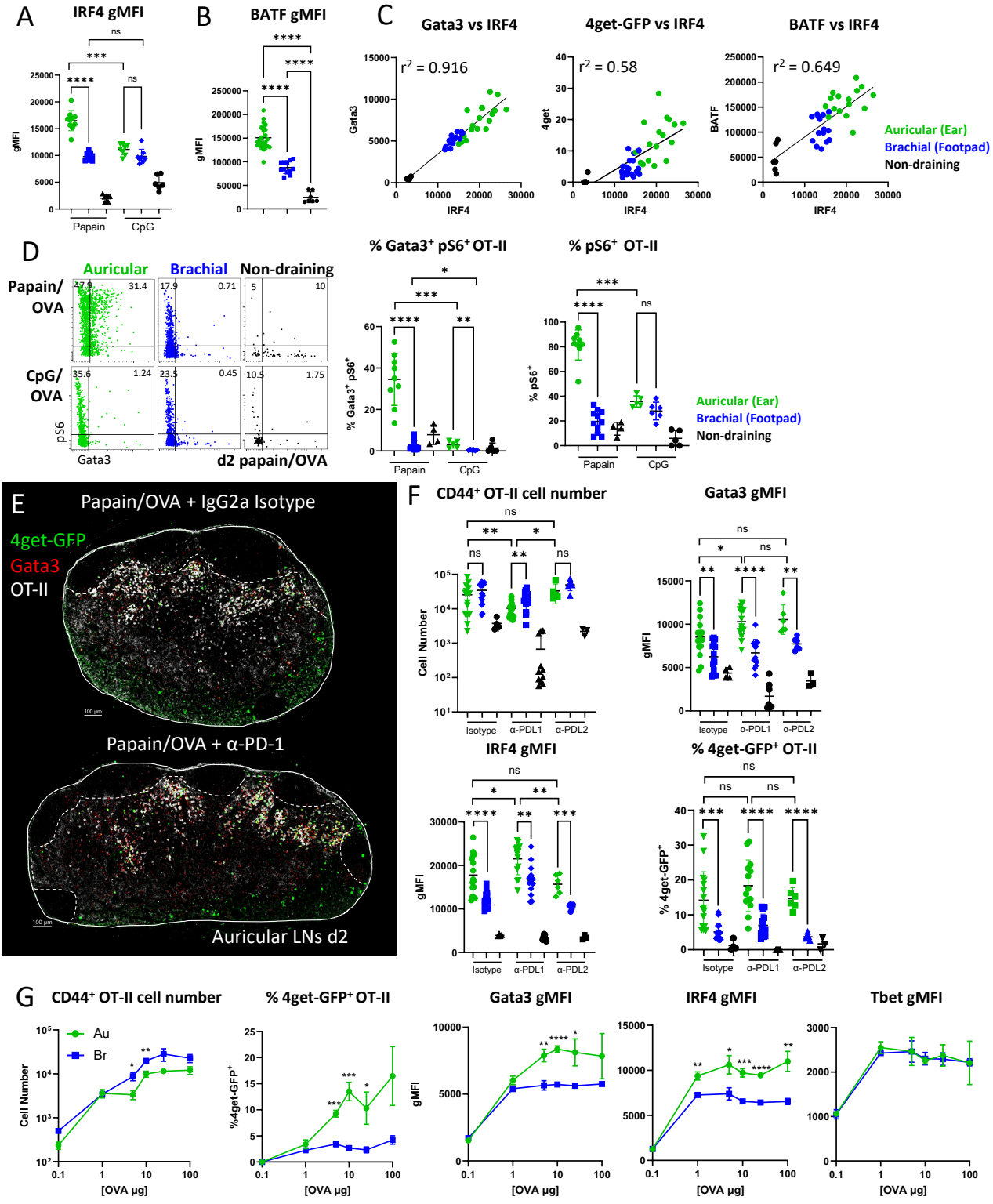

Figure 3.3. Non-equivalent activation of T cells across skin-draining LNs.

A-F) Naïve Ly5.2 4get.OT-II cells were transferred to Ly5.1 mice, injected with papain OVA or CpG OVA in the ear pinnae or front footpad, treated intraperitoneally with α-CD62L 6 hours post immunization, and dLNs were harvested and assessed by histo-cytometry or flow cytometry at 48 hours. A-C) Expression of IRF4 and BATF on activated $CD44^+$ OT-II cells and correlation plots with Gata3 gMFI and frequency of 4get-GFP^+ cells across different dLNs is shown. D) Representative histo-cytometry plots and quantification of pS6 and Gata3 expression in activated $Ki67^+IRF4^+$ OT-II T cells. E) Representative images of OT-II macro-clustering and differentiation with the indicated markers shown after treatment with anti-PD-1 blocking antibody or isotype control 24 hours post immunization. F) Flow cytometry data quantifying $CD44^+$ OT-II cell number, frequency of 4get-GFP^+ cells, and Gata3, IRF4 gMFI expression on $CD44^+$ OT-II cells after treatment with anti-PD-L1, anti-PD-L2, or isotype control. G) Naïve Ly5.2 4get.OT-II cells were transferred to Ly5.1 mice and injected with a fixed concentration of papain and increasing concentrations of OVA in the ear pinnae or front footpad. Mice were treated intraperitoneally with α-CD62L 6 hours post immunization and dLNs were harvested and assessed by flow cytometry at 48 hours. $CD44^+$ OT-II cell number, frequency of 4get-GFP^+ cells, and Gata3, IRF4, and Tbet gMFI expression on $CD44^+$ OT-II cells are shown. Data are representative of at least 3 independent experiments.

Together, these findings suggested that after papain immunization, monoclonal CD4 T cells within ear draining auricular LNs experienced increased overall stimulation compared to forepaw draining brachial LNs, and these effects could be moderately enhanced following checkpoint blockade. While being consistent with differential expression of costimulatory molecules by migratory cDC2s, and with otherwise limited differences in the number and composition of antigen-bearing migratory cDCs across the sites, it was still possible that insufficient delivery of antigen to brachial LNs after paw immunization was mediating the reduced T cell activation and Th2 programming in this compartment. To test this possibility, we titrated the amount of OVA administered into the skin sites along with a fixed concentration of papain. Although increasing the OVA dose at each site up to 10x the original amount did increase OT-II clonal expansion in both draining LNs, this did not enhance Th2 responses in brachial LNs, suggesting that the total amount of antigen was not a limiting factor in driving reduced Th2 differentiation after footpad immunization (Figure 3.3G). Of note, increased antigen delivery also did not elicit increased Tbet

expression in responding T cells, indicating that high antigen dose availability does not necessarily promote Th1 skewing in papain immunization settings (Figure 3.3G).

Based on the above observations, we next directly tested the requirements for costimulatory molecule expression on Th2 differentiation *in vivo*. For this, we performed a timed blockade of CD28 by administering an anti-CD28 antibody 24 hours post immunization and harvesting LNs 24 hours later. Delayed anti-CD28 administration allows the T cells to mount initial cognate interactions with cDCs for early priming and activation, but would limit the prolonged costimulatory contacts during the differentiation phase[75]. Indeed, delayed CD28 blockade resulted in very modest reductions of OT-II cellularity, indicating relatively normal initial activation (Figure 3.4A), but markedly decreased the expression of 4get-GFP, Gata3, BATF, and pS6 in both auricular and brachial LNs (Figure 3.4A-C). Delayed CD28 blockade also resulted in reduced macro-cluster formation within auricular LNs, instead driving more homogeneous and non-clustered distribution of OT-II cells throughout the T zone, akin to responses observed in footpad draining brachial LNs (Figure 3.4B, D). Furthermore, delayed CD28 blockade also reduced endogenous polyclonal Th2 cell differentiation, suggesting these effects are mediated across an array of TCR affinities (Figure 3.5A). Given that costimulation is thought to promote general T cell activation for all helper cell lineages, we next tested whether prolonged costimulatory sensing was important in Th1 inducing settings after CpG OVA immunization. Delayed CD28 blockade elicited much more modest effects on CXCR3 and Tbet expression (Figure 3.5B), overall indicating that prolonged costimulation was less essential in Th1-inducing settings.

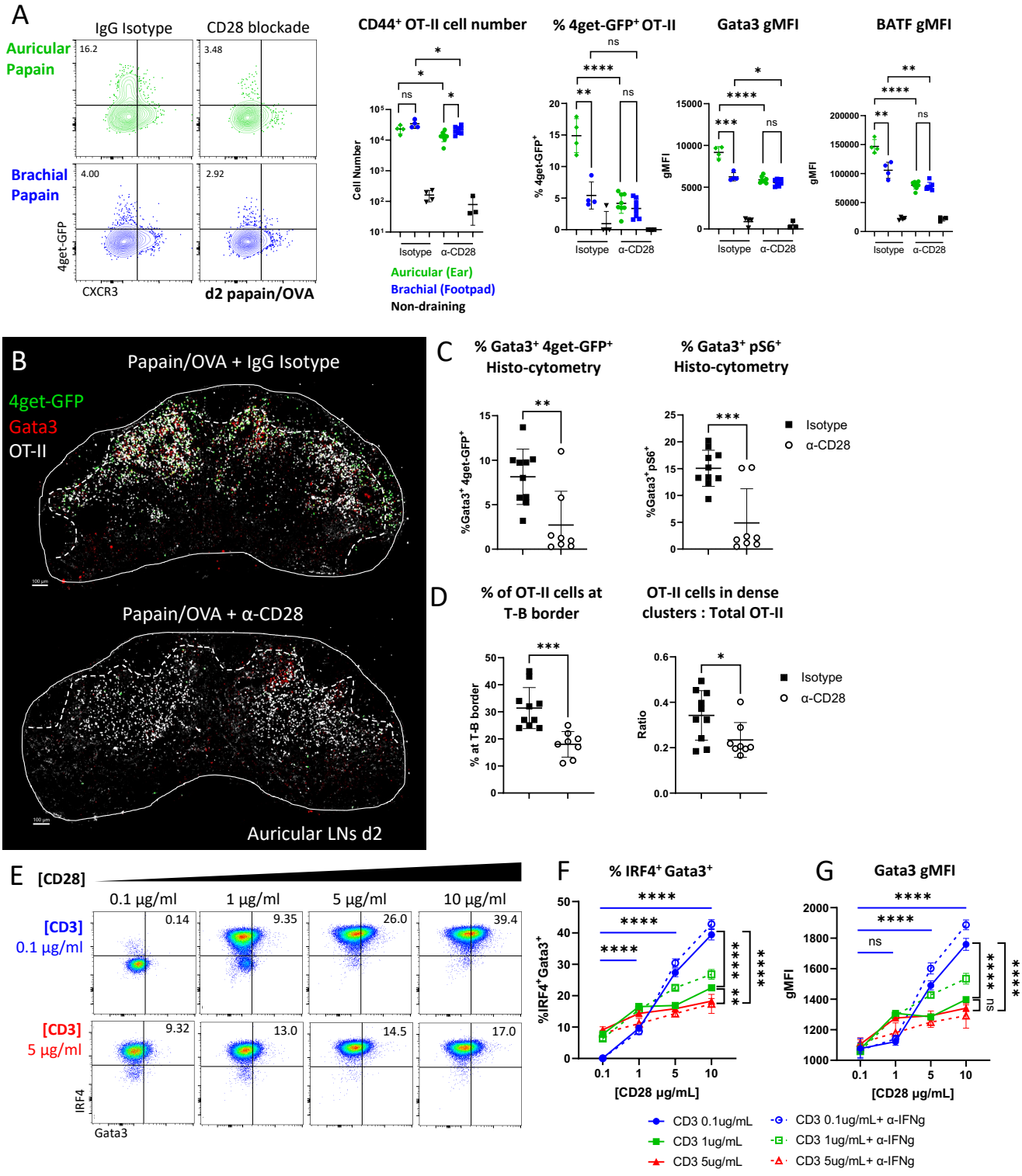

Figure 3.4. Site-specific T cell responses are mediated through non-equivalent expression of costimulatory molecules by migratory cDCs.

A-D) Naïve Ly5.2 4get.OT-II cells were transferred to Ly5.1 mice and injected with papain OVA in the ear pinnae or front footpad. Mice were treated intraperitoneally with α-CD62L 6 hours post

immunization, treated intraperitoneally with α-CD28 blocking antibody or IgG isotype control 24 hours post immunization, and dLNs were harvested and assessed by histo-cytometry or flow cytometry at 48 hours. A) Representative flow plots and quantification of $CD44^+$ OT-II cell number, 4get-GFP^+ frequency and Gata3 and IRF4 gMFI of $CD44^+$ OT-II cells after α-CD28 or isotype control treatment. B) Representative images depicting OT-II responses in auricular dLN treated with isotype control (top) or α-CD28 blocking antibody (bottom). Dashed lines represent the T-B border. C-D) Histo-cytometry analysis of 4get-GFP and Gata3 expression, OT-II localization, and frequency of macro-clustered OT-II cells. E-G) Naïve OT-II cells were cultured *in vitro* with the indicated concentrations of α-CD3 and α-CD28. α-IFNγ was added to cultures in some conditions (dashed lines). Cells were harvested 48 hours later and assessed for expression of Gata3 and IRF4 by flow cytometry. Representative plots of IRF4 and Gata3 expression are shown with quantification. A-D are representative of at least 2 independent experiments. E-G are representative of 4 independent experiments.

To examine if increasing costimulation can directly modulate Gata3 expression and Th2 differentiation *in vitro*, we next cultured naïve OT-II T cells in non-polarizing culture conditions with varying concentrations of plate-bound anti-CD3 and anti-CD28 for 48 hours. We found that increasing the concentration of available CD28 significantly enhanced Gata3 expression in T cells, and this was particularly evident at low anti-CD3 concentrations (Figure 3.4E-G). IRF4 was also increased in a CD28-dependent manner, indicating that this transcription factor can be regulated by both TCR and costimulation (Figure 3.4E-F). Additional blockade of IFN-γ further increased Gata3 expression across both low and intermediate anti-CD3 culture conditions, supporting its role in suppressing Th2 cell differentiation (Figure 3.4F-G). Moreover, dose-dependent CD28-mediated effects on Gata3 expression were also observed in Th2-polarizing culture conditions, albeit Gata3 and IRF4 expression was significantly greater than in non-polarizing settings (Figure 3.5C). Together, these data suggest that increasing concentrations of costimulatory molecules can drive Gata3 and IRF4 expression in responding T cells and initiate Th2 differentiation even at low CD3 concentrations.

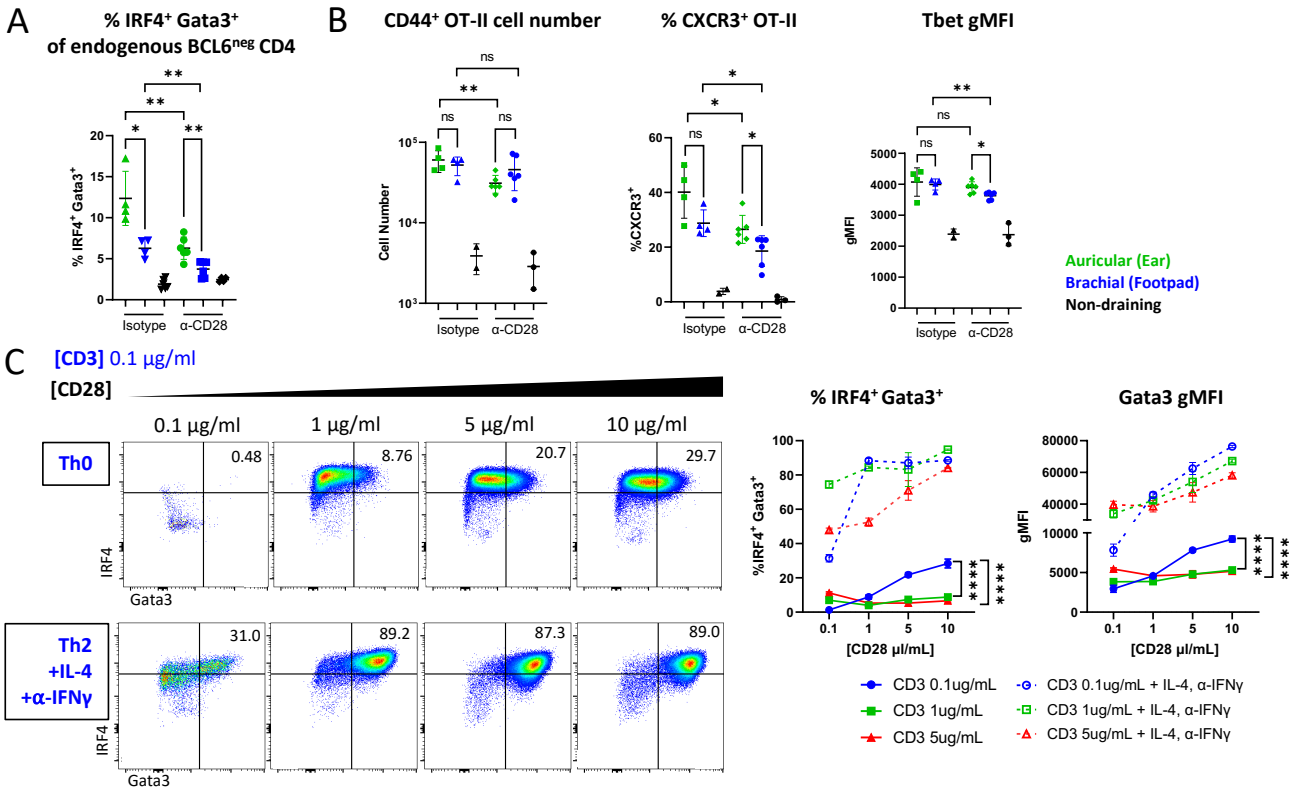

Figure 3.5. Late CD28 blockade has a minimal effect on Th1 differentiation.

A-B) Naïve Ly5.2 4get.OT-II cells were transferred to Ly5.1 mice and injected with Papain OVA or CpG OVA in the ear pinnae or front footpad. Mice were treated intraperitoneally with α-CD62L 6 hours post immunization, treated intraperitoneally with α-CD28 blocking antibody or IgG isotype control 24 hours post immunization, and dLNs were harvested and assessed by flow cytometry at 48 hours. A) Frequency of IRF4$^+$Gata3$^+$ endogenous T cells is shown. B) Quantification of CD44$^+$ OT-II cell number, frequency of CXCR3$^+$ cells, and Tbet gMFI on CD44$^+$ OT-II cells are shown. C) Naïve OT-II cells were cultured *in vitro* with the indicated concentrations of α-CD3 and α-CD28. IL-4 and α-IFNγ were added to the culture in some conditions (dashed lines). Cells were harvested for flow cytometry 48 hours later and assessed for expression of Gata3 and IRF4. Representative plots of IRF4 and Gata3 expression are shown with quantification. A-B is representative of 2 independent experiments. C is representative of 4 independent experiments.

3.3 Discussion

Here, we find that costimulatory molecule expression coupled with low pMHC-II expression by antigen-bearing migratory cDC2s promotes Th2 differentiation. Modulating costimulatory

signaling or TCR signal strength tuned Th2 differentiation both *in vivo* and *in* vitro. Furthermore, costimulatory molecule expression is more highly expressed on cDC2s migrating from the ear skin into the auricular dLNs as compared to the footpad, and these sites tightly correspond to Th2 differentiation. It is important to note that costimulatory molecules on their own are not thought to constitute a Th2 polarizing stimulus and can be involved in promoting general T cell activation. However, we find that prolonged costimulation was less essential for adjuvant induced Th1 responses, indicating differential requirements of costimulation for generation of distinct helper cell lineages. While additional factors expressed by cDC2s to selectively initiate Th2 skewing remain unknown[46], costimulatory molecule expression by cDCs can promote type-II cytokine production by *in vitro* stimulated T cells[77-82]. Similarly, TSLP-driven OX40L costimulatory molecule expression by cDCs has been positively linked with Th2 responses *in vivo*[53,84,162].

Our data also suggest that during papain exposure, antigen-bearing migratory cDC2s have low levels of pMHC complexes on the cell surface, accompanied by high amounts of costimulatory molecules. This was in stark contrast to surface pMHC-II expression after CpG immunization that induced robust detection of the Eα peptide on MHC-II. Mechanisms of how type-II inflammation impacts antigen processing and presentation, as well as whether it extends to other type-II settings remains to be determined, but could be driven in part by modulating the cytoskeletal properties of cDCs[144]. Together with TCR engagement, costimulation appears to enable prolonged T cell – cDC interactions, as well as reduces the threshold of TCR signaling required for T cell activation, overall being consistent with our findings that low levels of pMHC-II can still lead to robust T cell responses[163]. Together, these data suggest that costimulation can directly enhance T cell activation and Th2 differentiation by inducing IRF4 and Gata3 expression, and that differences in T cell

differentiation across the distinct skin draining LNs are most likely driven by non-equivalent expression of costimulatory molecules by migratory cDC2s.

Chapter 4. TH2 MACRO-CLUSTERING AND DIFFERENTIATION IS DRIVEN BY PROLONGED ICAM-1-MEDIATED DC-T CELL CONTACTS AND PROMOTES LOCALIZED CYTOKINE EXCHANGE

4.1 INTRODUCTION

In the previous chapters, we showed that Th2 differentiation is associated with T cell macro-cluster formation and requires migratory cDC2s and costimulatory molecule expression. We next explored the molecular mechanisms of macro-cluster formation and if this is required for Th2 differentiation. The integrin ICAM-1 is upregulated on DCs during maturation, and is downstream of costimulatory molecule signaling[164]. We therefore tested if costimulatory molecule signaling was promoting LFA-1 integrin mediated T – DC contacts and leading to macro-cluster formation. Of note, LFA-1 has also been shown to reduce the threshold of TCR / costimulatory signaling required for T cell activation thus enabling increased activation in setting of low pMHC-II[163].

We also investigated how these contacts could promote localized cytokine exchange from recently activated T cells thus impacting Th2 differentiation within LN microenvironments. The initial cellular source of IL-4 in draining LNs has not been clearly defined, yet recently stimulated T cells can produce IL-4 in a TCR-dependent manner *in vitro*[88,89]. Mice deficient in IL-4Rα also retain the capacity to secrete IL-4, suggesting that T cells can produce IL-4 without a requirement for prior IL-4 sensing[165]. Consistent with this, IL-4 secretion by T cells can be achieved by the activation of BATF/IRF4/Jun complexes downstream of costimulatory molecule / TCR engagement in a Gata3-independent manner[151-159]. Indeed, as shown previously, we observe robust expression of IRF4 and BATF in activated T cells within ear draining auricular LNs, suggesting

these transcription factors may be sufficient to induce initial IL-4 production by responding T cells within macro-clusters, and these can then be further amplified by canonical IL-4/IL-4Rα/pSTAT6 driven Gata3 expression. Thus, we hypothesized that enhanced costimulatory molecule and TCR mediated signaling induces production of IL-2 and IL-4 from responding T cells within the macro-clusters, and these in turn signal locally on to reinforce the Th2 differentiation program. Here, we find that prolonged T – DC contacts were essential for promoting macro-clustering and localized cytokine exchange. These contacts were ICAM-1 / LFA-1 mediated and delayed LFA-1 blockade reduced Th2, but not Th1 differentiation.

4.2 RESULTS

The above findings indicated that T cell macro-clustering was dependent on prolonged costimulatory molecule availability from migratory cDC2s (Figure 3.4A-B). We next tested how these T cell – DC contacts were mediated *in vivo*. The integrin LFA-1 is rapidly upregulated on T cells following activation, and its ligand, ICAM-1, is expressed on DCs after maturation to mediate T cell – DC interactions[129,164]. We observed marked ICAM-1 upregulation on activated antigen-bearing EαGFP^{+} migratory DCs after papain administration in both brachial and auricular LNs, and this was also elevated as compared to ICAM-1 expression after CpG immunization (Figure 4.1A). To test if T cell macro-clustering and Th2 differentiation was mediated via prolonged integrin-driven T – DC interactions, we performed a delayed LFA-1 blockade, treating mice with an anti-LFA-1 blocking antibody 24 hours post papain OVA administration and examining responses in auricular and brachial LNs 24 hours later[129,166]. Delayed LFA-1 blockade did not markedly alter OT-II T cell proliferation, indicating relatively normal initial activation and cognate interactions (Figure 4.1C). In contrast, 4get-GFP, Gata3, and IRF4 expression were all

significantly decreased in draining LNs after delayed LFA-1 blockade, indicating reduced Th2 differentiation (Figure 4.1B, D-E). LFA-1 blockade also disrupted the T cell macro-clustering at the T-B border, indicating limited formation of Th2 microenvironments in these settings (Figure 4.1E, F). Delayed LFA-1 blockade also reduced polyclonal Th2 differentiation after papain immunization indicating that DC – T cell contacts were critical for T cells of diverse TCR affinities (Figure 4.2C). To further test if prolonged T – DC contacts were important for driving Th2 response formation in other Type-II inflammation settings, we treated mice that had been subcutaneously infected with *N.b.* with delayed LFA-1 blockade at days 2 and 3 post infection and harvested inguinal draining LNs to examine Th2 response formation at day 4. We found that LFA-1 blockade significantly reduced Gata3 and pS6 expression in responding $Ki67^+$ T cells as well as minimizing Th2 cluster formation (Figure 4.1G-H). These data indicate that prolonged T – DC interactions were critical for Th2 induction across multiple models. In contrast to papain exposure and *N.b.* infection, delayed LFA-1 blockade had a minimal effect on Th1 differentiation after CpG OVA immunization (Figure 4.2A-B), suggesting that prolonged LFA-1 integrin mediated cell interactions are less important in these settings.

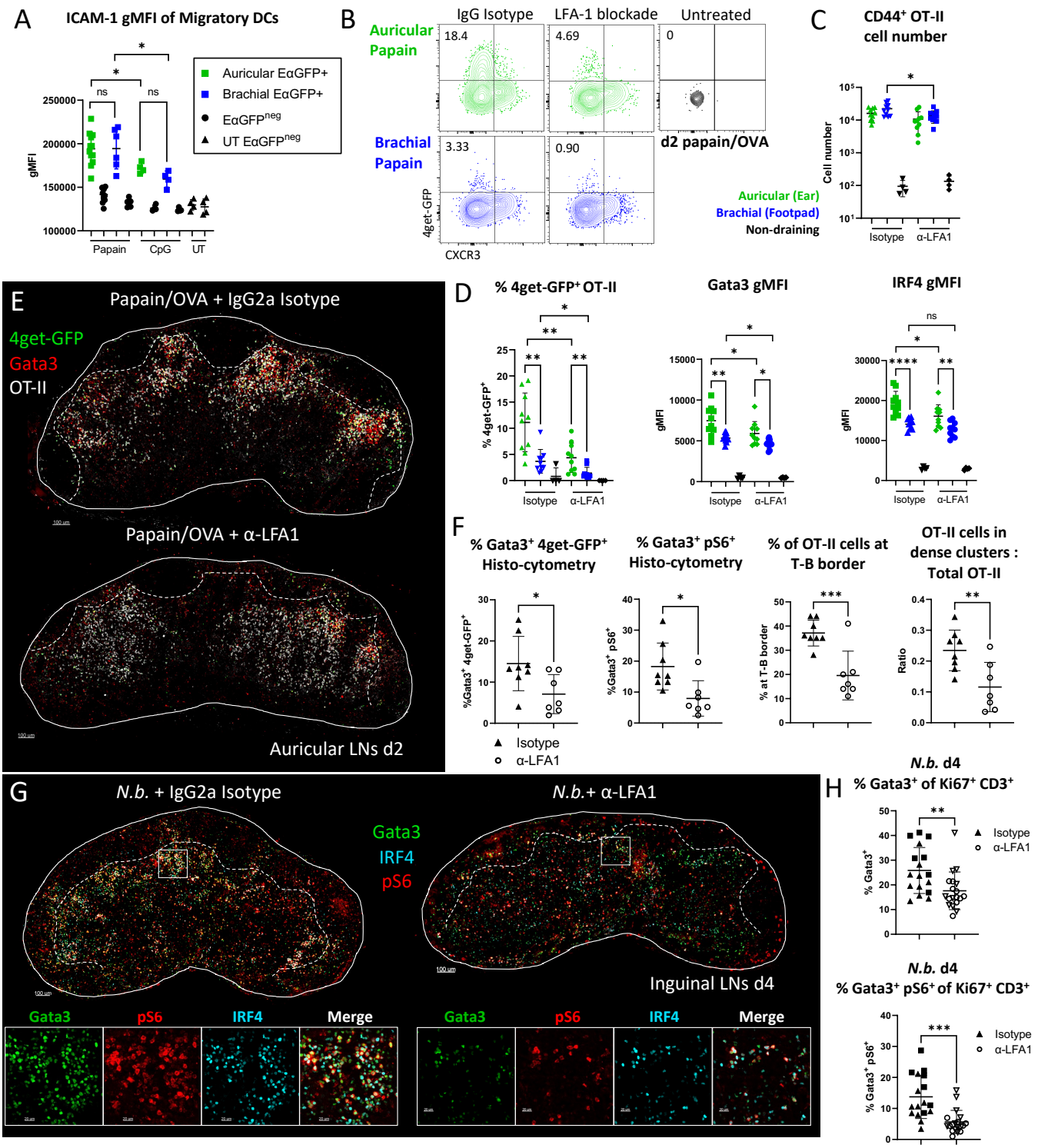

Figure 4.1. Th2 macro-clustering and differentiation is LFA-1 dependent.

A) B6 mice were immunized in the ear pinnae and front footpad with papain or CpG plus EαGFP and harvested for flow cytometry 48 hours later. Expression of ICAM-1 on EαGFP^{+} and EαGFP^{neg}

or naïve migratory DCs in the indicated LNs is shown. B-F) Naïve Ly5.2 4get.OT-II cells were transferred to Ly5.1 mice and injected with papain OVA in the ear pinnae or front footpad. Mice were treated intraperitoneally with α-CD62L 6 hours post immunization, treated intraperitoneally with α-LFA1 blocking antibody or IgG isotype control 24 hours post immunization, and dLNs were harvested and assessed by flow cytometry and imaging at 48 hours. B) Representative flow plots showing 4get-GFP and CXCR3 expression on $CD44^+$ OT-II cells. C) Quantification of the number of $CD44^+$ OT-II cells and D) frequency of 4get-GFP^+ cells, and Gata3 and IRF4 gMFI of $CD44^+$ OT-II cells after α-LFA1 or isotype control treatment. E) Representative microscopy images depicting OT-II responses in auricular dLN treated with isotype control (top) or α-LFA1 blocking antibody (bottom). Dashed lines represent T-B border. F) Histo-cytometry analysis of 4get-GFP and Gata3 expression, OT-II localization, and frequency of macro-clustered OT-II cells in auricular LNs with the indicated treatments. G-H) B6 mice were inoculated subcutaneously at the tail base with 500 *N.b.* L3 larvae, treated with α-LFA1or isotype control 2- and 3-days post infection, and the draining inguinal LNs were harvested 4 days later for confocal microscopy. Expression of the indicated markers is shown. H) Quantification of Gata3 and pS6 expression in responding endogenous T cells. A, G-H are representative of 2 independent experiments. B-F are representative of 4 independent experiments.

After activation, T cells can also express ICAM-1 on the cell surface, and in addition to T – DC interactions could potentially engage in homotypic T – T cell contacts[129]. To dissect whether delayed LFA-1 blockade was primarily affecting T – DC or T – T cell interactions, we generated ICAM1.KO OT-II cells (Figure 4.2D) and compared these responses to WT OT-II cells. In these experimental settings, ICAM1.KO OT-II T cells retain normal LFA-1 integrin functionality and can interact with ICAM1-expressing cDCs but lack the ability to engage in homotypic T – T cell contacts. We found no defects in Th2 differentiation in ICAM-1 deficient OT-II T cells, indicating that LFA-1 / ICAM-1 mediated homotypic T – T interactions are not required for early Th2 responses (Figure 4.2E). Together, these data suggest that enhanced T cell activation via costimulatory molecule expression by cDCs promotes prolonged LFA1 integrin-mediated T – DC interactions within auricular ear draining LNs, in turn reducing the threshold for TCR signaling required for activation. These contacts thus drive the formation of T cell macro-clusters and promote Th2 differentiation.

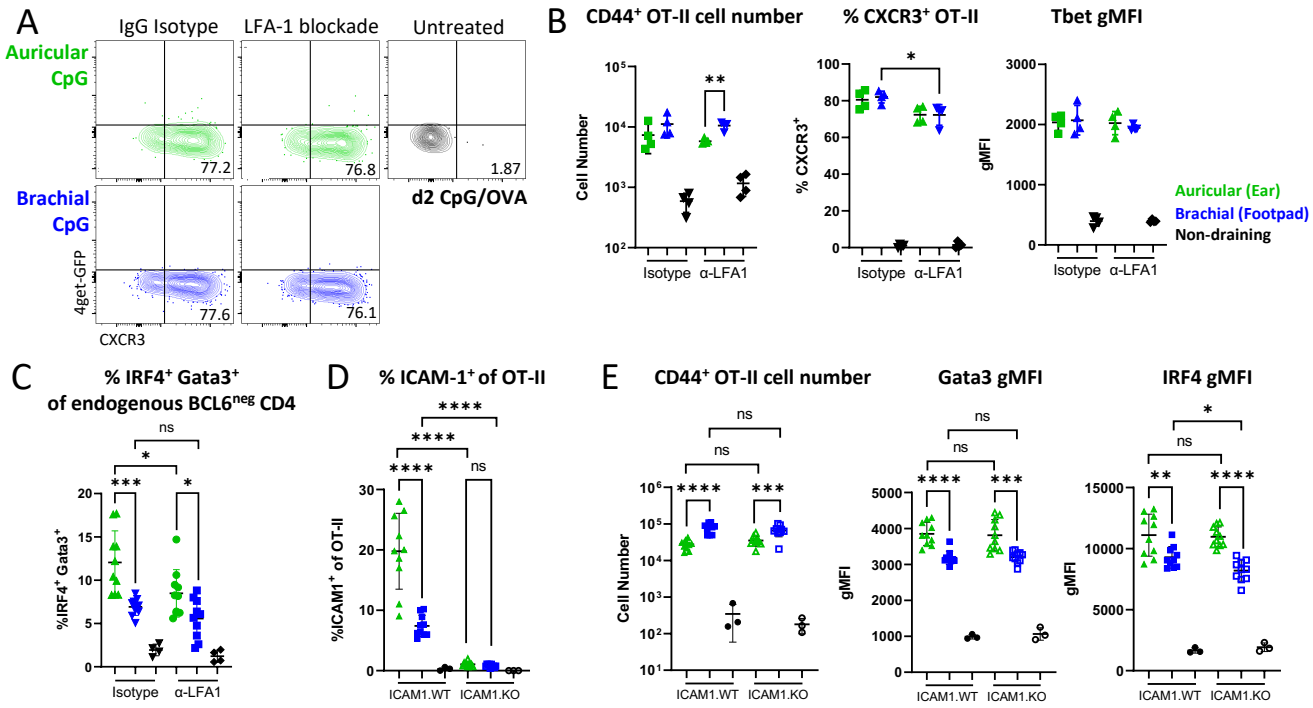

Figure 4.2. Late LFA-1 blockade has a minimal effect on Th1 differentiation.

A-C) Naïve Ly5.2 4get.OT-II cells were transferred to Ly5.1 mice and injected with CpG OVA in the ear pinnae or front footpad. Mice were treated intraperitoneally with α-CD62L 6 hours post immunization, treated intraperitoneally with α-LFA1 blocking antibody or IgG isotype control 24 hours post immunization, and dLNs were harvested and assessed by flow cytometry at 48 hours. A) Representative plots showing 4get-GFP and CXCR3 expression on $CD44^+$ OT-II cells. B) Quantification of $CD44^+$ OT-II cell number, frequency of $CXCR3^+$ cells, and Tbet gMFI on $CD44^+$ OT-II is shown. C) Frequency of $IRF4^+Gata3^+$ responding endogenous T cells. D-E) Naïve ICAM-1.KO or ICAM-1.WT OT-II cells were transferred to $CD45.1^+$ B6 recipients and injected with papain OVA in the ear pinnae or front footpad, treated intraperitoneally with α-CD62L 6 hours post immunization, and dLNs were harvested and assessed by flow cytometry at 48 hours. D) Frequency of ICAM-1^+ OT-II cells from ICAM-1.WT and ICAM-1.KO mice. E) Quantification of the number of $CD44^+$ OT-II cells, and Gata3 and IRF4 gMFI of $CD44^+$ OT-II cells. WT = wild type; KO = knockout. Data are representative of 2 independent experiments.

Costimulation promotes the production of IL-2 by activated T cells, as well as can elicit the production of the Th2 cytokine IL-4 *in vitro*[74,77-81,149,150]. IL-2 signaling in turn increases expression of the IL-4 receptor, IL-4Rα, such that IL-2 stimulated T cells become more receptive to IL-4[167]. T cell costimulation and macro-clustering could thus promote increased local

bioavailability of the cytokines IL-2 and IL-4, produced directly by activated T cells, which may reinforce localized Th2 differentiation within the macro-clusters. Indeed, we found CD25 was highly expressed on the activated $CD44^{+}$ $Gata3^{+}$ OT-II Th2 cells (Figure 4.3A). Further, early $Gata3^{+}CD25^{+}$ Th2 cells had increased expression of phosphorylated (p)STAT5 and pSTAT6, indicating enhanced and/or sustained IL-2 and IL-4 signaling, respectively, as compared with $Gata3^{neg}CD25^{neg}$ non-Th2 cells (Figure 4.3B).

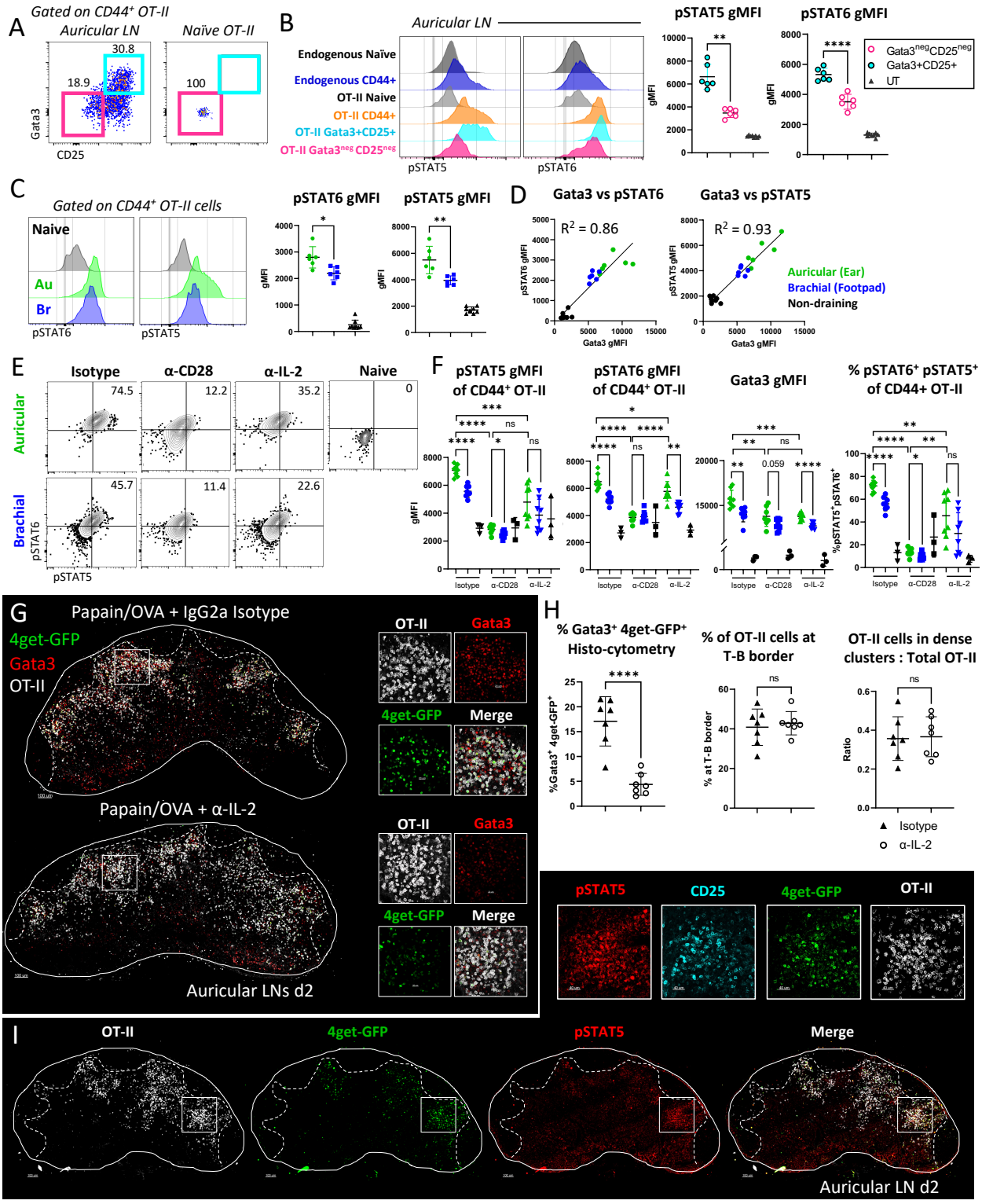

Figure 4.3. Increased costimulation in auricular draining LNs promotes increased cytokine signaling and Th2 differentiation.

A-D) Naïve Ly5.1 OT-II T cells were transferred to B6 mice and injected with papain OVA in the ear pinnae or front footpad. Mice were treated intraperitoneally with α-CD62L blocking antibody 6 hours post immunization and dLNs were harvested and assessed by flow cytometry at 48 hours. A) Representative flow plots of Gata3 and CD25 expression on $CD44^+$ OT-II cells in auricular dLNs. B) Representative histograms and quantification of pSTAT5 and pSTAT6 staining for the indicated cell subsets within the same sample. C) Representative histograms and quantification of pSTAT5 and pSTAT6 expression in auricular and brachial LNs and D) pSTAT5 and pSTAT6 correlation with Gata3 gMFI on $CD44^+$ OT-II cells is shown. E-F) Naïve Ly5.1 OT-II cells were transferred to B6 mice and injected with papain OVA in the ear pinnae or front footpad. Mice were treated intraperitoneally with α-CD62L 6 hours post immunization, treated intraperitoneally with α-CD28 blocking antibody, α-IL-2 blocking antibody, or IgG isotype control 24 hours post immunization, and dLNs were harvested and assessed by flow cytometry at 48 hours. Quantification of frequency of $pSTAT5^+$ and $pSTAT6^+$ cells, gMFI of pSTAT5 and pSTAT6, and Gata3 expression on $CD44^+$ OT-II cells are shown. G-I) Naïve Ly5.2 4get.OT-II cells were transferred to Ly5.1 mice and injected with Papain OVA in the ear pinnae or front footpad. Mice were treated intraperitoneally with α-CD62L 6 hours post immunization, treated intraperitoneally with α-IL-2 blocking antibody or IgG isotype control 24 hours post immunization, and dLNs were harvested and assessed by confocal microscopy at 48 hours. G) Representative microscopy images depicting OT-II responses in auricular dLN treated with isotype control (top) or α-IL-2 blocking antibody (bottom). Dashed lines represent T-B border. H) Histo-cytometry analysis of 4get-GFP and Gata3 expression, OT-II localization, and frequency of macro-clustered OT-II cells in auricular LNs with the indicated treatments. I) Representative microscopy images depicting pSTAT5 staining within OT-II macro-clusters. Data are representative of at least 2 independent experiments.

Consistent with non-equivalent T cell activation and differentiation in different draining LNs, both pSTAT5 and pSTAT6 in responding OT-II cells were significantly elevated in auricular as compared to brachial draining LNs (Figure 4.3C). pSTAT levels were also directly correlated with non-equivalent GATA3 expression across the sites (Figure 4.3D), suggesting direct involvement in Th2 differentiation. We thus tested whether differential sensing of costimulatory molecules by the responding T cells in distinct draining LNs resulted in non-equivalent cytokine signaling and Th2 differentiation. For this, we again utilized the timed CD28 blockade and examined phosphorylation of STAT5 and STAT6 molecules 24 hours later. Indeed, we found that delayed anti-CD28 treatment significantly reduced pSTAT5 and pSTAT6 expression in auricular draining LNs, and completely abrogated the differences between the tissues (Figure 4.3E-F). Similar effects

were observed after *in vivo* anti-IL-2 blockade, and both anti-CD28 and anti-IL-2 treatments resulted in comparable decreases in STAT5, and to a lesser extent STAT6, phosphorylation (Figure 4.3E-F). Both anti-CD28 and IL-2 blockade markedly reduced Gata3 expression in responding OT-II cells indicating a clear link between prolonged costimulation, cytokine sensing, and Th2 differentiation (Figure 4.3F). We next investigated whether blockade of IL-2 would affect Th2 macro-cluster formation and differentiation. We examined Th2 response formation after delayed IL-2 blockade and found that although clustering and T-B border localization were maintained, Gata3 and 4get-GFP expression in OT-II cells was significantly reduced as compared to isotype controls (Figure 4.3G-H). These results support the hypothesis that macro-cluster formation is costimulation and integrin mediated, while localized cytokine exchange within clusters promoted optimal Th2 differentiation such that in settings of IL-2 blockade, macro-clusters could still form as expected yet Th2 differentiation was abrogated. Finally, we detected pSTAT5 expression in responding Th2 cells within macro-clusters, which also colocalized with 4get-GFP and CD25 signal (Figure 4.3I). In sum, our data indicate that increased sensing of costimulatory molecules by early differentiating T cells in ear draining auricular LNs is associated with enhanced integrin-mediated T cell macro-clustering, increased local IL-2 and IL-4 cytokine production and sensing, and amplified early Th2 differentiation.

4.3 DISCUSSION

The above findings indicate that Th2 macro-clustering and differentiation is driven by ICAM-1 mediated T – DC contacts, which in turn promotes localize cytokine exchange amongst neighboring T cells. Additional integrin-mediated homotypic interactions among activated T cells may also take place, albeit likely not via ICAM-1 / LFA-1 interactions. Of note, a recent study has

demonstrated a role for the integrin αVβ3, for Th2 differentiation *in vitro*, and this integrin has also been previously linked with migratory behavior of Th2 cells in inflamed tissues[168,169].

Our data do support the notion that costimulation is essential for inducing IL-2 and IL-4 cytokine production by activated T cells[87-90,170-172], and likely for eliciting IL-4Rα upregulation, in turn allowing IL-2-experienced T cells to become more receptive to IL-4 signaling to drive enhanced Th2 differentiation[167]. IL-2 also skews responding T cells away from the Tfh lineage, thus supporting additional specification of helper cell fate[133,137,138]. Conversely, the spatial proximity of macro-clusters near B cell follicles could also directly support Tfh differentiation by enhancing the probability of interactions between those activated T cells which receive less IL-2 and neighboring B cells presenting cognate antigens, thereby explaining the involvement of migratory cDC2s in both Th2 and Tfh responses[173].While our studies do not examine other potential sources of IL-2 and IL-4 in LNs, our findings do suggest that T cells within the macro-clusters experience more extensive cytokine signaling than those outside the clusters, and this further enhances Th2 differentiation within local microenvironments. Supporting this idea are past observations that both IL-2 and IL-4 are secreted by T cells in a broadcasted, non-polarized fashion which suggests these cytokines could be available within the specialized microenvironments to promote optimal Th2 differentiation[174,175]. Taken together, our data indicates that migratory cDC2s are critical for initiation of Th2 differentiation by promoting the formation of specialized Th2 microenvironments which enable optimized Th2 differentiation (Figure 4.4). Low TCR signaling in combination with high costimulatory signaling provided by antigen bearing cDC2s initiates a cascade of Th2 cell differentiation by promotion of ICAM-1/ LFA-1 integrin mediated prolonged contacts, enabling localized cytokine exchange of IL-2 and IL-4 from activated T cells. Blockade of integrin mediated

contacts, costimulatory signaling, or cDC2 trafficking to dLNs abrogated Th2 differentiation. Notably, we utilized the observation that migratory cDC2s lack this activated costimulatory phenotype in brachial dLNs to compare and contrast Th2 responses across skin sites. Future studies will be required to understand the skin specific factors that differentially activate dermal DCs. Understanding how Th2 responses are initiated in the skin will be critical for the development of future therapies to treat allergic diseases.

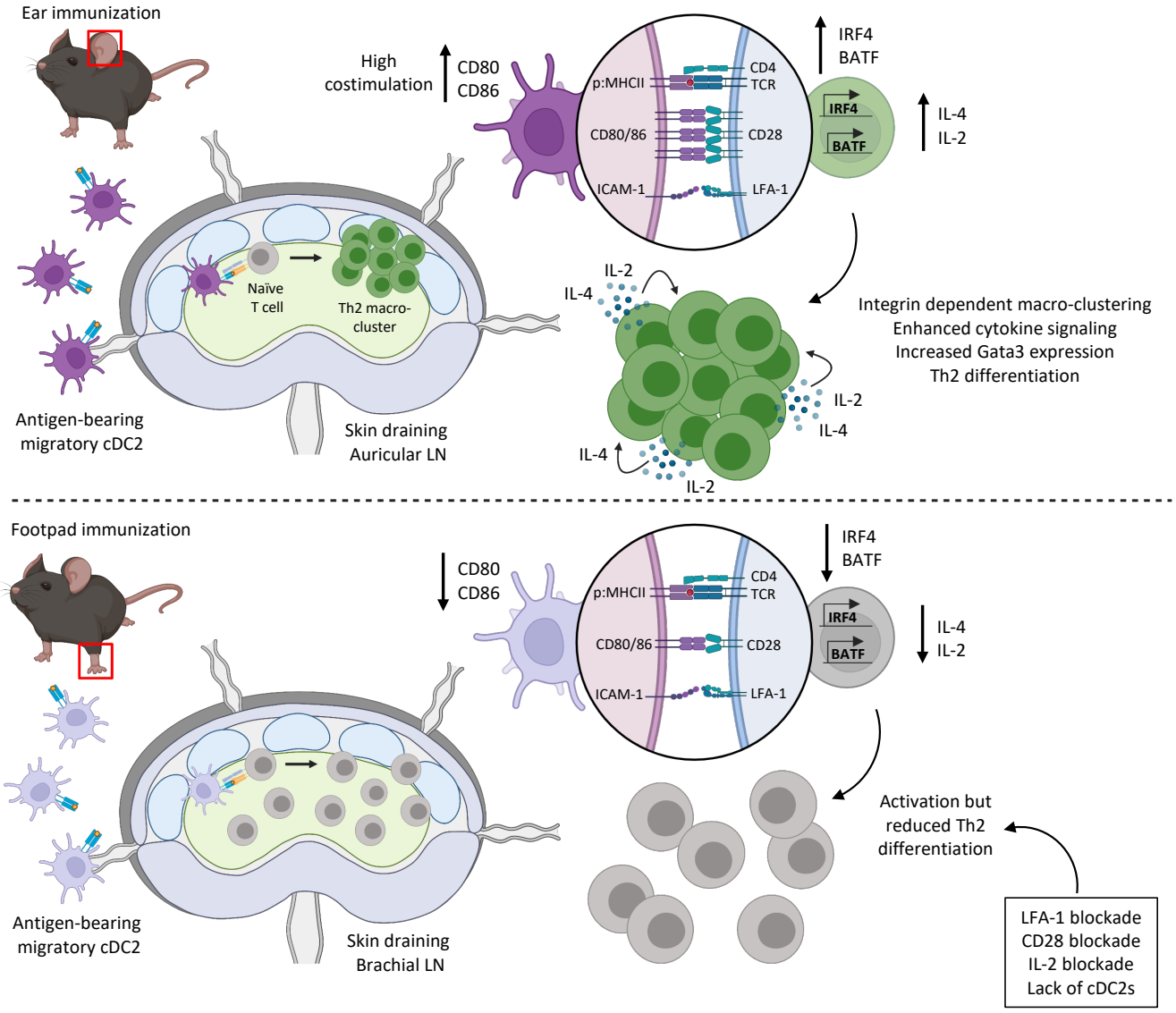

Figure 4.4. Proposed model for initiation of Th2 differentiation in skin draining LNs.

Proposed model for initiation of Th2 differentiation in skin draining LNs. Papain immunization of the skin elicits the maturation and migration of migratory antigen-bearing cDC2 to draining LNs where they induce Th2 responses within dedicated microenvironments localized at the T-B border. Th2 differentiation is driven by prolonged T – DC contacts leading to T cell activation through low levels of pMHC and high levels of costimulatory molecules on cDC2s thus driving integrin-mediated macro-clustering, efficient cytokine exchange, and localized Th2 differentiation. Certain skin sites, such as the paw, induce reduced expression of costimulatory molecules on cDC2s which leads to reduced Th2 responses within corresponding draining LNs.

Chapter 5. SUMMARY AND IMPACT

We used quantitative microscopy to investigate the early stages of *in vivo* Th2 differentiation after cutaneous administration of the allergen, papain, and other type-II stimuli, as well as compared these responses to Th1 differentiation with TLR agonist immunization. In contrast to the predicted limited cellular activation in Th2 settings, we observed enhanced T cell signaling and extensive clustering, here termed 'macro-clustering', of early differentiating Th2 cells which primarily occurred near the T-B border of the LN paracortex. Macro-clustering was integrin-mediated and was associated with enhanced cytokine signaling, suggesting that the spatial proximity of activated T cells enables optimized cytokine exchange for Th2 differentiation (Figure 4.4). Enhanced T cell signaling and macro-clustering were also distinct from that seen with adjuvant induced Th1 responses. Surprisingly, formation of Th2 responses was highly dependent on the specific site of type-II agonist administration, with footpad-delivered stimuli eliciting markedly reduced Th2 responses as compared to other skin sites, but without compromised ability to elicit Th1 differentiation across different tissues. Differences across the sites were driven by divergent activation states of migratory cDC2, with enhanced costimulatory molecule expression by cDC2 in Th2-inducing LNs promoting T cell macro-clustering, cytokine signaling, and Th2 differentiation (Figure 4.4). Collectively, our findings demonstrate that enhanced costimulation and integrin-driven prolonged T - DC crosstalk promotes T cell macro-clustering and generates LN microenvironments which drive Th2 response formation *in vivo*. Our data also support the emerging notion that generation of T cell responses is heavily impacted by upstream barrier tissues[176,177], raising fundamental questions on the mechanisms leading to divergent responses among skin sites and having clear implications for allergic disease development.

In vivo mechanisms driving early Th2 differentiation in LNs have remained enigmatic, in large part due to the complex role of TCR signaling in directing T cell effector fates and the lack of clear understanding of which molecules expressed by cDCs, or other innate cells in LNs, selectively induce Th2 polarization[90]. Our studies indicate that early differentiating Th2 cells undergo enhanced T cell signaling and activation, and that this is mediated through macro-clustering at the T-B border with migratory cDC2s displaying high levels of costimulatory molecules and integrin ligands but relatively low levels of surface pMHC. This in turn appears to promote efficient cytokine exchange, in particular for IL-2 and IL-4, among neighboring activated T cells to reinforce localized Th2 differentiation and to support prolonged proliferation. Thus, formation of discrete spatial microenvironments within LNs in which T cells integrate quantitatively strong activation signals from cDC2s coupled with qualitative cytokine sensing from nearby T cells promotes the initiation of large-scale Th2 responses *in vivo*.

Past studies have demonstrated that *in vitro* stimulation of CD4 T cells with strong TCR agonists or high dose of peptide promotes Th1 differentiation, while low dose signals elicit Th2 differentiation[72,73]. This has also been supported by *in vivo* work using peptide-pulsed DCs, which showed that TCR signal strength serves as a rheostat to control cytokine receptor expression, in turn modulating the ability of T cells to sense cytokines and undergo T helper cell differentiation[72-74]. Our studies are consistent with this hierarchy model, showing that cells undergoing the greatest degree of activation become more differentiated. However, we show that during *in vivo* allergen exposure and helminth infection, prolonged and enhanced T activation leads to Th2 and Tfh, not Th1 polarization, and that Th1 differentiation occurs at minimal rates for these responses. Differences in these observations are likely explained by the fact that environmental allergens such

as papain elicit inflammatory functions via proteolytic disruption of the epithelial barrier and release of the alarmin IL-33[103], and this in turn induces cDC maturation and costimulatory molecule expression through local ILC2 activation[53,83,122,178], thus necessitating *in vivo* administration to appropriately instruct cDCs. Further, activated T cells appear confined within microenvironments rich in other T cells and cDC2s and away from other potential cellular sources of IL-12, which could suppress early Th2 differentiation[100,101]. In this regard, we previously showed that papain administration does not elicit robust monocyte recruitment to the draining LNs[16], as these cells can also produce copious amounts of IL-12 during type-I inflammation[179]. Altogether, these findings suggest there is limited availability of Th1 inducing factors in draining LNs after papain administration, indicating that highly activated T cells undergoing prolonged interactions with cDC2s receive Th2 polarizing cytokines in the absence of Th1-promoting factors, leading to the generation of large-scale Th2 responses. Notably, the formation of T cell macro-clusters appears far less critical for Th1 responses *in vivo*. This may be due to comparatively lower expression of integrin ligands by cDC2s to mediate prolonged clustering, high abundance of inflammatory cytokines across vast regions of the LN parenchyma, and presence of chemokines which would drive CXCR3-expressing early Th1 cells away from sites of initial T – DC contacts[16,127].

An unexpected finding in our work was that not all types of skin generated equivalent Th2 responses in the draining LNs. We primarily characterized the ear and footpad draining LNs, finding that cDC2s within these different tissue compartments had distinct transcriptional profiles and expression of costimulatory molecules after exposure to the same agonist. How these DCs are differentially programmed within tissues remains a major open question. Therefore, skin should

not be thought of as a single barrier tissue, but unique compartments that may respond differently to environmental triggers. A possible evolutionally benefit of reduced Th2 responses after footpad allergen administration could reflect the need for dampened inflammation in tissues with constant mechanical stress, environmental exposure, and likely damage, while still retaining the ability to induce robust Th1 responses to microbial challenges, thus raising questions about human vaccine administration, which are typically delivered intramuscularly or intradermally.

Finally, a common feature of Th2 allergic responses is atopic march development, in which initial skin sensitization leads to downstream pathology across peripheral organs. It will therefore be important to understand how different regions of the skin, the largest barrier tissue in the body, respond to allergen exposure and drive disease development in humans.

Chapter 6. MATERIALS AND METHODS

6.1 MICE

C57BL/6J, BALB/cJ, B6.Cg-Tg(Itgax-cre)1-1Reiz/J (CD11c-Cre), B6.129S1-Irf4^{tm1Rdf}/J (IRF4$^{fl/fl}$), and B6.129S4-*Icam1*^{tm1Jcgr}/J (ICAM-1.KO) were obtained from Jackson Laboratory. B6.SJL-*Ptprc*^{a}*Pepc*^{b}/BoyCrl (CD45.1) mouse strain was obtained from Charles River Laboratory. CD45.1^{+} B6.Cg-Tg(TcraTcrb)425Cbn/J (OT-II) mice were obtained from a donating investigator (P.J. Fink, University of Washington) and crossed with CD45.2^{+} C57BL/6J mice to generate CD45.1^{+} OT-II and CD45.1^{+}CD45.2^{+} OT-II lines that were used interchangeably based on recipient congenic status. The KN2 and 4get-GFP mouse strains on a B6 background were obtained from a donating investigator (M. Pepper, University of Washington). 4get-GFP and ICAM-1.KO mice were crossed to OT-II to generate 4get-GFP OT-II and ICAM-1.KO OT-II lines respectively.

Six- to twelve-week-old male and female mice were kept in specific pathogen-free (SPF) conditions at an Association for Assessment and Accreditation of Laboratory Animal Care-accredited facility at the University of Washington, South Lake Union campus. All procedures were approved by the University of Washington Institutional Animal Care and Use Committee.

6.2 ADOPTIVE TRANSFERS

For adoptive transfers, naïve CD45.1^{+} OT-II, CD45.1^{+}CD45.2^{+} OT-II, or CD45.2^{+} 4get-GFP OT-II T cells were isolated from LNs and spleens using the naïve CD4^{+} T cell isolation kit (Miltenyi Biotec). The average purity of OT-II cells was approximately 75-80% for all experiments. 1x10^{6}

(unless otherwise noted) naïve OT-II cells were transferred into hosts intravenously via retro-orbital injection 1-3 days prior to immunization.

6.3 IMMUNIZATIONS AND BLOCKING ANTIBODIES

The following adjuvants and amounts per immunization site were used: 20µg of CpG ODN 1668 (AdipoGen), Alhydrogel ("Alum") (Invivogen) diluted 1:2 with PBS, Dibutyl pthalate ("DBP") (Sigma Aldrich) diluted 1:1 with 100% Acetone, 50µg Papain (Sigma-Aldrich), and 10µg Endotoxin-free Ovalbumin ("OVA") (Invivogen). In some studies, the dose of OVA given ranged from 0.1-100µg per injection. For antigen presentation studies, 10µg of LPS-free EαGFP (gift from M. K. Jenkins, University of Minnesota) plus 50µg of papain were injected intradermally in the ear pinnae or the forepaw. Adjuvants were mixed with PBS in a 20µl total volume per immunization site and injected in the hind or front footpads, subcutaneously in the flank skin, at the tail base, or intradermally in the ear pinnae (to target the popliteal, Brachial, Inguinal, and Auricular dLNs, respectively) as indicated. For some studies, DBP was "painted" onto ear or footpad skin by pipetting 20µl volume slowly, allowing drying between drops with the mouse under anesthesia until liquid was completely dried. For *Nippostrongylus brasiliensis* infections, infectious third-stage larvae (L3) were raised and maintained as described[180]. Mice were infected subcutaneously at the base of the tail to target the inguinal draining LN with 500 *Nippostrongylus brasiliensis* L3.

For *in vivo* antibody blocking studies, 100µg of anti-CD62L (clone Mel-14, BioXcell) was injected intraperitoneally 6 hours post immunization. In some studies 100µg anti-LFA-1α (clone M17/4, BioXcell), 100µg rat IgG2a isotype control (BioXcell), 100µg anti-CD28 (clone 37.51, BioXcell), 100µg polyclonal Syrian hamster IgG (BioXcell), 100µg anti-PD-L1 (clone B7-H1, BioXcell),

100µg anti-PD-L2 (clone B7-DC, BioXcell), 100µg anti-PD-1 (clone RMP1-14, BioXcell), or 100µg anti-IL-2 (clone JES6-1A12, BioXcell) was injected intraperitoneally 24 hours post immunization.

6.4 CONFOCAL MICROSCOPY

For confocal imaging, PFA-fixed and sectioned LN or skin tissues were imaged as previously described using a Leica SP8 microscope[14]. Briefly, isolated LN or skin tissues were fixed using BD Cytofix (BD Biosciences) diluted 1:3 in PBS for 24 hours at 4°C then dehydrated with 30% sucrose solution for 24-48 hours at 4°C. LNs were then embedded in OCT compound (Tissue-Tek) and stored at -20°C. LNs were section on a Thermo Scientific Micron HM550 cryostat into 20µm sections and stained as previously described[14]. A Leica SP8 tiling confocal microscope equipped with a 40x 1.3NA oil objective was used for image acquisition. All raw imaging data was processed and analyzed using Imaris (Bitplane).

6.5 HISTO-CYTOMETRY AND CYTOMAP

Histo-cytometry analysis was performed as previously described[14,16]. Briefly, multiparameter confocal images were corrected for fluorophore spillover using the built-in Leica Channel Dye Separation module. Single stained controls were acquired using UltraComp eBeads (Invitrogen) that were incubated with fluorescently conjugated antibodies, mounted on slides with Fluormount-G slide mounting media (ThermoFisher), and imaged. All images were visualized and analyzed using Imaris (Bitplane). For analysis of myeloid cells, a combinatorial myeloid channel was created by adding normalized signals for CD11c, MHC-II, CD207, CD301b, and Sirpα using the Imaris XT channel arithmetic module, and this sum myeloid channel was used for myeloid isosurface object creation. For T cells, a combined activated T cell channel was created by adding

normalized signals for Ki67 and IRF4; T cell isosurface objects were next created on this channel and then further gated on the congenic CD45.1 or CD45.2 signal. For visual clarity, 4get-GFP signal was masked outside of CD45.2$^+$ OT-II cells. In all analyses, object statistics were exported to FlowJo software (FlowJo, LLC) for gating and phenotypic characterization. T-B border regions were manually created using B220 or MHC-II (B cell follicles) and CD3 (T cell zone) staining and represented as a surface. T-B border localization was calculated as the frequency of OT-II cells within the T-B border surface region. Clustering analysis was performed by creating isosurfaces on CD45.1 congenic signal without cell splitting. Surfaces were then filtered by volume and surfaces exceeding 1400μm^3 (defining dense clusters) were added and presented as a ratio of dense macro-clustered surface volume (greater than 1400 μm^3) to total OT-II surface volume. Spatial correlation analysis was performed in CytoMAP[18]. In brief, the position of all myeloid and T cell objects within LNs was used for virtual raster scanning with 50-μm radius neighborhoods. The Pearson correlation coefficient was calculated for the number of cells of the different cell types within these neighborhoods. Raster-scanned neighborhoods were also used for clustering based on cell type abundance to identify distinct region types, and these regions were used for heatmap and positional visualization of regions in dLNs.

6.6 CELL ISOLATION AND FLOW CYTOMETRY

For myeloid cell analysis, LN tissues were mechanically disrupted and subject to digestion in PBS with 10% fetal bovine serum (FBS) with DNase I (100μg/mL; Sigma), Dispase II (800μg/mL; Sigma), and Collagenase P (200μg/mL; Sigma) at 37°C shaking at 150rpm for 30 minutes with periodic manual disruption. Flow cytometric studies of T cells in lymph nodes did not use enzymatic digestion. In some studies, mice were injected intravenously with 1μg of anti-Thy1.2-BUV395 (clone 30-H12; BD Biosciences) ~5 minutes prior to sacrifice. Lung tissue was digested

in complete RPMI with Liberase (70µg/mL; Roche) and Aminoguanidine (10mM; Sigma) and tissue was dissociated on the gentleMACS Dissociator (Miltenyi Biotec) as previously described[91]. Cell staining was conducted in the presence of Fc Block (2.4G2, Tonbo Biosciences) at 4°C for 30 minutes for all surface markers except CXCR5-biotin which was stained at room temperature for 45 minutes. Intracellular staining was performed for 45 minutes at 4°C after fixation with the FOXP3 Fix/perm kit (Invitrogen). In some studies, an additional permeabilization step was performed in 90% ice-cold methanol prior to intracellular staining for pSTAT5 and pSTAT6. Data were acquired on an Aurora flow cytometer (Cytek) and analyzed using FlowJo software (BD Biosciences).

6.7 $CD4^+$ T CELL ISOLATION AND CULTURE

For *in vitro* T cell stimulation experiments, naïve $CD4^+$ T cells were isolated from LNs and spleens using the naïve $CD4^+$ T cell isolation kit (Miltenyi Biotec) into complete RPMI media. 400,000 cells were then plated on pre-treated plates coated with the indicated concentrations of anti-CD3ε (145-2C11, Thermo Scientific) and anti-CD28 (37.51, Thermo Scientific) under Th0, +anti-IFNγ 10ug/mL; (XMG1.2, Biolegend), or Th2 (anti-IFNγ 10µg/mL (XMG1.2, Biolegend), rIL-4 50ng/mL (Peprotech)) conditions. Cells were cultured for 48 hours at 37°C and 5% CO_2 before fixation and flow cytometric analysis.

6.8 RNA SEQUENCING

Single cell suspensions from tissues were prepared as described above for myeloid cells. Cells were sorted from pooled dLNs from 3 individual mice for each group. 500 of each cDC2 cell type was sorted on an Aria III (BD Biosciences) directly into reaction buffer from the SMART-Seq v4 Ultra Low Input RNA Kit for Sequencing (Takara), and reverse transcription was performed

followed by PCR amplification to generate full length amplified cDNA. Sequencing libraries were constructed using the NexteraXT DNA sample preparation kit with unique dual indexes (Illumina) to generate Illumina-compatible barcoded libraries. Libraries were pooled and quantified using a Qubit Fluorometer (Life Technologies). Sequencing of pooled libraries was carried out on a NextSeq 2000 sequencer (Illumina) with paired-end 59-base reads, using NextSeq P2 sequencing kits (Illumina) with a target depth of 5 million reads per sample. Base calls were processed to FASTQs on BaseSpace (Illumina), and a base call quality-trimming step was applied to remove low-confidence base calls from the ends of reads. The FASTQs were aligned to the GRCm38 mouse reference genome, using STAR v.2.4.2a and gene counts were generated using htseq-count. QC and metrics analysis was performed using the Picard family of tools (v1.134). Further downstream analysis was performed using publicly available RNAseq toolkits. The Degust toolkit[181] (v4.1.1) with integrated Voom/Limma R package was used for differentially expressed gene analysis and generation of volcano plots. Only genes with count per million (CPM) ≥ 10 were analyzed further. Genes were filtered based on a false discovery rate cutoff ≤ 0.05 and a minimum expression fold change ≥ 2. DEGs were input into the WebGestalt gene set analysis toolkit[182] to identify Biological Processes Gene Ontology (GO) terms and generate the associated graphs. Heatmap data tables were generated by inputting DEG data into the BIOMEX toolkit[183]. PCA plots were generated via the DEBrowser toolkit[184] (v1.26.3), where only genes with CPM ≥ 10 were analyzed.

6.9 ANTIBODIES AND STAINING REAGENTS

Antibodies used for staining sections for confocal imaging or isolated cells for flow cytometry include: CD64 (clone X54-57.1; BioLegend), B220 (clone RA3-6B2; Biolegend), SIRPα (clone

P84; BD Biosciences), CD11c (clone N418; BD Biosciences), CD11b (clone M1/70; Biolegend), MHCII (clone M5/114.15.2; BioLegend), IRF4 (clone IRF4.3E4; BioLegend), CD45.1 (clone A20; BioLegend), Ki67 (clone B56; BD Biosciences), Y-Ae (clone eBioY-Ae; ThermoFisher Scientific), Thy1.2 (clone 30-H12; BD Biosciences), CD3 (clone 17A2; BD Biosciences), Tbet (clone 4B10; BioLegend), NK1.1 (clone PK136; BioLegend), CD19 (clone 6D5; BioLegend), CD44 (clone IM7; BioLegend), XCR1 (clone ZET; BioLegend), GATA3 (clone L50-823; BD Biosciences), CXCR3 (clone CXCR3-173; BioLegend), CXCR5 (clone 2G8; BD Biosciences), pS6 (clone 2F9; Cell Signaling Technologies), PD-1 (clone RMP1-30; BioLegend), CD45.2 (clone 104; BioLegend), CD25 (clone PC61; ThermoFisher Scientific), EpCAM (clone G8.8; ThermoFisher Scientific), CD103 (clone M290; BD Biosciences), CD301b (clone URA-1; BioLegend), CD80 (clone 16-10A1; ThermoFisher Scientific), CD86 (clone GL1; BD Biosciences), PDL-1 (clone MIH5; ThermoFisher Scientific), PDL-2 (clone MIH37; BD Biosciences), BCL6 (clone K112-91; BD Biosciences), BATF (clone D7C5 rabbit; Cell Signaling Technologies), Anti-GFP (goat; Novus Biologics), ICAM-1 (clone 3E2; BD Biosciences), CD207 (clone 929F3.01; Dendritics), CD4 (clone GK1.5; BD Biosciences), huCD2 (clone RPA-2.10; ThermoFisher Scientific), pSTAT5 (clone 47/STAT5(pY694); BD Biosciences), pSTAT6 (clone J71-773.58.11; BD Biosciences), LIVE/DEAD Near-IR (ThermoFisher), Chicken anti-goat (ThermoFisher) and Donkey anti-rabbit (ThermoFisher).

6.10 STATISTICS

Statistical analysis was performed using GraphPad Prism software. The statistical significance of differences in mean values between two groups was analyzed by a two-tailed unpaired student's *t* test with Welch's correction. Paired *t* tests were performed when comparing responses within the same experimental tissue. In bar graphs for all figures, data is shown as mean with standard

deviation. ****$p<0.0001$; ***$p<0.001$; **$p<0.01$; *$p<0.05$; $p>0.05$ not significant (ns). Unless otherwise noted, all data points represent independent LNs.

REFERENCES

1. Oliver, G., Kipnis, J., Randolph, G.J., and Harvey, N.L. (2020). The Lymphatic Vasculature in the 21(st) Century: Novel Functional Roles in Homeostasis and Disease. Cell *182*, 270-296. 10.1016/j.cell.2020.06.039.
2. Petrova, T.V., and Koh, G.Y. (2020). Biological functions of lymphatic vessels. Science *369*. 10.1126/science.aax4063.
3. Randolph, G.J., Ivanov, S., Zinselmeyer, B.H., and Scallan, J.P. (2017). The Lymphatic System: Integral Roles in Immunity. Annu Rev Immunol *35*, 31-52. 10.1146/annurev-immunol-041015-055354.
4. Clement, C.C., Cannizzo, E.S., Nastke, M.D., Sahu, R., Olszewski, W., Miller, N.E., Stern, L.J., and Santambrogio, L. (2010). An expanded self-antigen peptidome is carried by the human lymph as compared to the plasma. PLoS One *5*, e9863. 10.1371/journal.pone.0009863.
5. Pflicke, H., and Sixt, M. (2009). Preformed portals facilitate dendritic cell entry into afferent lymphatic vessels. J Exp Med *206*, 2925-2935. 10.1084/jem.20091739.
6. Schineis, P., Runge, P., and Halin, C. (2019). Cellular traffic through afferent lymphatic vessels. Vascul Pharmacol *112*, 31-41. 10.1016/j.vph.2018.08.001.
7. Stern, L.J., and Santambrogio, L. (2016). The melting pot of the MHC II peptidome. Curr Opin Immunol *40*, 70-77. 10.1016/j.coi.2016.03.004.
8. Bogoslowski, A., and Kubes, P. (2018). Lymph Nodes: The Unrecognized Barrier against Pathogens. ACS Infect Dis *4*, 1158-1161. 10.1021/acsinfecdis.8b00111.
9. Qi, H., Kastenmüller, W., and Germain, R.N. (2014). Spatiotemporal basis of innate and adaptive immunity in secondary lymphoid tissue. Annu Rev Cell Dev Biol *30*, 141-167. 10.1146/annurev-cellbio-100913-013254.
10. Eisenbarth, S.C. (2019). Dendritic cell subsets in T cell programming: location dictates function. Nat Rev Immunol *19*, 89-103. 10.1038/s41577-018-0088-1.
11. Grant, S.M., Lou, M., Yao, L., Germain, R.N., and Radtke, A.J. (2020). The lymph node at a glance - how spatial organization optimizes the immune response. J Cell Sci *133*. 10.1242/jcs.241828.
12. Gray, E.E., and Cyster, J.G. (2012). Lymph node macrophages. J Innate Immun *4*, 424-436. 10.1159/000337007.
13. Moran, I., Grootveld, A.K., Nguyen, A., and Phan, T.G. (2019). Subcapsular Sinus Macrophages: The Seat of Innate and Adaptive Memory in Murine Lymph Nodes. Trends Immunol *40*, 35-48. 10.1016/j.it.2018.11.004.
14. Gerner, M.Y., Kastenmuller, W., Ifrim, I., Kabat, J., and Germain, R.N. (2012). Histo-cytometry: a method for highly multiplex quantitative tissue imaging analysis applied to dendritic cell subset microanatomy in lymph nodes. Immunity *37*, 364-376. 10.1016/j.immuni.2012.07.011.
15. Gerner, M.Y., Torabi-Parizi, P., and Germain, R.N. (2015). Strategically localized dendritic cells promote rapid T cell responses to lymph-borne particulate antigens. Immunity *42*, 172-185. 10.1016/j.immuni.2014.12.024.
16. Leal, J.M., Huang, J.Y., Kohli, K., Stoltzfus, C., Lyons-Cohen, M.R., Olin, B.E., Gale, M., and Gerner, M.Y. (2021). Innate cell microenvironments in lymph nodes shape the generation of T cell responses during type I inflammation. Sci Immunol *6*. 10.1126/sciimmunol.abb9435.

17. Gerner, M.Y., Casey, K.A., Kastenmuller, W., and Germain, R.N. (2017). Dendritic cell and antigen dispersal landscapes regulate T cell immunity. J Exp Med *214*, 3105-3122. 10.1084/jem.20170335.
18. Stoltzfus, C.R., Filipek, J., Gern, B.H., Olin, B.E., Leal, J.M., Wu, Y., Lyons-Cohen, M.R., Huang, J.Y., Paz-Stoltzfus, C.L., Plumlee, C.R., et al. (2020). CytoMAP: A Spatial Analysis Toolbox Reveals Features of Myeloid Cell Organization in Lymphoid Tissues. Cell Rep *31*, 107523. 10.1016/j.celrep.2020.107523.
19. Eickhoff, S., Brewitz, A., Gerner, M.Y., Klauschen, F., Komander, K., Hemmi, H., Garbi, N., Kaisho, T., Germain, R.N., and Kastenmüller, W. (2015). Robust Anti-viral Immunity Requires Multiple Distinct T Cell-Dendritic Cell Interactions. Cell *162*, 1322-1337. 10.1016/j.cell.2015.08.004.
20. Hor, J.L., Whitney, P.G., Zaid, A., Brooks, A.G., Heath, W.R., and Mueller, S.N. (2015). Spatiotemporally Distinct Interactions with Dendritic Cell Subsets Facilitates CD4+ and CD8+ T Cell Activation to Localized Viral Infection. Immunity *43*, 554-565. 10.1016/j.immuni.2015.07.020.
21. Ruhland, M.K., Roberts, E.W., Cai, E., Mujal, A.M., Marchuk, K., Beppler, C., Nam, D., Serwas, N.K., Binnewies, M., and Krummel, M.F. (2020). Visualizing Synaptic Transfer of Tumor Antigens among Dendritic Cells. Cancer Cell *37*, 786-799.e785. 10.1016/j.ccell.2020.05.002.
22. Granot, T., Senda, T., Carpenter, D.J., Matsuoka, N., Weiner, J., Gordon, C.L., Miron, M., Kumar, B.V., Griesemer, A., Ho, S.H., et al. (2017). Dendritic Cells Display Subset and Tissue-Specific Maturation Dynamics over Human Life. Immunity *46*, 504-515. 10.1016/j.immuni.2017.02.019.
23. Baratin, M., Foray, C., Demaria, O., Habbeddine, M., Pollet, E., Maurizio, J., Verthuy, C., Davanture, S., Azukizawa, H., Flores-Langarica, A., et al. (2015). Homeostatic NF-κB Signaling in Steady-State Migratory Dendritic Cells Regulates Immune Homeostasis and Tolerance. Immunity *42*, 627-639. 10.1016/j.immuni.2015.03.003.
24. Cabeza-Cabrerizo, M., Cardoso, A., Minutti, C.M., Pereira da Costa, M., and Reis, E.S.C. (2021). Dendritic Cells Revisited. Annu Rev Immunol *39*, 131-166. 10.1146/annurev-immunol-061020-053707.
25. Devi, K.S., and Anandasabapathy, N. (2017). The origin of DCs and capacity for immunologic tolerance in central and peripheral tissues. Semin Immunopathol *39*, 137-152. 10.1007/s00281-016-0602-0.
26. Manicassamy, S., and Pulendran, B. (2011). Dendritic cell control of tolerogenic responses. Immunol Rev *241*, 206-227. 10.1111/j.1600-065X.2011.01015.x.
27. Bastow, C.R., Bunting, M.D., Kara, E.E., McKenzie, D.R., Caon, A., Devi, S., Tolley, L., Mueller, S.N., Frazer, I.H., Harvey, N., et al. (2021). Scavenging of soluble and immobilized CCL21 by ACKR4 regulates peripheral dendritic cell emigration. Proc Natl Acad Sci U S A *118*. 10.1073/pnas.2025763118.
28. Weber, M., Hauschild, R., Schwarz, J., Moussion, C., de Vries, I., Legler, D.F., Luther, S.A., Bollenbach, T., and Sixt, M. (2013). Interstitial dendritic cell guidance by haptotactic chemokine gradients. Science *339*, 328-332. 10.1126/science.1228456.
29. Worbs, T., Hammerschmidt, S.I., and Förster, R. (2017). Dendritic cell migration in health and disease. Nat Rev Immunol *17*, 30-48. 10.1038/nri.2016.116.
30. Kissenpfennig, A., Henri, S., Dubois, B., Laplace-Builhé, C., Perrin, P., Romani, N., Tripp, C.H., Douillard, P., Leserman, L., Kaiserlian, D., et al. (2005). Dynamics and

function of Langerhans cells in vivo: dermal dendritic cells colonize lymph node areas distinct from slower migrating Langerhans cells. Immunity *22*, 643-654. 10.1016/j.immuni.2005.04.004.

31. Kitano, M., Yamazaki, C., Takumi, A., Ikeno, T., Hemmi, H., Takahashi, N., Shimizu, K., Fraser, S.E., Hoshino, K., Kaisho, T., and Okada, T. (2016). Imaging of the cross-presenting dendritic cell subsets in the skin-draining lymph node. Proc Natl Acad Sci U S A *113*, 1044-1049. 10.1073/pnas.1513607113.
32. Connor, L.M., Tang, S.C., Cognard, E., Ochiai, S., Hilligan, K.L., Old, S.I., Pellefigues, C., White, R.F., Patel, D., Smith, A.A., et al. (2017). Th2 responses are primed by skin dendritic cells with distinct transcriptional profiles. J Exp Med *214*, 125-142. 10.1084/jem.20160470.
33. Kumamoto, Y., Linehan, M., Weinstein, J.S., Laidlaw, B.J., Craft, J.E., and Iwasaki, A. (2013). CD301b^{+} dermal dendritic cells drive T helper 2 cell-mediated immunity. Immunity *39*, 733-743. 10.1016/j.immuni.2013.08.029.
34. Ochiai, S., Roediger, B., Abtin, A., Shklovskaya, E., Fazekas de St Groth, B., Yamane, H., Weninger, W., Le Gros, G., and Ronchese, F. (2014). CD326(lo)CD103(lo)CD11b(lo) dermal dendritic cells are activated by thymic stromal lymphopoietin during contact sensitization in mice. J Immunol *193*, 2504-2511. 10.4049/jimmunol.1400536.
35. Klein, L., Kyewski, B., Allen, P.M., and Hogquist, K.A. (2014). Positive and negative selection of the T cell repertoire: what thymocytes see (and don't see). Nat Rev Immunol *14*, 377-391. 10.1038/nri3667.
36. Liu, Z., Gerner, M.Y., Van Panhuys, N., Levine, A.G., Rudensky, A.Y., and Germain, R.N. (2015). Immune homeostasis enforced by co-localized effector and regulatory T cells. Nature *528*, 225-230. 10.1038/nature16169.
37. Wong, H.S., Park, K., Gola, A., Baptista, A.P., Miller, C.H., Deep, D., Lou, M., Boyd, L.F., Rudensky, A.Y., Savage, P.A., et al. (2021). A local regulatory T cell feedback circuit maintains immune homeostasis by pruning self-activated T cells. Cell *184*, 3981-3997.e3922. 10.1016/j.cell.2021.05.028.
38. Gratz, I.K., and Campbell, D.J. (2014). Organ-specific and memory treg cells: specificity, development, function, and maintenance. Front Immunol *5*, 333. 10.3389/fimmu.2014.00333.
39. Smigiel, K.S., Richards, E., Srivastava, S., Thomas, K.R., Dudda, J.C., Klonowski, K.D., and Campbell, D.J. (2014). CCR7 provides localized access to IL-2 and defines homeostatically distinct regulatory T cell subsets. J Exp Med *211*, 121-136. 10.1084/jem.20131142.
40. Buszko, M., and Shevach, E.M. (2020). Control of regulatory T cell homeostasis. Curr Opin Immunol *67*, 18-26. 10.1016/j.coi.2020.07.001.
41. Hilligan, K.L., and Ronchese, F. (2020). Antigen presentation by dendritic cells and their instruction of CD4+ T helper cell responses. Cell Mol Immunol *17*, 587-599. 10.1038/s41423-020-0465-0.
42. Gao, Y., Nish, S.A., Jiang, R., Hou, L., Licona-Limón, P., Weinstein, J.S., Zhao, H., and Medzhitov, R. (2013). Control of T helper 2 responses by transcription factor IRF4-dependent dendritic cells. Immunity *39*, 722-732. 10.1016/j.immuni.2013.08.028.
43. Williams, J.W., Tjota, M.Y., Clay, B.S., Vander Lugt, B., Bandukwala, H.S., Hrusch, C.L., Decker, D.C., Blaine, K.M., Fixsen, B.R., Singh, H., et al. (2013). Transcription

factor IRF4 drives dendritic cells to promote Th2 differentiation. Nat Commun *4*, 2990. 10.1038/ncomms3990.

44. Plantinga, M., Guilliams, M., Vanheerswynghels, M., Deswarte, K., Branco-Madeira, F., Toussaint, W., Vanhoutte, L., Neyt, K., Killeen, N., Malissen, B., et al. (2013). Conventional and monocyte-derived CD11b(+) dendritic cells initiate and maintain T helper 2 cell-mediated immunity to house dust mite allergen. Immunity *38*, 322-335. 10.1016/j.immuni.2012.10.016.
45. Tussiwand, R., Everts, B., Grajales-Reyes, G.E., Kretzer, N.M., Iwata, A., Bagaitkar, J., Wu, X., Wong, R., Anderson, D.A., Murphy, T.L., et al. (2015). Klf4 expression in conventional dendritic cells is required for T helper 2 cell responses. Immunity *42*, 916-928. 10.1016/j.immuni.2015.04.017.
46. Hilligan, K.L., Tang, S.C., Hyde, E.J., Roussel, E., Mayer, J.U., Yang, J., Wakelin, K.A., Schmidt, A.J., Connor, L.M., Sher, A., et al. (2020). Dermal IRF4+ dendritic cells and monocytes license CD4+ T helper cells to distinct cytokine profiles. Nat Commun *11*, 5637. 10.1038/s41467-020-19463-9.
47. Yin, X., Chen, S., and Eisenbarth, S.C. (2021). Dendritic Cell Regulation of T Helper Cells. Annu Rev Immunol *39*, 759-790. 10.1146/annurev-immunol-101819-025146.
48. Sokol, C.L., Camire, R.B., Jones, M.C., and Luster, A.D. (2018). The Chemokine Receptor CCR8 Promotes the Migration of Dendritic Cells into the Lymph Node Parenchyma to Initiate the Allergic Immune Response. Immunity *49*, 449-463.e446. 10.1016/j.immuni.2018.07.012.
49. León, B., Ballesteros-Tato, A., Browning, J.L., Dunn, R., Randall, T.D., and Lund, F.E. (2012). Regulation of T(H)2 development by CXCR5+ dendritic cells and lymphotoxin-expressing B cells. Nat Immunol *13*, 681-690. 10.1038/ni.2309.
50. Liu, Q., Liu, Z., Rozo, C.T., Hamed, H.A., Alem, F., Urban, J.F., Jr., and Gause, W.C. (2007). The role of B cells in the development of CD4 effector T cells during a polarized Th2 immune response. J Immunol *179*, 3821-3830. 10.4049/jimmunol.179.6.3821.
51. Randolph, D.A., Huang, G., Carruthers, C.J., Bromley, L.E., and Chaplin, D.D. (1999). The role of CCR7 in TH1 and TH2 cell localization and delivery of B cell help in vivo. Science *286*, 2159-2162. 10.1126/science.286.5447.2159.
52. León, B., and Lund, F.E. (2019). Compartmentalization of dendritic cell and T-cell interactions in the lymph node: Anatomy of T-cell fate decisions. Immunol Rev *289*, 84-100. 10.1111/imr.12758.
53. Ito, T., Wang, Y.H., Duramad, O., Hori, T., Delespesse, G.J., Watanabe, N., Qin, F.X., Yao, Z., Cao, W., and Liu, Y.J. (2005). TSLP-activated dendritic cells induce an inflammatory T helper type 2 cell response through OX40 ligand. J Exp Med *202*, 1213-1223. 10.1084/jem.20051135.
54. Kitajima, M., and Ziegler, S.F. (2013). Cutting edge: identification of the thymic stromal lymphopoietin-responsive dendritic cell subset critical for initiation of type 2 contact hypersensitivity. J Immunol *191*, 4903-4907. 10.4049/jimmunol.1302175.
55. Tindemans, I., Peeters, M.J.W., and Hendriks, R.W. (2017). Notch Signaling in T Helper Cell Subsets: Instructor or Unbiased Amplifier? Front Immunol *8*, 419. 10.3389/fimmu.2017.00419.
56. Walker, J.A., and McKenzie, A.N.J. (2018). T H 2 cell development and function. Nat Rev Immunol *18*, 121-133. 10.1038/nri.2017.118.

57. King, I.L., and Mohrs, M. (2009). IL-4-producing CD4+ T cells in reactive lymph nodes during helminth infection are T follicular helper cells. J Exp Med *206*, 1001-1007. 10.1084/jem.20090313.
58. Glatman Zaretsky, A., Taylor, J.J., King, I.L., Marshall, F.A., Mohrs, M., and Pearce, E.J. (2009). T follicular helper cells differentiate from Th2 cells in response to helminth antigens. J Exp Med *206*, 991-999. 10.1084/jem.20090303.
59. Prout, M.S., Kyle, R.L., Ronchese, F., and Le Gros, G. (2018). IL-4 Is a Key Requirement for IL-4- and IL-4/IL-13-Expressing CD4 Th2 Subsets in Lung and Skin. Front Immunol *9*, 1211. 10.3389/fimmu.2018.01211.
60. Sokol, C.L., Barton, G.M., Farr, A.G., and Medzhitov, R. (2008). A mechanism for the initiation of allergen-induced T helper type 2 responses. Nat Immunol *9*, 310-318. 10.1038/ni1558.
61. Tang, H., Cao, W., Kasturi, S.P., Ravindran, R., Nakaya, H.I., Kundu, K., Murthy, N., Kepler, T.B., Malissen, B., and Pulendran, B. (2010). The T helper type 2 response to cysteine proteases requires dendritic cell-basophil cooperation via ROS-mediated signaling. Nat Immunol *11*, 608-617. 10.1038/ni.1883.
62. Sokol, C.L., Chu, N.Q., Yu, S., Nish, S.A., Laufer, T.M., and Medzhitov, R. (2009). Basophils function as antigen-presenting cells for an allergen-induced T helper type 2 response. Nat Immunol *10*, 713-720. 10.1038/ni.1738.
63. Hammad, H., Plantinga, M., Deswarte, K., Pouliot, P., Willart, M.A., Kool, M., Muskens, F., and Lambrecht, B.N. (2010). Inflammatory dendritic cells--not basophils--are necessary and sufficient for induction of Th2 immunity to inhaled house dust mite allergen. J Exp Med *207*, 2097-2111. 10.1084/jem.20101563.
64. Kim, S., Prout, M., Ramshaw, H., Lopez, A.F., LeGros, G., and Min, B. (2010). Cutting edge: basophils are transiently recruited into the draining lymph nodes during helminth infection via IL-3, but infection-induced Th2 immunity can develop without basophil lymph node recruitment or IL-3. J Immunol *184*, 1143-1147. 10.4049/jimmunol.0902447.
65. He, K., Hettinga, A., Kale, S.L., Hu, S., Xie, M.M., Dent, A.L., Ray, A., and Poholek, A.C. (2020). Blimp-1 is essential for allergen-induced asthma and Th2 cell development in the lung. J Exp Med *217*. 10.1084/jem.20190742.
66. Bosteels, C., Neyt, K., Vanheerswynghels, M., van Helden, M.J., Sichien, D., Debeuf, N., De Prijck, S., Bosteels, V., Vandamme, N., Martens, L., et al. (2020). Inflammatory Type 2 cDCs Acquire Features of cDC1s and Macrophages to Orchestrate Immunity to Respiratory Virus Infection. Immunity *52*, 1039-1056.e1039. 10.1016/j.immuni.2020.04.005.
67. Li, J., Lu, E., Yi, T., and Cyster, J.G. (2016). EBI2 augments Tfh cell fate by promoting interaction with IL-2-quenching dendritic cells. Nature *533*, 110-114. 10.1038/nature17947.
68. Krishnaswamy, J.K., Gowthaman, U., Zhang, B., Mattsson, J., Szeponik, L., Liu, D., Wu, R., White, T., Calabro, S., Xu, L., et al. (2017). Migratory CD11b + conventional dendritic cells induce T follicular helper cell–dependent antibody responses. Sci Immunol *2*. 10.1126/sciimmunol.aam9169.
69. De Giovanni, M., Cutillo, V., Giladi, A., Sala, E., Maganuco, C.G., Medaglia, C., Di Lucia, P., Bono, E., Cristofani, C., Consolo, E., et al. (2020). Spatiotemporal regulation

of type I interferon expression determines the antiviral polarization of CD4. Nat Immunol *21*, 321-330. 10.1038/s41590-020-0596-6.

70. Crotty, S. (2019). T Follicular Helper Cell Biology: A Decade of Discovery and Diseases. Immunity *50*, 1132-1148. 10.1016/j.immuni.2019.04.011.
71. Kumamoto, Y., Hirai, T., Wong, P.W., Kaplan, D.H., and Iwasaki, A. (2016). CD301b + dendritic cells suppress T follicular helper cells and antibody responses to protein antigens. Elife *5*. 10.7554/eLife.17979.
72. van Panhuys, N., Klauschen, F., and Germain, R.N. (2014). T-cell-receptor-dependent signal intensity dominantly controls CD4(+) T cell polarization In Vivo. Immunity *41*, 63-74. 10.1016/j.immuni.2014.06.003.
73. van Panhuys, N. (2016). TCR Signal Strength Alters T-DC Activation and Interaction Times and Directs the Outcome of Differentiation. Front Immunol *7*, 6. 10.3389/fimmu.2016.00006.
74. Bhattacharyya, N.D., and Feng, C.G. (2020). Regulation of T Helper Cell Fate by TCR Signal Strength. Front Immunol *11*, 624. 10.3389/fimmu.2020.00624.
75. Mempel, T.R., Henrickson, S.E., and Von Andrian, U.H. (2004). T-cell priming by dendritic cells in lymph nodes occurs in three distinct phases. Nature *427*, 154-159. 10.1038/nature02238.
76. Zhu, J., Jankovic, D., Oler, A.J., Wei, G., Sharma, S., Hu, G., Guo, L., Yagi, R., Yamane, H., Punkosdy, G., et al. (2012). The transcription factor T-bet is induced by multiple pathways and prevents an endogenous Th2 cell program during Th1 cell responses. Immunity *37*, 660-673. 10.1016/j.immuni.2012.09.007.
77. Tao, X., Constant, S., Jorritsma, P., and Bottomly, K. (1997). Strength of TCR signal determines the costimulatory requirements for Th1 and Th2 CD4+ T cell differentiation. J Immunol *159*, 5956-5963.
78. Rulifson, I.C., Sperling, A.I., Fields, P.E., Fitch, F.W., and Bluestone, J.A. (1997). CD28 costimulation promotes the production of Th2 cytokines. J Immunol *158*, 658-665.
79. van Rijt, L.S., Vos, N., Willart, M., Kleinjan, A., Coyle, A.J., Hoogsteden, H.C., and Lambrecht, B.N. (2004). Essential role of dendritic cell CD80/CD86 costimulation in the induction, but not reactivation, of TH2 effector responses in a mouse model of asthma. J Allergy Clin Immunol *114*, 166-173. 10.1016/j.jaci.2004.03.044.
80. King, C.L., Stupi, R.J., Craighead, N., June, C.H., and Thyphronitis, G. (1995). CD28 activation promotes Th2 subset differentiation by human CD4+ cells. Eur J Immunol *25*, 587-595. 10.1002/eji.1830250242.
81. Gause, W.C., Chen, S.J., Greenwald, R.J., Halvorson, M.J., Lu, P., Zhou, X.D., Morris, S.C., Lee, K.P., June, C.H., Finkelman, F.D., et al. (1997). CD28 dependence of T cell differentiation to IL-4 production varies with the particular type 2 immune response. J Immunol *158*, 4082-4087.
82. Liu, Z., Liu, Q., Pesce, J., Anthony, R.M., Lamb, E., Whitmire, J., Hamed, H., Morimoto, M., Urban, J.F., and Gause, W.C. (2004). Requirements for the development of IL-4-producing T cells during intestinal nematode infections: what it takes to make a Th2 cell in vivo. Immunol Rev *201*, 57-74. 10.1111/j.0105-2896.2004.00186.x.
83. Besnard, A.G., Togbe, D., Guillou, N., Erard, F., Quesniaux, V., and Ryffel, B. (2011). IL-33-activated dendritic cells are critical for allergic airway inflammation. Eur J Immunol *41*, 1675-1686. 10.1002/eji.201041033.

84. Stanbery, A.G., Shuchi Smita, Jakob von Moltke, Tait Wojno, E.D., and Ziegler, S.F. (2022). TSLP, IL-33, and IL-25: Not just for allergy and helminth infection. J Allergy Clin Immunol *150*, 1302-1313. 10.1016/j.jaci.2022.07.003.
85. Hung, L.Y., Tanaka, Y., Herbine, K., Pastore, C., Singh, B., Ferguson, A., Vora, N., Douglas, B., Zullo, K., Behrens, E.M., et al. (2020). Cellular context of IL-33 expression dictates impact on anti-helminth immunity. Sci Immunol *5*. 10.1126/sciimmunol.abc6259.
86. Kopp, E.B., Agaronyan, K., Licona-Limón, I., Nish, S.A., and Medzhitov, R. (2023). Modes of type 2 immune response initiation. Immunity *56*, 687-694. 10.1016/j.immuni.2023.03.015.
87. Chu, D.K., Mohammed-Ali, Z., Jiménez-Saiz, R., Walker, T.D., Goncharova, S., Llop-Guevara, A., Kong, J., Gordon, M.E., Barra, N.G., Gillgrass, A.E., et al. (2014). T helper cell IL-4 drives intestinal Th2 priming to oral peanut antigen, under the control of OX40L and independent of innate-like lymphocytes. Mucosal Immunol *7*, 1395-1404. 10.1038/mi.2014.29.
88. Noben-Trauth, N., Hu-Li, J., and Paul, W.E. (2000). Conventional, naive CD4+ T cells provide an initial source of IL-4 during Th2 differentiation. J Immunol *165*, 3620-3625. 10.4049/jimmunol.165.7.3620.
89. Noben-Trauth, N., Hu-Li, J., and Paul, W.E. (2002). IL-4 secreted from individual naive CD4+ T cells acts in an autocrine manner to induce Th2 differentiation. Eur J Immunol *32*, 1428-1433. 10.1002/1521-4141(200205)32:5<1428::AID-IMMU1428>3.0.CO;2-0.
90. Paul, W.E., and Zhu, J. (2010). How are T(H)2-type immune responses initiated and amplified? Nat Rev Immunol *10*, 225-235. 10.1038/nri2735.
91. Hondowicz, B.D., An, D., Schenkel, J.M., Kim, K.S., Steach, H.R., Krishnamurty, A.T., Keitany, G.J., Garza, E.N., Fraser, K.A., Moon, J.J., et al. (2016). Interleukin-2-Dependent Allergen-Specific Tissue-Resident Memory Cells Drive Asthma. Immunity *44*, 155-166. 10.1016/j.immuni.2015.11.004.
92. Sabatos, C.A., Doh, J., Chakravarti, S., Friedman, R.S., Pandurangi, P.G., Tooley, A.J., and Krummel, M.F. (2008). A synaptic basis for paracrine interleukin-2 signaling during homotypic T cell interaction. Immunity *29*, 238-248. 10.1016/j.immuni.2008.05.017.
93. DiToro, D., Winstead, C.J., Pham, D., Witte, S., Andargachew, R., Singer, J.R., Wilson, C.G., Zindl, C.L., Luther, R.J., Silberger, D.J., et al. (2018). Differential IL-2 expression defines developmental fates of follicular versus nonfollicular helper T cells. Science *361*. 10.1126/science.aao2933.
94. Longhi, M.P., Trumpfheller, C., Idoyaga, J., Caskey, M., Matos, I., Kluger, C., Salazar, A.M., Colonna, M., and Steinman, R.M. (2009). Dendritic cells require a systemic type I interferon response to mature and induce CD4+ Th1 immunity with poly IC as adjuvant. J Exp Med *206*, 1589-1602. 10.1084/jem.20090247.
95. Wang, Y., Cella, M., Gilfillan, S., and Colonna, M. (2010). Cutting edge: polyinosinic:polycytidylic acid boosts the generation of memory CD8 T cells through melanoma differentiation-associated protein 5 expressed in stromal cells. J Immunol *184*, 2751-2755. 10.4049/jimmunol.0903201.
96. Irvine, D.J., Aung, A., and Silva, M. (2020). Controlling timing and location in vaccines. Adv Drug Deliv Rev *158*, 91-115. 10.1016/j.addr.2020.06.019.
97. Schudel, A., Francis, D.M., and Thomas, S.N. (2019). Material design for lymph node drug delivery. Nat Rev Mater *4*, 415-428. 10.1038/s41578-019-0110-7.

98. Blecher-Gonen, R., Bost, P., Hilligan, K.L., David, E., Salame, T.M., Roussel, E., Connor, L.M., Mayer, J.U., Bahar Halpern, K., Tóth, B., et al. (2019). Single-Cell Analysis of Diverse Pathogen Responses Defines a Molecular Roadmap for Generating Antigen-Specific Immunity. Cell Syst *8*, 109-121.e106. 10.1016/j.cels.2019.01.001.
99. León, B. (2023). A model of Th2 differentiation based on polarizing cytokine repression. Trends Immunol *44*, 399-407. 10.1016/j.it.2023.04.004.
100. Everts, B., Tussiwand, R., Dreesen, L., Fairfax, K.C., Huang, S.C., Smith, A.M., O'Neill, C.M., Lam, W.Y., Edelson, B.T., Urban, J.F., et al. (2016). Migratory CD103+ dendritic cells suppress helminth-driven type 2 immunity through constitutive expression of IL-12. J Exp Med *213*, 35-51. 10.1084/jem.20150235.
101. Conejero, L., Khouili, S.C., Martínez-Cano, S., Izquierdo, H.M., Brandi, P., and Sancho, D. (2017). Lung CD103+ dendritic cells restrain allergic airway inflammation through IL-12 production. JCI Insight *2*. 10.1172/jci.insight.90420.
102. Vance, R.E., Isberg, R.R., and Portnoy, D.A. (2009). Patterns of pathogenesis: discrimination of pathogenic and nonpathogenic microbes by the innate immune system. Cell Host Microbe *6*, 10-21. 10.1016/j.chom.2009.06.007.
103. Cayrol, C., Duval, A., Schmitt, P., Roga, S., Camus, M., Stella, A., Burlet-Schiltz, O., Gonzalez-de-Peredo, A., and Girard, J.P. (2018). Environmental allergens induce allergic inflammation through proteolytic maturation of IL-33. Nat Immunol *19*, 375-385. 10.1038/s41590-018-0067-5.
104. Pulendran, B., and Artis, D. (2012). New paradigms in type 2 immunity. Science *337*, 431-435. 10.1126/science.1221064.
105. Wan, H., Winton, H.L., Soeller, C., Gruenert, D.C., Thompson, P.J., Cannell, M.B., Stewart, G.A., Garrod, D.R., and Robinson, C. (2000). Quantitative structural and biochemical analyses of tight junction dynamics following exposure of epithelial cells to house dust mite allergen Der p 1. Clin Exp Allergy *30*, 685-698. 10.1046/j.1365-2222.2000.00820.x.
106. Sharafutdinov, I., Esmaeili, D.S., Harrer, A., Tegtmeyer, N., Sticht, H., and Backert, S. (2020). Serine Protease HtrA Cleaves the Tight Junction Component Claudin-8. Front Cell Infect Microbiol *10*, 590186. 10.3389/fcimb.2020.590186.
107. Donnelly, S., Dalton, J.P., and Loukas, A. (2006). Proteases in helminth- and allergen-induced inflammatory responses. Chem Immunol Allergy *90*, 45-64. 10.1159/000088880.
108. Caffrey, C.R., Goupil, L., Rebello, K.M., Dalton, J.P., and Smith, D. (2018). Cysteine proteases as digestive enzymes in parasitic helminths. PLoS Negl Trop Dis *12*, e0005840. 10.1371/journal.pntd.0005840.
109. Schneider, C., Shen, C., Gopal, A.A., Douglas, T., Forestell, B., Kauffman, K.D., Rogers, D., Artusa, P., Zhang, Q., Jing, H., et al. (2020). Migration-induced cell shattering due to DOCK8 deficiency causes a type 2-biased helper T cell response. Nat Immunol *21*, 1528-1539. 10.1038/s41590-020-0795-1.
110. Ronchese, F., Hilligan, K.L., and Mayer, J.U. (2020). Dendritic cells and the skin environment. Curr Opin Immunol *64*, 56-62. 10.1016/j.coi.2020.03.006.
111. Sumpter, T.L., Balmert, S.C., and Kaplan, D.H. (2019). Cutaneous immune responses mediated by dendritic cells and mast cells. JCI Insight *4*. 10.1172/jci.insight.123947.
112. Roan, F., Obata-Ninomiya, K., and Ziegler, S.F. (2019). Epithelial cell-derived cytokines: more than just signaling the alarm. J Clin Invest *129*, 1441-1451. 10.1172/JCI124606.

113. Bell, B.D., Kitajima, M., Larson, R.P., Stoklasek, T.A., Dang, K., Sakamoto, K., Wagner, K.U., Kaplan, D.H., Reizis, B., Hennighausen, L., and Ziegler, S.F. (2013). The transcription factor STAT5 is critical in dendritic cells for the development of TH2 but not TH1 responses. Nat Immunol *14*, 364-371. 10.1038/ni.2541.
114. Larson, R.P., Zimmerli, S.C., Comeau, M.R., Itano, A., Omori, M., Iseki, M., Hauser, C., and Ziegler, S.F. (2010). Dibutyl phthalate-induced thymic stromal lymphopoietin is required for Th2 contact hypersensitivity responses. J Immunol *184*, 2974-2984. 10.4049/jimmunol.0803478.
115. Rank, M.A., Kobayashi, T., Kozaki, H., Bartemes, K.R., Squillace, D.L., and Kita, H. (2009). IL-33-activated dendritic cells induce an atypical TH2-type response. J Allergy Clin Immunol *123*, 1047-1054. 10.1016/j.jaci.2009.02.026.
116. Chu, D.K., Llop-Guevara, A., Walker, T.D., Flader, K., Goncharova, S., Boudreau, J.E., Moore, C.L., Seunghyun In, T., Waserman, S., Coyle, A.J., et al. (2013). IL-33, but not thymic stromal lymphopoietin or IL-25, is central to mite and peanut allergic sensitization. J Allergy Clin Immunol *131*, 187-200.e181-188. 10.1016/j.jaci.2012.08.002.
117. de Kleer, I.M., Kool, M., de Bruijn, M.J., Willart, M., van Moorleghem, J., Schuijs, M.J., Plantinga, M., Beyaert, R., Hams, E., Fallon, P.G., et al. (2016). Perinatal Activation of the Interleukin-33 Pathway Promotes Type 2 Immunity in the Developing Lung. Immunity *45*, 1285-1298. 10.1016/j.immuni.2016.10.031.
118. Carroll-Portillo, A., Cannon, J.L., te Riet, J., Holmes, A., Kawakami, Y., Kawakami, T., Cambi, A., and Lidke, D.S. (2015). Mast cells and dendritic cells form synapses that facilitate antigen transfer for T cell activation. J Cell Biol *210*, 851-864. 10.1083/jcb.201412074.
119. Shimokawa, C., Kanaya, T., Hachisuka, M., Ishiwata, K., Hisaeda, H., Kurashima, Y., Kiyono, H., Yoshimoto, T., Kaisho, T., and Ohno, H. (2017). Mast Cells Are Crucial for Induction of Group 2 Innate Lymphoid Cells and Clearance of Helminth Infections. Immunity *46*, 863-874.e864. 10.1016/j.immuni.2017.04.017.
120. Suto, H., Nakae, S., Kakurai, M., Sedgwick, J.D., Tsai, M., and Galli, S.J. (2006). Mast cell-associated TNF promotes dendritic cell migration. J Immunol *176*, 4102-4112. 10.4049/jimmunol.176.7.4102.
121. Halim, T.Y., Steer, C.A., Mathä, L., Gold, M.J., Martinez-Gonzalez, I., McNagny, K.M., McKenzie, A.N., and Takei, F. (2014). Group 2 innate lymphoid cells are critical for the initiation of adaptive T helper 2 cell-mediated allergic lung inflammation. Immunity *40*, 425-435. 10.1016/j.immuni.2014.01.011.
122. Halim, T.Y., Hwang, Y.Y., Scanlon, S.T., Zaghouani, H., Garbi, N., Fallon, P.G., and McKenzie, A.N. (2016). Group 2 innate lymphoid cells license dendritic cells to potentiate memory TH2 cell responses. Nat Immunol *17*, 57-64. 10.1038/ni.3294.
123. Dahlgren, M.W., Jones, S.W., Cautivo, K.M., Dubinin, A., Ortiz-Carpena, J.F., Farhat, S., Yu, K.S., Lee, K., Wang, C., Molofsky, A.V., et al. (2019). Adventitial Stromal Cells Define Group 2 Innate Lymphoid Cell Tissue Niches. Immunity *50*, 707-722.e706. 10.1016/j.immuni.2019.02.002.
124. Dahlgren, M.W., and Molofsky, A.B. (2019). Adventitial Cuffs: Regional Hubs for Tissue Immunity. Trends Immunol *40*, 877-887. 10.1016/j.it.2019.08.002.
125. Perner, C., Flayer, C.H., Zhu, X., Aderhold, P.A., Dewan, Z.N.A., Voisin, T., Camire, R.B., Chow, O.A., Chiu, I.M., and Sokol, C.L. (2020). Substance P Release by Sensory

Neurons Triggers Dendritic Cell Migration and Initiates the Type-2 Immune Response to Allergens. Immunity *53*, 1063-1077.e1067. 10.1016/j.immuni.2020.10.001.

126. Webb, L.M., Lundie, R.J., Borger, J.G., Brown, S.L., Connor, L.M., Cartwright, A.N., Dougall, A.M., Wilbers, R.H., Cook, P.C., Jackson-Jones, L.H., et al. (2017). Type I interferon is required for T helper (Th) 2 induction by dendritic cells. EMBO J *36*, 2404-2418. 10.15252/embj.201695345.
127. Groom, J.R., Richmond, J., Murooka, T.T., Sorensen, E.W., Sung, J.H., Bankert, K., von Andrian, U.H., Moon, J.J., Mempel, T.R., and Luster, A.D. (2012). CXCR3 chemokine receptor-ligand interactions in the lymph node optimize CD4+ T helper 1 cell differentiation. Immunity *37*, 1091-1103. 10.1016/j.immuni.2012.08.016.
128. Mohrs, M., Shinkai, K., Mohrs, K., and Locksley, R.M. (2001). Analysis of type 2 immunity in vivo with a bicistronic IL-4 reporter. Immunity *15*, 303-311. 10.1016/s1074-7613(01)00186-8.
129. Gérard, A., Khan, O., Beemiller, P., Oswald, E., Hu, J., Matloubian, M., and Krummel, M.F. (2013). Secondary T cell-T cell synaptic interactions drive the differentiation of protective CD8+ T cells. Nat Immunol *14*, 356-363. 10.1038/ni.2547.
130. von Moltke, J., Ji, M., Liang, H.E., and Locksley, R.M. (2016). Tuft-cell-derived IL-25 regulates an intestinal ILC2-epithelial response circuit. Nature *529*, 221-225. 10.1038/nature16161.
131. Jiang, W., Lederman, M.M., Harding, C.V., Rodriguez, B., Mohner, R.J., and Sieg, S.F. (2007). TLR9 stimulation drives naïve B cells to proliferate and to attain enhanced antigen presenting function. Eur J Immunol *37*, 2205-2213. 10.1002/eji.200636984.
132. Crotty, S. (2014). T follicular helper cell differentiation, function, and roles in disease. Immunity *41*, 529-542. 10.1016/j.immuni.2014.10.004.
133. Johnston, R.J., Choi, Y.S., Diamond, J.A., Yang, J.A., and Crotty, S. (2012). STAT5 is a potent negative regulator of TFH cell differentiation. J Exp Med *209*, 243-250. 10.1084/jem.20111174.
134. Ruterbusch, M., Pruner, K.B., Shehata, L., and Pepper, M. (2020). In Vivo CD4+ T Cell Differentiation and Function: Revisiting the Th1/Th2 Paradigm. Annu Rev Immunol *38*, 705-725. 10.1146/annurev-immunol-103019-085803.
135. Fang, D., and Zhu, J. (2017). Dynamic balance between master transcription factors determines the fates and functions of CD4 T cell and innate lymphoid cell subsets. J Exp Med *214*, 1861-1876. 10.1084/jem.20170494.
136. Chandler, J., Prout, M., Old, S., Morgan, C., Ronchese, F., Benoist, C., and Le Gros, G. (2022). BCL6 deletion in CD4 T cells does not affect Th2 effector mediated immunity in the skin. Immunol Cell Biol *100*, 791-804. 10.1111/imcb.12589.
137. Johnston, R.J., Poholek, A.C., DiToro, D., Yusuf, I., Eto, D., Barnett, B., Dent, A.L., Craft, J., and Crotty, S. (2009). Bcl6 and Blimp-1 are reciprocal and antagonistic regulators of T follicular helper cell differentiation. Science *325*, 1006-1010. 10.1126/science.1175870.
138. Pepper, M., Pagán, A.J., Igyártó, B.Z., Taylor, J.J., and Jenkins, M.K. (2011). Opposing signals from the Bcl6 transcription factor and the interleukin-2 receptor generate T helper 1 central and effector memory cells. Immunity *35*, 583-595. 10.1016/j.immuni.2011.09.009.

139. Mohrs, K., Wakil, A.E., Killeen, N., Locksley, R.M., and Mohrs, M. (2005). A two-step process for cytokine production revealed by IL-4 dual-reporter mice. Immunity *23*, 419-429. 10.1016/j.immuni.2005.09.006.
140. Yi, T., and Cyster, J.G. (2013). EBI2-mediated bridging channel positioning supports splenic dendritic cell homeostasis and particulate antigen capture. Elife *2*, e00757. 10.7554/eLife.00757.
141. Castellanos, C.A., Ren, X., Gonzalez, S.L., Li, H.K., Schroeder, A.W., Liang, H.E., Laidlaw, B.J., Hu, D., Mak, A.C.Y., Eng, C., et al. (2021). Lymph node–resident dendritic cells drive T H 2 cell development involving MARCH1. Sci Immunol *6*, eabh0707. 10.1126/sciimmunol.abh0707.
142. Allenspach, E.J., Lemos, M.P., Porrett, P.M., Turka, L.A., and Laufer, T.M. (2008). Migratory and lymphoid-resident dendritic cells cooperate to efficiently prime naive CD4 T cells. Immunity *29*, 795-806. 10.1016/j.immuni.2008.08.013.
143. Hsieh, C.S., Macatonia, S.E., O'Garra, A., and Murphy, K.M. (1995). T cell genetic background determines default T helper phenotype development in vitro. J Exp Med *181*, 713-721. 10.1084/jem.181.2.713.
144. Steinfelder, S., Andersen, J.F., Cannons, J.L., Feng, C.G., Joshi, M., Dwyer, D., Caspar, P., Schwartzberg, P.L., Sher, A., and Jankovic, D. (2009). The major component in schistosome eggs responsible for conditioning dendritic cells for Th2 polarization is a T2 ribonuclease (omega-1). J Exp Med *206*, 1681-1690. 10.1084/jem.20082462.
145. Mayer, J.U., Hilligan, K.L., Chandler, J.S., Eccles, D.A., Old, S.I., Domingues, R.G., Yang, J., Webb, G.R., Munoz-Erazo, L., Hyde, E.J., et al. (2021). Homeostatic IL-13 in healthy skin directs dendritic cell differentiation to promote T. Nat Immunol *22*, 1538-1550. 10.1038/s41590-021-01067-0.
146. Ricardo-Gonzalez, R.R., Van Dyken, S.J., Schneider, C., Lee, J., Nussbaum, J.C., Liang, H.E., Vaka, D., Eckalbar, W.L., Molofsky, A.B., Erle, D.J., and Locksley, R.M. (2018). Tissue signals imprint ILC2 identity with anticipatory function. Nat Immunol *19*, 1093-1099. 10.1038/s41590-018-0201-4.
147. Tong, P.L., Roediger, B., Kolesnikoff, N., Biro, M., Tay, S.S., Jain, R., Shaw, L.E., Grimbaldeston, M.A., and Weninger, W. (2015). The skin immune atlas: three-dimensional analysis of cutaneous leukocyte subsets by multiphoton microscopy. J Invest Dermatol *135*, 84-93. 10.1038/jid.2014.289.
148. Itano, A.A., McSorley, S.J., Reinhardt, R.L., Ehst, B.D., Ingulli, E., Rudensky, A.Y., and Jenkins, M.K. (2003). Distinct dendritic cell populations sequentially present antigen to CD4 T cells and stimulate different aspects of cell-mediated immunity. Immunity *19*, 47-57. 10.1016/s1074-7613(03)00175-4.
149. Chen, L., and Flies, D.B. (2013). Molecular mechanisms of T cell co-stimulation and co-inhibition. Nat Rev Immunol *13*, 227-242. 10.1038/nri3405.
150. Acuto, O., and Michel, F. (2003). CD28-mediated co-stimulation: a quantitative support for TCR signalling. Nat Rev Immunol *3*, 939-951. 10.1038/nri1248.
151. Huber, M., and Lohoff, M. (2014). IRF4 at the crossroads of effector T-cell fate decision. Eur J Immunol *44*, 1886-1895. 10.1002/eji.201344279.
152. Iwata, A., Durai, V., Tussiwand, R., Briseño, C.G., Wu, X., Grajales-Reyes, G.E., Egawa, T., Murphy, T.L., and Murphy, K.M. (2017). Quality of TCR signaling determined by differential affinities of enhancers for the composite BATF-IRF4 transcription factor complex. Nat Immunol *18*, 563-572. 10.1038/ni.3714.

153. Krishnamoorthy, V., Kannanganat, S., Maienschein-Cline, M., Cook, S.L., Chen, J., Bahroos, N., Sievert, E., Corse, E., Chong, A., and Sciammas, R. (2017). The IRF4 Gene Regulatory Module Functions as a Read-Write Integrator to Dynamically Coordinate T Helper Cell Fate. Immunity *47*, 481-497.e487. 10.1016/j.immuni.2017.09.001.
154. Kuwahara, M., Ise, W., Ochi, M., Suzuki, J., Kometani, K., Maruyama, S., Izumoto, M., Matsumoto, A., Takemori, N., Takemori, A., et al. (2016). Bach2-Batf interactions control Th2-type immune response by regulating the IL-4 amplification loop. Nat Commun *7*, 12596. 10.1038/ncomms12596.
155. Li, P., Spolski, R., Liao, W., Wang, L., Murphy, T.L., Murphy, K.M., and Leonard, W.J. (2012). BATF-JUN is critical for IRF4-mediated transcription in T cells. Nature *490*, 543-546. 10.1038/nature11530.
156. Lohoff, M., Mittrücker, H.W., Prechtl, S., Bischof, S., Sommer, F., Kock, S., Ferrick, D.A., Duncan, G.S., Gessner, A., and Mak, T.W. (2002). Dysregulated T helper cell differentiation in the absence of interferon regulatory factor 4. Proc Natl Acad Sci U S A *99*, 11808-11812. 10.1073/pnas.182425099.
157. Rengarajan, J., Mowen, K.A., McBride, K.D., Smith, E.D., Singh, H., and Glimcher, L.H. (2002). Interferon regulatory factor 4 (IRF4) interacts with NFATc2 to modulate interleukin 4 gene expression. J Exp Med *195*, 1003-1012. 10.1084/jem.20011128.
158. Bao, K., Carr, T., Wu, J., Barclay, W., Jin, J., Ciofani, M., and Reinhardt, R.L. (2016). BATF Modulates the Th2 Locus Control Region and Regulates CD4+ T Cell Fate during Antihelminth Immunity. J Immunol *197*, 4371-4381. 10.4049/jimmunol.1601371.
159. Sahoo, A., Alekseev, A., Tanaka, K., Obertas, L., Lerman, B., Haymaker, C., Clise-Dwyer, K., McMurray, J.S., and Nurieva, R. (2015). Batf is important for IL-4 expression in T follicular helper cells. Nat Commun *6*, 7997. 10.1038/ncomms8997.
160. Chan, W., Cao, Y.M., Zhao, X., Schrom, E.C., Jia, D., Song, J., Sibener, L.V., Dong, S., Fernandes, R.A., Bradfield, C.J., et al. (2023). TCR ligand potency differentially impacts PD-1 inhibitory effects on diverse signaling pathways. J Exp Med *220*. 10.1084/jem.20231242.
161. Kamphorst, A.O., Wieland, A., Nasti, T., Yang, S., Zhang, R., Barber, D.L., Konieczny, B.T., Daugherty, C.Z., Koenig, L., Yu, K., et al. (2017). Rescue of exhausted CD8 T cells by PD-1-targeted therapies is CD28-dependent. Science *355*, 1423-1427. 10.1126/science.aaf0683.
162. Zhou, B., Comeau, M.R., De Smedt, T., Liggitt, H.D., Dahl, M.E., Lewis, D.B., Gyarmati, D., Aye, T., Campbell, D.J., and Ziegler, S.F. (2005). Thymic stromal lymphopoietin as a key initiator of allergic airway inflammation in mice. Nat Immunol *6*, 1047-1053. 10.1038/ni1247.
163. Wang, Y., Shibuya, K., Yamashita, Y., Shirakawa, J., Shibata, K., Kai, H., Yokosuka, T., Saito, T., Honda, S., Tahara-Hanaoka, S., and Shibuya, A. (2008). LFA-1 decreases the antigen dose for T cell activation in vivo. Int Immunol *20*, 1119-1127. 10.1093/intimm/dxn070.
164. Gérard, A., Cope, A.P., Kemper, C., Alon, R., and Köchl, R. (2021). LFA-1 in T cell priming, differentiation, and effector functions. Trends Immunol *42*, 706-722. 10.1016/j.it.2021.06.004.
165. Noben-Trauth, N., Shultz, L.D., Brombacher, F., Urban, J.F., Gu, H., and Paul, W.E. (1997). An interleukin 4 (IL-4)-independent pathway for CD4+ T cell IL-4 production is

revealed in IL-4 receptor-deficient mice. Proc Natl Acad Sci U S A *94*, 10838-10843. 10.1073/pnas.94.20.10838.

166. Krummel, M.F., Mahale, J.N., Uhl, L.F.K., Hardison, E.A., Mujal, A.M., Mazet, J.M., Weber, R.J., Gartner, Z.J., and Gérard, A. (2018). Paracrine costimulation of IFN-γ signaling by integrins modulates CD8 T cell differentiation. Proc Natl Acad Sci U S A *115*, 11585-11590. 10.1073/pnas.1804556115.
167. Liao, W., Schones, D.E., Oh, J., Cui, Y., Cui, K., Roh, T.Y., Zhao, K., and Leonard, W.J. (2008). Priming for T helper type 2 differentiation by interleukin 2-mediated induction of interleukin 4 receptor alpha-chain expression. Nat Immunol *9*, 1288-1296. 10.1038/ni.1656.
168. Szeto, A.C.H., Ferreira, A.C.F., Mannion, J., Clark, P.A., Sivasubramaniam, M., Heycock, M.W.D., Crisp, A., Jolin, H.E., Kozik, P., Knolle, M.D., and McKenzie, A.N.J. (2023). An αvβ3 integrin checkpoint is critical for efficient T. Nat Immunol *24*, 123-135. 10.1038/s41590-022-01378-w.
169. Gaylo-Moynihan, A., Prizant, H., Popović, M., Fernandes, N.R.J., Anderson, C.S., Chiou, K.K., Bell, H., Schrock, D.C., Schumacher, J., Capece, T., et al. (2019). Programming of Distinct Chemokine-Dependent and -Independent Search Strategies for Th1 and Th2 Cells Optimizes Function at Inflamed Sites. Immunity *51*, 298-309.e296. 10.1016/j.immuni.2019.06.026.
170. Liu, Z., Liu, Q., Hamed, H., Anthony, R.M., Foster, A., Finkelman, F.D., Urban, J.F., and Gause, W.C. (2005). IL-2 and autocrine IL-4 drive the in vivo development of antigen-specific Th2 T cells elicited by nematode parasites. J Immunol *174*, 2242-2249. 10.4049/jimmunol.174.4.2242.
171. Fraser, J.D., Irving, B.A., Crabtree, G.R., and Weiss, A. (1991). Regulation of interleukin-2 gene enhancer activity by the T cell accessory molecule CD28. Science *251*, 313-316. 10.1126/science.1846244.
172. June, C.H., Ledbetter, J.A., Gillespie, M.M., Lindsten, T., and Thompson, C.B. (1987). T-cell proliferation involving the CD28 pathway is associated with cyclosporine-resistant interleukin 2 gene expression. Mol Cell Biol *7*, 4472-4481. 10.1128/mcb.7.12.4472-4481.1987.
173. Crotty, S. (2011). Follicular helper CD4 T cells (TFH). Annu Rev Immunol *29*, 621-663. 10.1146/annurev-immunol-031210-101400.
174. Duan, L., Liu, D., Chen, H., Mintz, M.A., Chou, M.Y., Kotov, D.I., Xu, Y., An, J., Laidlaw, B.J., and Cyster, J.G. (2021). Follicular dendritic cells restrict interleukin-4 availability in germinal centers and foster memory B cell generation. Immunity *54*, 2256-2272.e2256. 10.1016/j.immuni.2021.08.028.
175. Huse, M., Lillemeier, B.F., Kuhns, M.S., Chen, D.S., and Davis, M.M. (2006). T cells use two directionally distinct pathways for cytokine secretion. Nat Immunol *7*, 247-255. 10.1038/ni1304.
176. Poholek, A.C. (2021). Tissue-Specific Contributions to Control of T Cell Immunity. Immunohorizons *5*, 410-423. 10.4049/immunohorizons.2000103.
177. Ataide, M.A., Knöpper, K., Cruz de Casas, P., Ugur, M., Eickhoff, S., Zou, M., Shaikh, H., Trivedi, A., Grafen, A., Yang, T., et al. (2022). Lymphatic migration of unconventional T cells promotes site-specific immunity in distinct lymph nodes. Immunity *55*, 1813-1828.e1819. 10.1016/j.immuni.2022.07.019.

178. von Moltke, J., and Pepper, M. (2018). Sentinels of the Type 2 Immune Response. Trends Immunol *39*, 99-111. 10.1016/j.it.2017.10.004.
179. De Koker, S., Van Hoecke, L., De Beuckelaer, A., Roose, K., Deswarte, K., Willart, M.A., Bogaert, P., Naessens, T., De Geest, B.G., Saelens, X., et al. (2017). Inflammatory monocytes regulate Th1 oriented immunity to CpG adjuvanted protein vaccines through production of IL-12. Sci Rep *7*, 5986. 10.1038/s41598-017-06236-6.
180. Nadjsombati, M.S., McGinty, J.W., Lyons-Cohen, M.R., Jaffe, J.B., DiPeso, L., Schneider, C., Miller, C.N., Pollack, J.L., Nagana Gowda, G.A., Fontana, M.F., et al. (2018). Detection of Succinate by Intestinal Tuft Cells Triggers a Type 2 Innate Immune Circuit. Immunity *49*, 33-41.e37. 10.1016/j.immuni.2018.06.016.
181. Powell, D. (2019). drpowell/degust 4.1.1 (4.1.1). Zenodo.
182. Liao, Y., Wang, J., Jaehnig, E.J., Shi, Z., and Zhang, B. (2019). WebGestalt 2019: gene set analysis toolkit with revamped UIs and APIs. Nucleic Acids Res *47*, W199-W205. 10.1093/nar/gkz401.
183. Taverna, F., Goveia, J., Karakach, T.K., Khan, S., Rohlenova, K., Treps, L., Subramanian, A., Schoonjans, L., Dewerchin, M., Eelen, G., and Carmeliet, P. (2020). BIOMEX: an interactive workflow for (single cell) omics data interpretation and visualization. Nucleic Acids Res *48*, W385-W394. 10.1093/nar/gkaa332.
184. Kucukural, A., Yukselen, O., Ozata, D.M., Moore, M.J., and Garber, M. (2019). DEBrowser: interactive differential expression analysis and visualization tool for count data. *BMC Genomics 20*. 10.1186/s12864-018-5362-x.